AD-A230 527

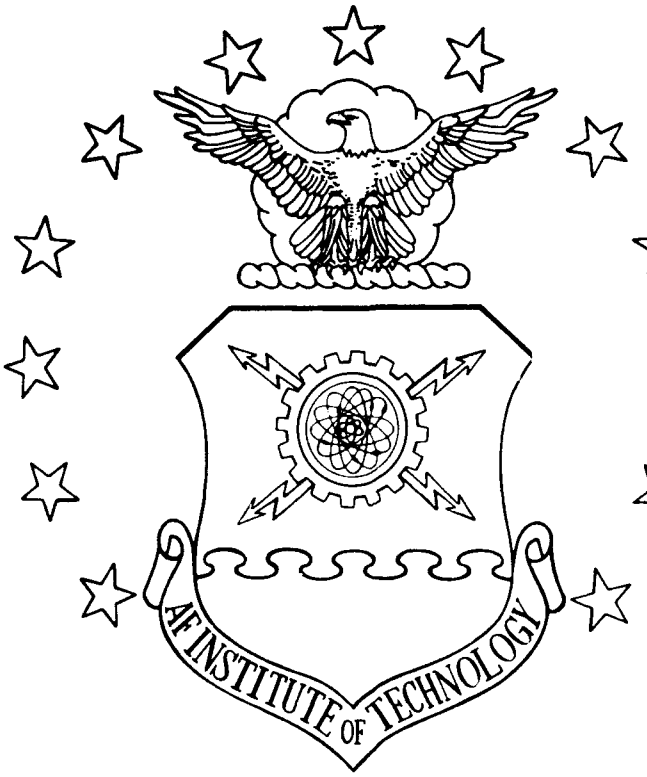

DTIC
ELECTE
JAN 07 1991
S B D

DEPARTMENT OF THE AIR FORCE

AIR UNIVERSITY

AIR FORCE INSTITUTE OF TECHNOLOGY

Wright-Patterson Air Force Base, Ohio

DISTRIBUTION STATEMENT A
Approved for public release;
Distribution Unlimited

AFIT/GAE/ENY/90D-08

INVESTIGATION OF STRAIN CHARACTERISTICS OF GRAPHITE POLYETHERETHER KETONE USING A NONLINEAR ANALYSIS AND EXPERIMENTAL METHODS

THESIS

Stephen C. Gould, Captain, USAF

AFIT/GAE/ENY/90D-08

Approved for public release; distribution unlimited

DTIC
ELECTE
JAN 07 1991
S B D

AFIT/GAE/ENY/90D-08

INVESTIGATION OF STRAIN CHARACTERISTICS OF GRAPHITE POLYETHERETHER KETONE USING A NONLINEAR ANALYSIS AND EXPERIMENTAL METHODS

THESIS

Presented to the Faculty of the School of Engineering
of the Air Force Institute of Technology
Air University
In Partial Fulfillment of the
Requirements for the Degree of
Master of Science in Aeronautical Engineering

Stephen C. Gould, B.S.
Captain, USAF

December 1990

Approved for public release; distribution unlimited

Preface

The purpose of this study was to develop a computer program which would provide an accurate method of predicting the stress/strain behavior of advanced composite laminates. The ability to predict the behavior of materials at large strain will allow the use of important ply lay-ups such as ±45° to its full capacity.

This thesis was clearly a group effort. I need to thank my thesis advisor, Dr. A. N. Palazotto, for his patience through some major problems. I am also deeply indebted to Dr R. S. Sandhu of the Flight Dynamics Laboratory for his continued assistance over the past year. Both of these individuals provided me with an insight of composites and computer programming that will benefit me throughout my career.

The people of the structures division:

1. Capt J. Daniels and Mr. K. Spitzer for insuring the specimens were C-scanned, cut, and ready for testing. Capt Daniels also helped me in understanding the computer systems.
2. Mr C. Hitchcock, and the instrumentation group who attached the strain gages.
3. Mr. D. Cook, Mr. L. Bates, and Mr H. Stalnaker, of the Fatigue, Fracture, and Reliability Group, who ran the testing.
4. Mr Gene Maddux and Don Webb, of the Photomechanics Facility, also provided support.

Accession For
NTIS GRA&I ☑
DTIC TAB ☐
Unannounced ☐
Justification
By
Distribution/
Availability Codes
Dist | Avail and/or Special
A-1

Table of Contents

List of Figures

List of Tables

Abstract

A geometric nonlinear technique is incorporated in a current finite element program. This nonlinear program allows material nonlinearity for calculating the stresses, strains and failure of composites. The improved program uses an updated Lagrangian to calculate the stresses and strains. In addition, it updates the fiber orientation due to displacement in order to calculate the updated stiffness matrix. This method is valuable for large strain values.

The analytical data were compared to experimental data obtained from Graphite PolyEtherEther Ketone (Gr/PEEK) $[\pm 45°]_{4s}$ laminates. To obtain data two geometries were used. Digitized photographs were used to measure the angle change for large strains.

INVESTIGATION OF STRAIN CHARACTERISTICS OF GRAPHITE POLYETHERETHER KETONE USING A NONLINEAR ANALYSIS AND EXPERIMENTAL METHODS

I. Introduction

Since the airplane first flew, persistent efforts have been made to make it lighter and stronger. The recent development of composites has added to this impetus. Graphite based composites are stronger and lighter than aluminum. Researchers have reduced the weights of engines, wings and several other aircraft parts through the use of composites.

In the past several years new composites have improved aircraft performance immeasurably. The Air Force uses hundreds of different composites in aircraft parts; researchers have introduced many of these materials in the past few years. Research at the Flight Dynamics Laboratory of Wright Research and Development Center have included many of these composites.

Graphite-epoxy is one of the most commonly used composites. The materials industry has recently introduced a potential substitute, graphite polyetherether ketone (Gr/PEEK). This thermoplastic material weighs less, has a greater operating temperature, and has better fracture toughness characteristics than graphite-epoxy.

Composite materials are the macroscopic blend of two or more different materials. Composites include cloth, wood, and several other materials which have been used for centuries. This research is concerned with "advanced" composites. Advanced composites are materials with high strength fibers blended into a plastic or metal matrix.

Manufacture of the composite can taylor differing properties as required. When the composite prepreg is manufactured, the fibers are laid such that the direction of the fibers is parallel. Each layer or laminae can be laid with a different orientation. (Figure 1-1) The matrix is then allowed to cure in an autoclave. The different temperatures of the curing process can produce different material properties. The data sheet from the production of the composites used in this thesis is provided in Appendix A.

"For the design to be satisfactory for an aircraft, it is essential to determine the stress-strain behavior and the ultimate strength of the laminates." (21:104) One way to examine the stress-strain characteristics is through computer modeling, using finite element models. Another way is by experimental observation. The best way is to do both and compare the results. This is the basis of this thesis.

A. Problem.

This research will compare the stress-strain analysis of several finite elements models with experimental data. Two separate specimen geometries were evaluated numerically . (Figure 1-2) The results of the models will be compared to experimental data.

Fiber Orientation

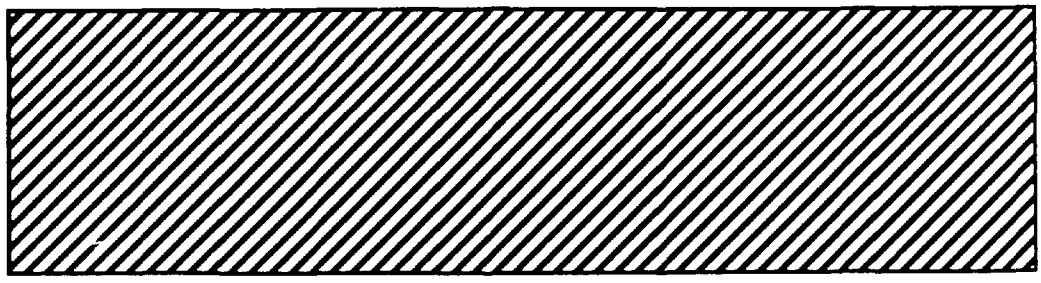

+45°

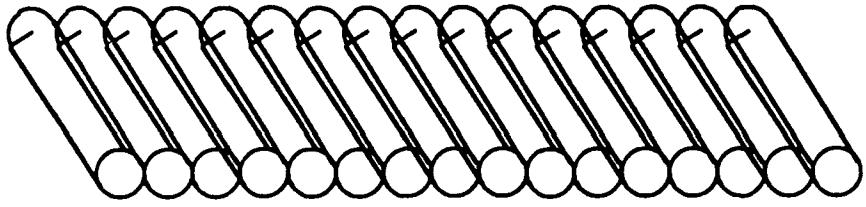

-45°

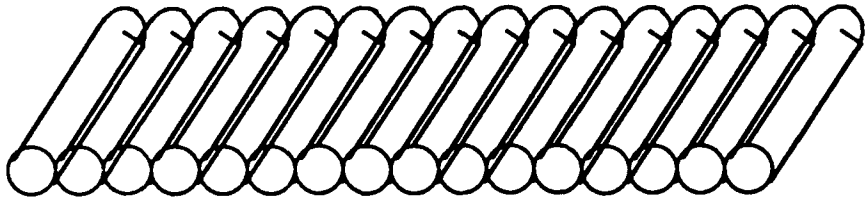

0°

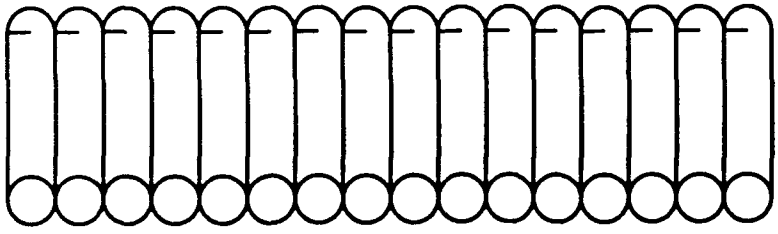

90°

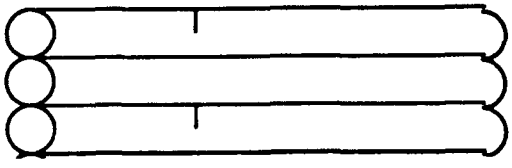

Figure 1-1. Usual Fiber Orientations

These specimen shapes were chosen for their high degree of strain provided. Originally a 0.4 inch diameter notched model was considered, however, to obtain high strains a 0.2 inch diameter notch was used. The width was increased to 1.125 inches for increased strain.

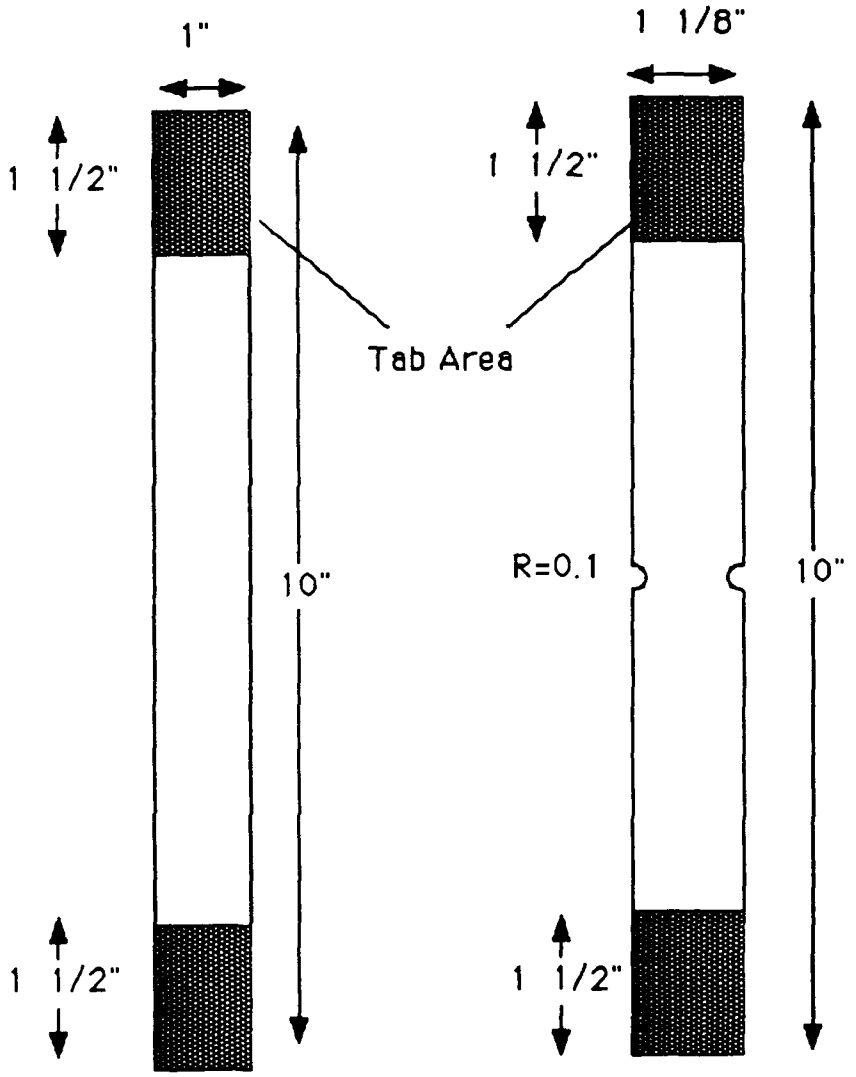

Figure 1-2. Specimens Dimensions

Other methods of obtaining high strain results are discussed in a recent article. (11) The strain field mappings similar to the contours shown in Section V.

Earlier versions of the modified program were used on several previous theses. (6,8,13) This thesis will update the program PLSTR2 to provide geometric nonlinearity along with the material nonlinearity shown in Capt Daniels's thesis. (6). The geometric nonlinearity will consist of updating the Lagrangian (shape functions) coordinates and updating the fiber orientation (ply angle) during each increment of loading. A ±45° orientation was used to observe the fullest use of these updates.

The experimentation will consist of strain gage measurements, and extensometer readings. The strain gages and the attaching adhesive are designed for up to 10-20 percent strain per the manufacturer. Photographs were taken during the loading process to determine angle changes and total displacement versus loading.

B. Current Knowledge.

Three recent AFIT theses examined the characteristics of Gr/PEEK. (6,8,13) Capt Martin studied the characteristics at room temperature with, and without concentric holes in the coupons. Capt Fisher studied the characteristics at high temperature with and without concentric holes. Capt Daniels studied the characteristics at room temperature with eccentric and concentric holes. Each thesis used different methods of evaluating the stress-strain characteristics.

All of these theses looked at ±45° laminates. They all had difficulty with the high strains obtained by these laminates. All three theses will be discussed and compared with the present research.

This research will be conducted solely on $(\pm 45°)_S$ Gr/PEEK 16 ply laminates.

These theses also contained finite element models. Capt Daniels used the program called PLSTREN (6:6-4) which incorporated nonlinear material properties. This research will take that same program and account for geometric nonlinearity as well. These changes are discussed fully in Section III.

This type of analysis is necessary for large strain. Mr. Nabil Y. Ghantos wrote a program for "Geometric Nonlinear Analysis of Plane Frame Structures". His thesis shows the enhanced predictions of using geometric nonlinearity in plane structures. (9,10-19) His thesis shows that if structures experience large stresses the shape of the structure will change. Therefore, during the loading process the change of new shape of the structure must be updated. This thesis uses that same concept only with a composite coupon instead of a structure.

Large strains have always been a difficult process to predict since the process is highly nonlinear. Linear equations are not accurate at high strains, and so the nonlinear analysis is necessary. All three AFIT theses done on this material looked at ±45° lay-ups. Most of the material properties which Capt Martin (13:116-118) derived will be used in this thesis. However, he decided to select a cut off point of 5% strain to separate interlaminar and intralaminar ahear strains. By using high elongation gages and high elongation adhesive, much higher strains than either Martin or Fisher were observed. Therefore, shearing stress and strain will be more accurate in these tests.

Several articles have been written on the subject of notched laminates (20). Notched specimens were also looked at in this study and will be compared with previous investigations.

II. Theory

The applicable theories used in this thesis include the constitutive equations of composite materials, failure theory, and nonlinear finite element theory,. The constitutive laws are utilized in the program and in the analysis of the data obtained experimentally.

This research will be looking at ±45° ply lay-ups. This will create large displacements and thus strains and the fiber orientation will change as the specimen strains. It is assumed that plasticity will not occur, but stress- strain relations can be considered nonlinear. Figures 2-1a, b and c show how the lay-up starts and is updated as stresses are applied. These figure show the directions of fiber orientation. Figure 2-1c show how the angle changes as the forces are applied. The stresses in the X direction are derived from the applied forces. The stresses in the Y direction are zero. The stresses in the fiber directions change.

The basic constitutive equations include Hooke's Law equation 2-1. (18:188)

$$\sigma_i = C_{ij}\,\varepsilon_j \qquad i = 1,..6 \qquad j = 1,..6 \qquad (2\text{-}1)$$

where:

σ_i = stresses

C_{ij} = stiffness matrix

e_j = strains

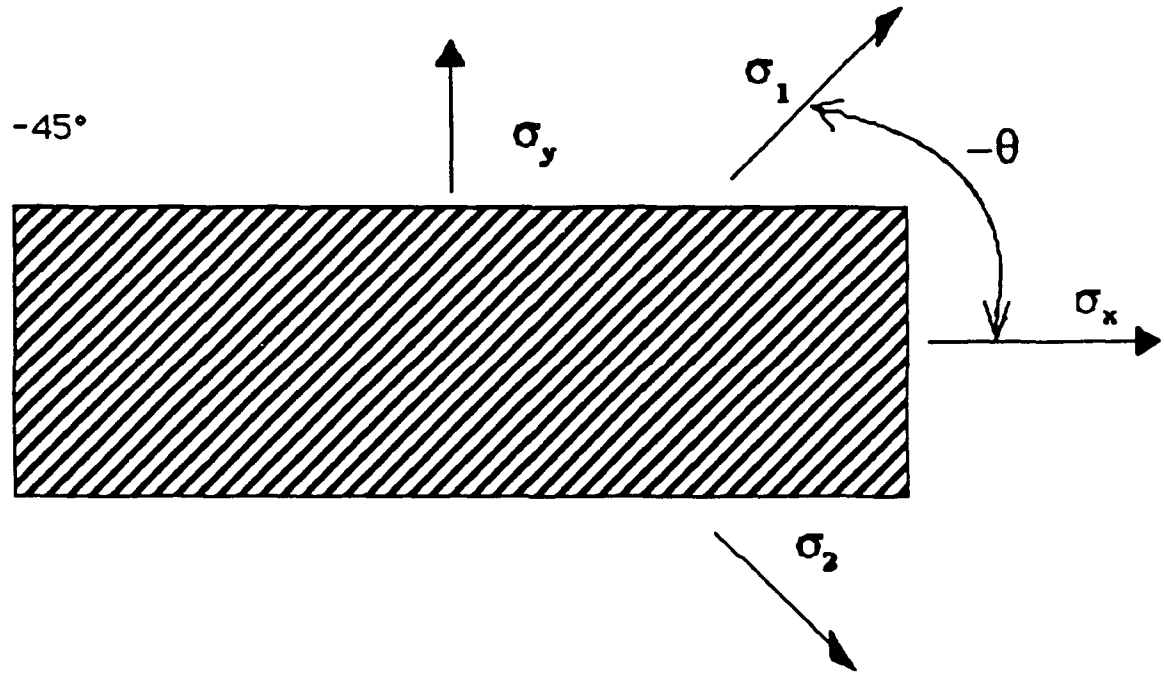

Figure 2-1a. Stress Directions in -45° Specimen

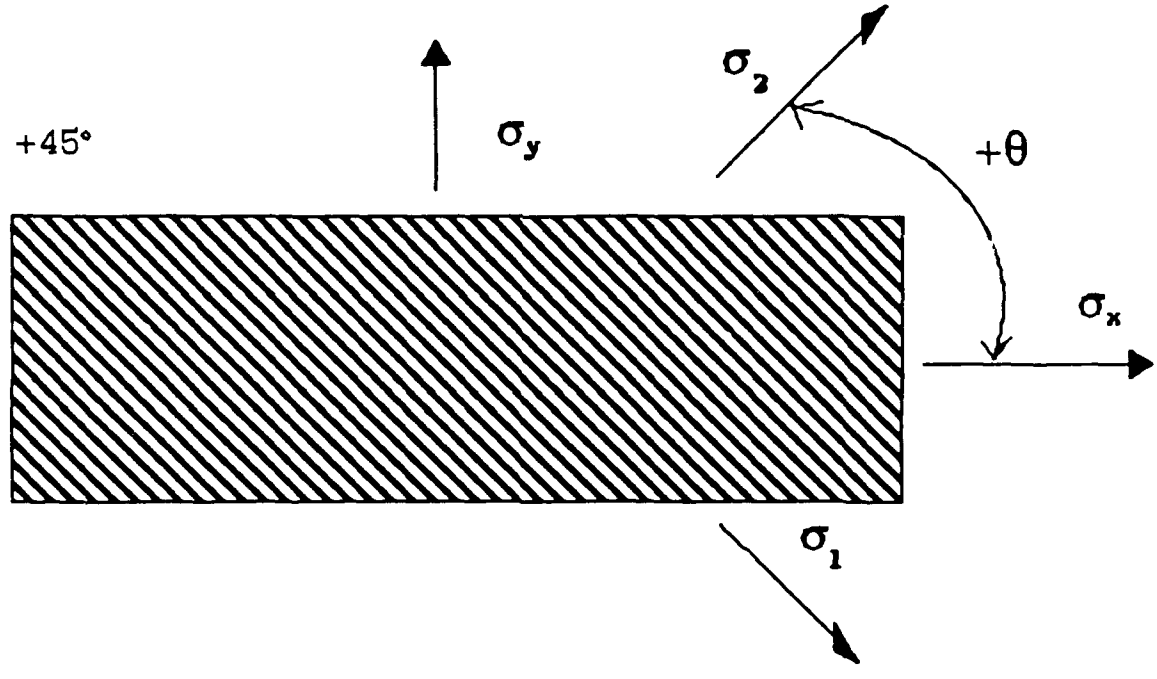

Figure 2-1b. Stress Directions in +45° Specimen

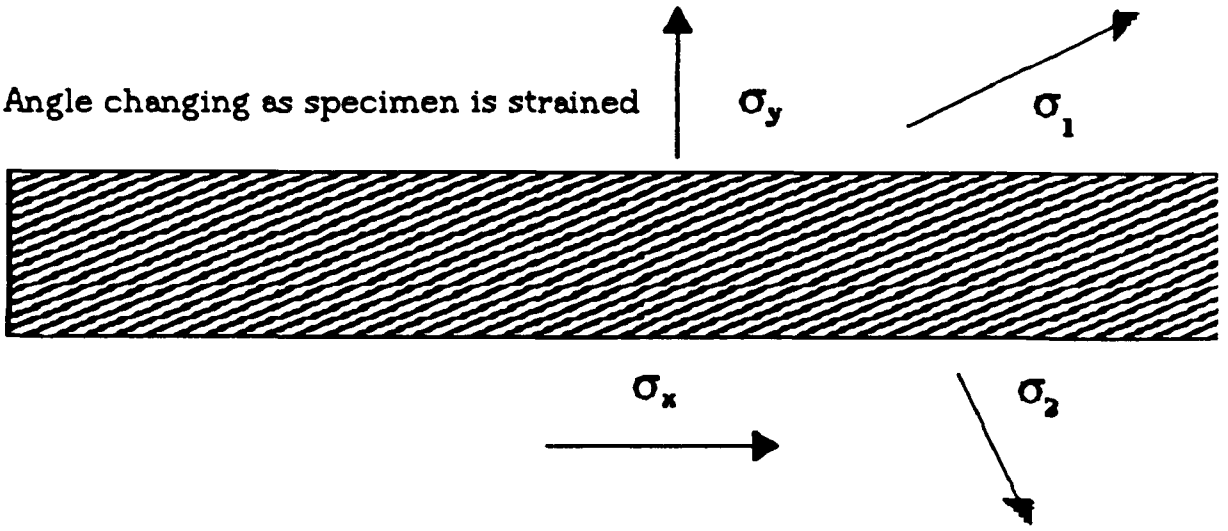

Figure 2-1c. Stress Directions After Deformation

For our purposes, only plane stress and plane strain will be looked at. In other words, three dimensional effects will not be considered. $\sigma_3,\tau_{13},\tau_{23}=0$; and $\varepsilon_3,\gamma_{13},\gamma_{23}=0$

Equation (2-2) shows the transformation matrix used to solve for the stresses.

$$\begin{Bmatrix} d\sigma_1 \\ d\sigma_2 \\ d\tau_{12} \end{Bmatrix} = \begin{bmatrix} m^2 & n^2 & -2mn \\ n^2 & m^2 & 2mn \\ nm & -mn & m^2-n^2 \end{bmatrix} \begin{Bmatrix} d\sigma_x \\ d\sigma_y \\ d\tau_{xy} \end{Bmatrix} \qquad (2\text{-}2)$$

Where:

$d\sigma_x$ = change of stress in direction of specimen.

$d\sigma_1$ = change of stress in fiber direction

$m = \cos\theta$

$n = \sin\theta$

θ = fiber orientation (updated throughout program)

A. Linear Finite Element Theory.

Finite element analysis utilizes the equations described above. It assumes that each element has the same properties throughout the element. At points where there is a stress concentration, a closely refined model is needed. In our study as many elements as feasible to get the best results will be considered. Figure 2-3a shows the original model. Figure 2-3b shows the quarter model. Symmetry was taken advantage of in the model.

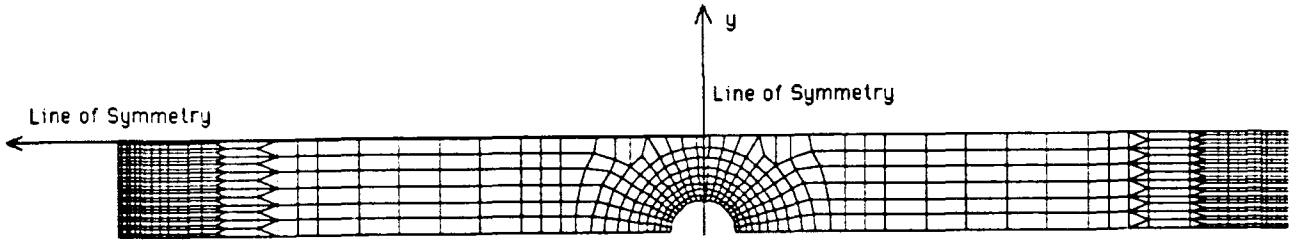

Figure 2-3a. Original Half Model

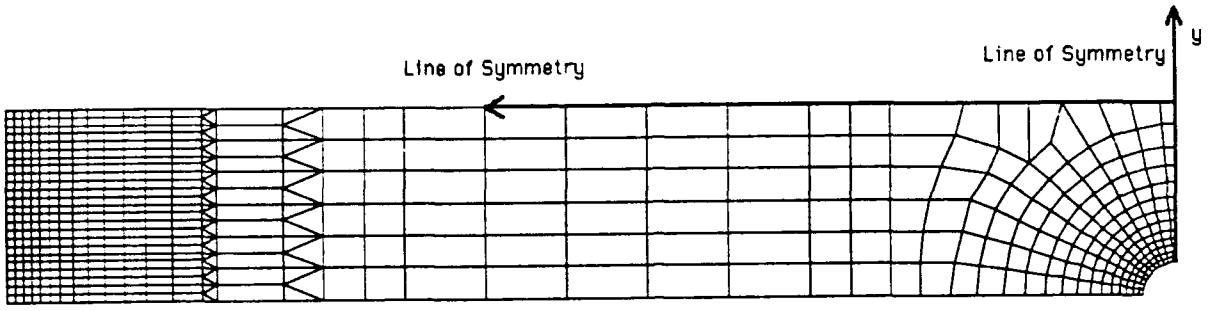

Figure 2-3b. Quarter Model

The program PLSTR2 uses quadrilateral elements consisting of constant strain triangular elements. This concept is described in detail in several books (2:98-101). The use of the concept in PLSTREN (linear) and PLSTR2(nonlinear material) is described in detail by Capt Daniels. (6:2-15 - 2-19) The constant strain triangle is shown in figure 2-9.

All element in this program are "Lagrange elements" (2:97-99). Therefore, the elements shape functions are derived using "Lagrange's Interpolation Formula". This formula is reduced to (2-4) for plane stress/plane strain problems.

$$u = \sum_{i=1}^{n} N_i u_i \quad \text{or} \quad u = N_1u_1 + N_2u_2 + ...+ N_nu_n \qquad (2\text{-}4)$$

$$v = \sum_{i=1}^{n} N_i v_i \quad \text{or} \quad v = N_1v_1 + N_2v_2 + ...+ N_nv_n$$

where: N= shape function

u= X direction component of displacement

v= Y direction component of displacement

n= 4 for a four noded element (3 in this program)

This program will divide all elements into triangles as discussed further on in this section.

The models used in this thesis use both triangular elements and condensed rectangular elements. The elements must be kept as close to square as possible close to either a material or geometric discontinuity.(Figure 2-4). This program updates the coordinates and thus the element's shape is updated as shown. Triangular elements are only used at uniform stress/strain locations (Figure 2-5).

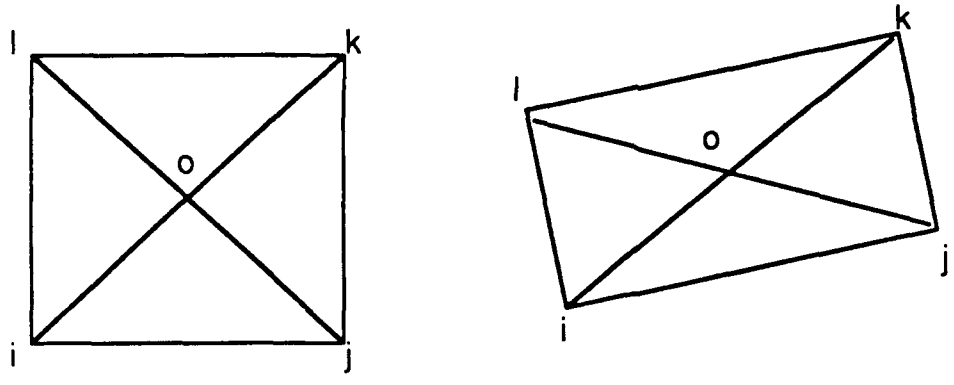

Figure 2-4. Degenerated Rectangular Elements

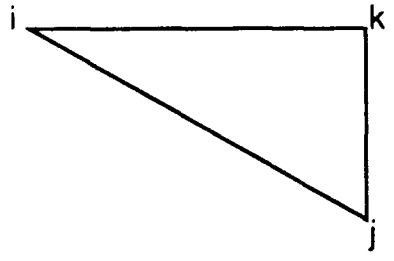

Figure 2-5. Triangular Elements

Elements are numbered counterclockwise. The centroid is then calculated and all stresses and strains are calculated for that point.

These relationships are used in both linear and nonlinear programs. The linear program is only used to compare with the nonlinear program and show the integrity of our models.

B. Material Nonlinear Constitutive Relations.

The material properties of Gr/PEEK have been shown by Capt Martin to change as the material is deformed. Material properties were obtained experimentally for tension, compression, and shear. He averaged the data by selecting suitable sets of strain values for all the stress strain curves required in this computer code.

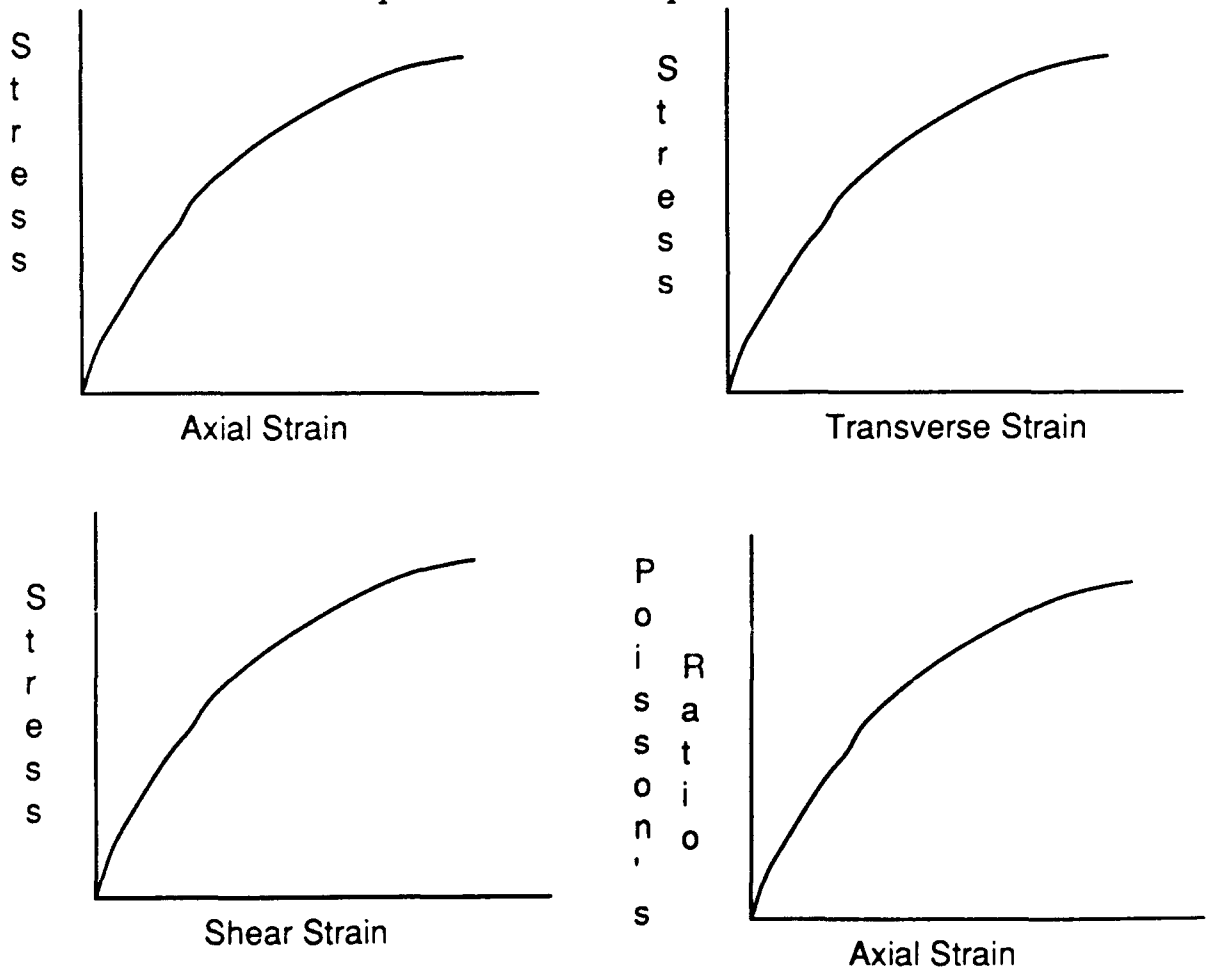

Figure 2-6. Examples of Cubic Splines Used in Program PLSTR2

As each increment of load is applied, new material properties are calculated using a predictive, corrective, and iterative technique. This process is described in detail by Capt Fisher. (8:2-15 - 2-29)

After enough load is applied to extend past the end of the curve, the program believes the material has failed. For our models failure occurred at approximately 6 times the level of strain experienced by Capt Martin. Therefore, experimental data from these experiments were used for the shear stress\strain curve with angle updates. (Figure 4-6). The curves for glass epoxy were also extended. (Figure 2-7)

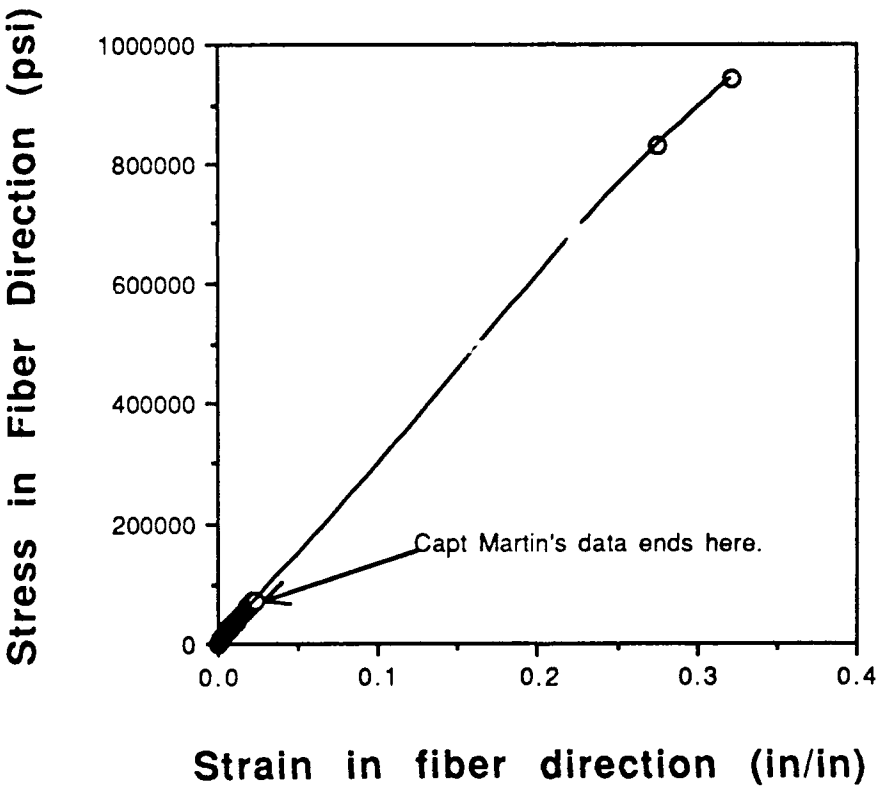

Figure 2-7 Extended Curve of Capt Martin's Data

C. Geometric Nonlinear Constitutive Relations.

The geometric nonlinearity provided by this program was done in two parts. The coordinates were updated after every increment of load was applied. Each time the strain increments were calculated the fiber orientation of each ply was updated. A description of the updated Lagrangian coordinate system is given by Owen and Hinton (15:382-388)

To update the coordinates, one first must calculate the $\bar{Q}$ matrix. By multiplying the Q matrix (equation 2-4) by the transformation matrix(equation 2-1) and it's inverse one can obtain the $\bar{Q}$ matrix(equation 2-4).

$$\begin{Bmatrix} d\sigma_1 \\ d\sigma_2 \\ d\tau_{12} \end{Bmatrix} = \begin{bmatrix} Q_{11} & Q_{12} & 0 \\ Q_{12} & Q_{22} & 0 \\ 0 & 0 & Q_{66} \end{bmatrix} \begin{Bmatrix} d\varepsilon_1 \\ d\varepsilon_2 \\ d\varepsilon_3 \end{Bmatrix} \qquad (2\text{-}4)$$

Where: $Q_{11} = \dfrac{E_1}{1-\nu_{12}\nu_{21}}$ $\quad Q_{12} = \dfrac{E_1\nu_{12}}{1-\nu_{12}\nu_{21}}$

$$Q_{22} = \frac{E_2}{1-\nu_{12}\nu_{21}} \qquad Q_{66} = G_{12}$$

$$\begin{Bmatrix} d\sigma_x \\ d\sigma_y \\ d\tau_{xy} \end{Bmatrix} = \begin{bmatrix} \bar{Q}_{11} & \bar{Q}_{12} & \bar{Q}_{16} \\ \bar{Q}_{12} & \bar{Q}_{22} & \bar{Q}_{26} \\ \bar{Q}_{16} & \bar{Q}_{26} & \bar{Q}_{66} \end{bmatrix} \begin{Bmatrix} d\varepsilon_x \\ d\varepsilon_y \\ d\gamma_{xy} \end{Bmatrix} \qquad (2\text{-}5)$$

Where: $\bar{Q}_{11} = Q_{11}m^4 + 2(Q_{12}+2Q_{66})n^2m^2 + Q_{22}n^4$

$\bar{Q}_{12} = (Q_{11}+Q_{22}-4Q_{66})n^2m^2 + Q_{12}(n^4+m^4)$

$\bar{Q}_{22} = Q_{11}n + 2(Q_{12}+2Q_{66})n^2m^2 + Q_{22}m^4$

$$\bar{Q}_{16} = (Q_{11}-Q_{12}-Q_{66})nm^3 + (Q_{12}-Q_{22}+2Q_{66})n^3m$$

$$\bar{Q}_{26} = (Q_{11}-Q_{12}-Q_{66})n^3m + (Q_{12}-Q_{22}+2Q_{66})nm^3$$

$$\bar{Q}_{66}=(Q_{11}+ Q_{22}-2Q_{12}-2Q_{66})n^2m^2 + Q_{66}(n^4+m^4)$$

$m = \cos\theta$

$n = \sin\theta$

θ = fiber orientation

Once the $\bar{Q}$ matrix has been calculated, one can determine the incremental strains from the incremental stresses. From the incremental strains one can now calculate the displacements.(equation 2-8) These equations were shown by Palazotto (16).

$$[K_{eq}] = A\sum_{i=1}^{n}[B]^T[\bar{Q}][B]t_i \qquad (2\text{-}6)$$

$$[dN] = \sum_{p=1}^{n} [\bar{Q}]_k \ [du]_k \ t_k \qquad (2\text{-}7)$$

$$[du] = [K_{eq}]^{-1}[dN] \qquad (2\text{-}8)$$

where: k = number of plies

t_k = thickness of kth ply

After the displacements are calculated, the new element is defined. One now has a new mesh from which to calculate stresses and strains (Figure 2-8).

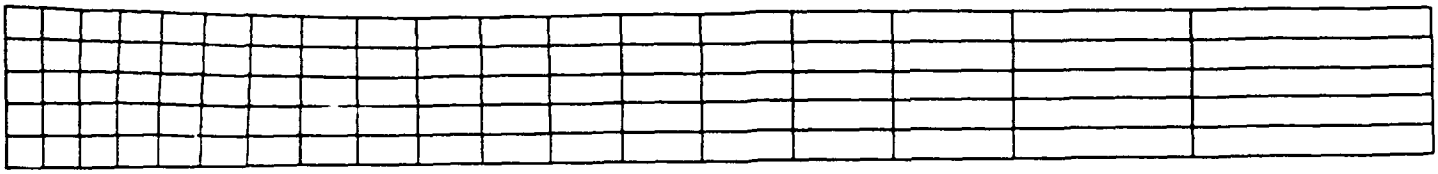

Figure 2-8 a. Old Mesh

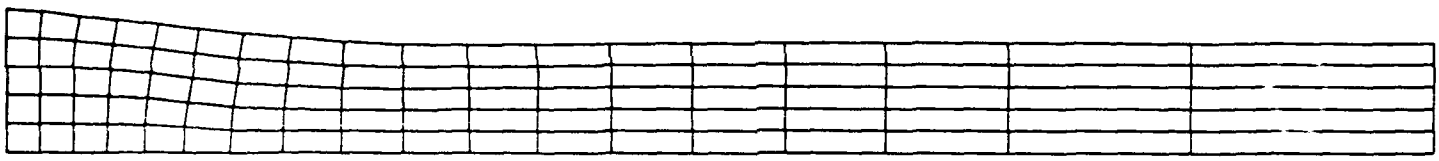

Figure 2-8 b. New Mesh

Calculation of the new ply orientation is done prior to calculating the $\bar{Q}$ matrix(equation 2-9). The accuracy of this equation is shown in figure 5-7 of the results.

$$d\theta = d\gamma_{xy}(180/\pi) \qquad (2\text{-}9)$$

Where: $d\theta$ = change in fiber orientation(degrees)

γ_{xy} = shear strain

D. Program Description.

"The laminate constitutive relations are initially assumed to be linear and the element stiffness matrices are computed" (19:182) This stiffness matrices are made into a global stiffness matrix and then condensed into a reduced stiffness matrix. The resulting equations are solved using the applied incremental loads. These equations are now used to solve for the displacements.

The calculated displacements from an incremental point of view can be written as vectors using the updated Lagrangian approach. The updated Lagrangian is acceptable from the small increments of displacement.

$$du=[\mathbf{X}]\{a_1 \;\; a_2 \;\; a_3\}^T \text{ and } dv=[\mathbf{X}]\{a_4 \;\; a_5 \;\; a_6\}^T \qquad (2\text{-}10)$$

where: $[\mathbf{X}]=[1 \;\; \bar{x} \;\; \bar{y}]$ from figure 2-7

$\bar{x}$ and $\bar{y}$ are the coordinate differential functions

These displacements are converted into strain. The higher order terms of the total Lagrangian are ignored due to small increments.

$$d\varepsilon_x=\frac{\partial du}{\partial x} \quad d\varepsilon_y=\frac{\partial dv}{\partial y} \quad d\gamma_{xy}=\frac{\partial du}{\partial y}+\frac{\partial dv}{\partial x} \qquad (2\text{-}11)$$

These strains are now used to calculate the strain-displacement matrix [B].

$$\begin{Bmatrix} d\varepsilon_x \\ d\varepsilon_y \\ d\gamma_{xy} \end{Bmatrix}=[B]\begin{Bmatrix} du_1 \\ dv_1 \\ du_2 \\ dv_2 \\ du_3 \\ dv_3 \end{Bmatrix} \qquad (2\text{-}12)$$

where:

$$[B]=\begin{bmatrix} 1 & 0 & 0 & 0 & 0 & 0 \\ 0 & 0 & 0 & 1 & 0 & 0 \\ 1 & 0 & 1 & 0 & 0 & 0 \end{bmatrix}[A]^{-1}$$

$$[A]=\begin{bmatrix} 1 & x1 & y1 \\ 1 & x2 & y2 \\ 1 & x3 & y3 \end{bmatrix}$$

previous coordinate before the increment of displacement.

[A] is calculated from the constant area triangle shown in figure 2-9.

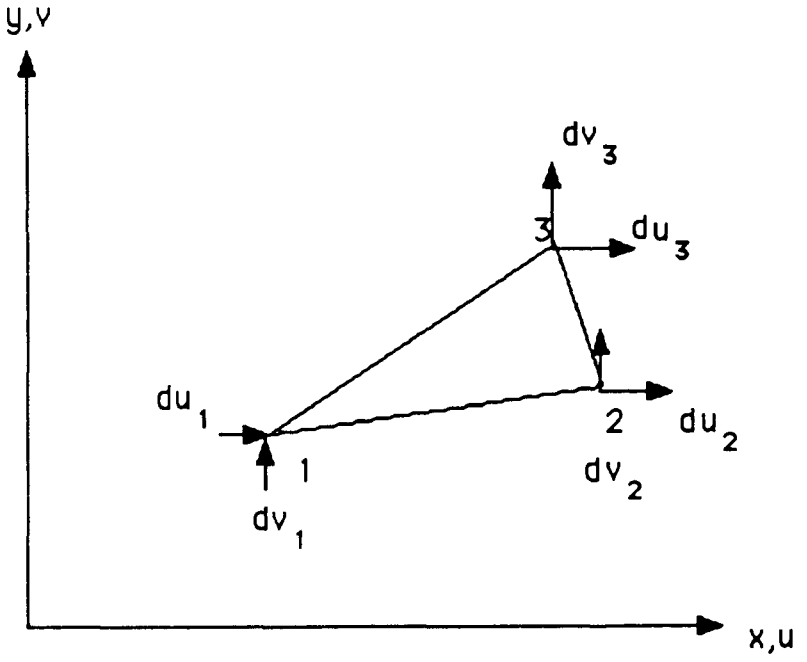

Figure 2-9. Constant Strain Triangle

The stiffness matrix [k] of an element can now be calculated from equation 2-13.

$$[k]_e=\int_A [B]^T [\bar{Q}][B]tdA=[B]^T [\bar{Q}][B]tA \qquad (2\text{-}13)$$

where: A is previous element area

$$\bar{Q} = \begin{bmatrix} \bar{Q}_{11} & \bar{Q}_{12} & \bar{Q}_{16} \\ \bar{Q}_{12} & \bar{Q}_{22} & \bar{Q}_{26} \\ \bar{Q}_{16} & \bar{Q}_{26} & \bar{Q}_{66} \end{bmatrix} \quad \text{At previous load}$$

Once the new strains are calculated, and the position of the nodes are determined, with these new positions it is possible to evaluate updated element areas and a check to see if the maximum strain has been reached for ply failure. It is then possible to calculate the stresses by adding the new increment of stress to previous total stress. A more complete discussion of these equations is provided in section III.

The failure criterion used on PLSTREN and PLSTR2 was discussed in many references and is explained fully in Technical Report AFFDL-TR-73-137 (23).

For this program, total strain energy determines the failure of laminates.

$$K_1W_1 + K_2W_2 + K_6W_6 \geq 1 \qquad (2\text{-}14)$$

Where:

$$W_i = \int_{e_i} \sigma_i de_i \qquad 1/K_i = \int_{e_{iu}} \sigma_i de_i \qquad (2\text{-}15)$$

The program considers the laminate as having failed if:

$$K_1W_1/(K_1W_1 + K_2W_2 + K_6W_6) \quad \begin{cases} \geq 0.1 \text{ for fiber failure} \\ < 0.1 \text{ for matrix failure} \end{cases} \qquad (2\text{-}16)$$

Two different types of unloading have been considered for this program. However, gradual unloading is most accurate for multidirectional laminates. For this program this is accomplished by setting NOPSHN equal to 2. For immediate unloading, set NOPSHN equal to 1. Upon failure the modulus of elasticity for the failed laminate is made negative. This unloads the laminate as the load increases and has been shown to be quite accurate with experimental data. (20:168)

This failure criteria is compared to numerous other criteria by Sandhu. (22) This method shows excellent results when compared to experimental data.

III. Analysis

This chapter includes a description of the geometry of the specimen, how the models were developed, and a convergence study to determine the integrity of the models.

This thesis compares the linear finite element model with the nonlinear models. The program diagram has not changed from Capt Daniels's thesis. We follow the subroutines on the nonlinear part of the program. The changes in the program were in the STON, and OUTPUT subroutines.

This thesis uses a conventional method of Finite Element Analysis (FEA). Betts discusses several different methods of FEA and commercially available FEA programs. As Betts states, the re-mesh of the model may create a potential for distorting element shapes(1:60). This could decrease accuracy. To show the integrity of our model we will compare with experimental results. The convergence study also proves the integrity of the models.

A. Finite Element Modeling.

This thesis modeled the specimens shown in Figure 1.2. The modeling consisted of highly refined elements around the discontinuities. This included both material and geometric discontinuities. Elements in between were made as geometrically convenient since stress and strain were reasonably constant. The use of triangles was a mistake. The program works better with four sided polygons as shown by Sandhu(20). For this reason a smaller model was used for some of our calculations. As shown in the section V, the smaller model provided better failure criteria. (Figure 5-4c)

The material properties for glass epoxy the linear program were taken from Cron's experimental results. (3) Cron ran tests on both Gr/epoxy and glass epoxy. His data had a constant value for the material properties. These properties of glass epoxy were also used by Capt Martin.

Using Capt Martin's model, it was observed that the differences in using the quarter model were small.(Figure 3-1) This graph shows the differences between strains from the linear program across the line of symmetry (Figure 3-2). Since the differences were less than 1 percent, we considered the model viable.

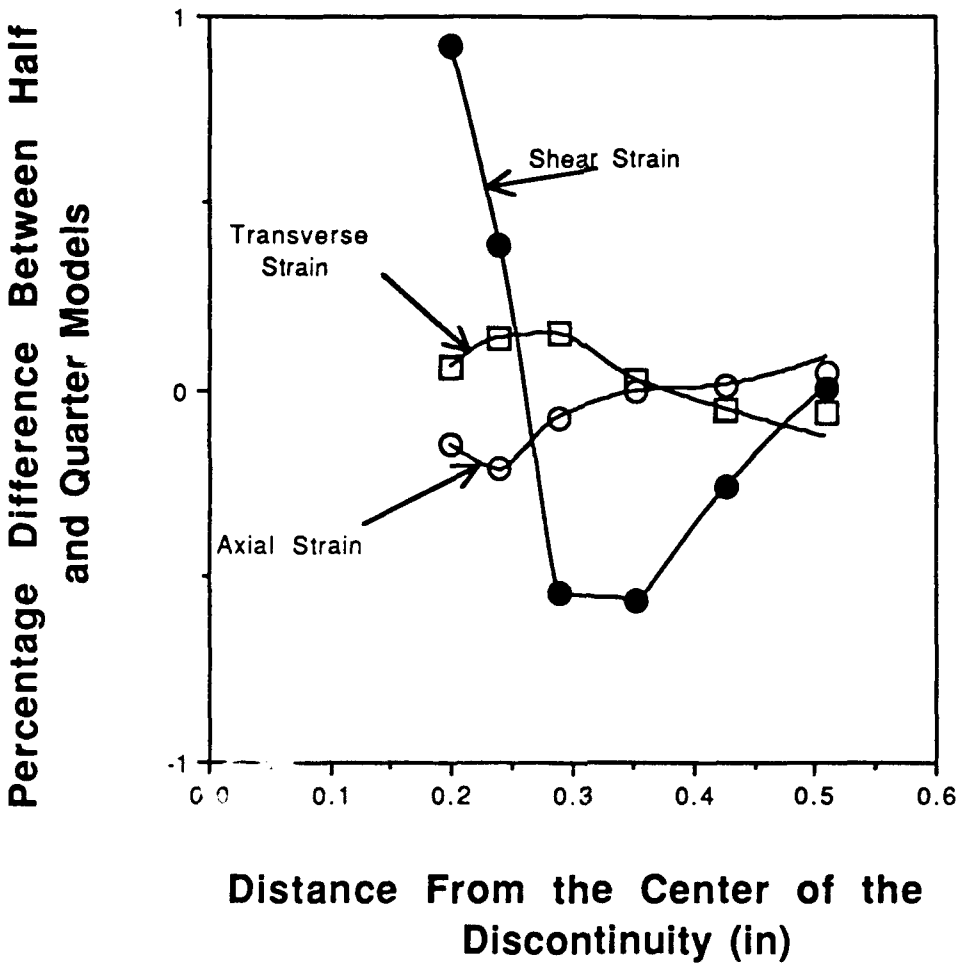

Figure 3-1. Half and Quarter Model Differences

Therefore, we assume that the differences are minimal using our models for determining stresses along the line of symmetry. (Figure 3-2) All other stresses and strains were nearly the same. Figure 3-3 shows the model used herein. This model has 629 nodes and 1284 elements which is about half the nodes and elements of the half model.

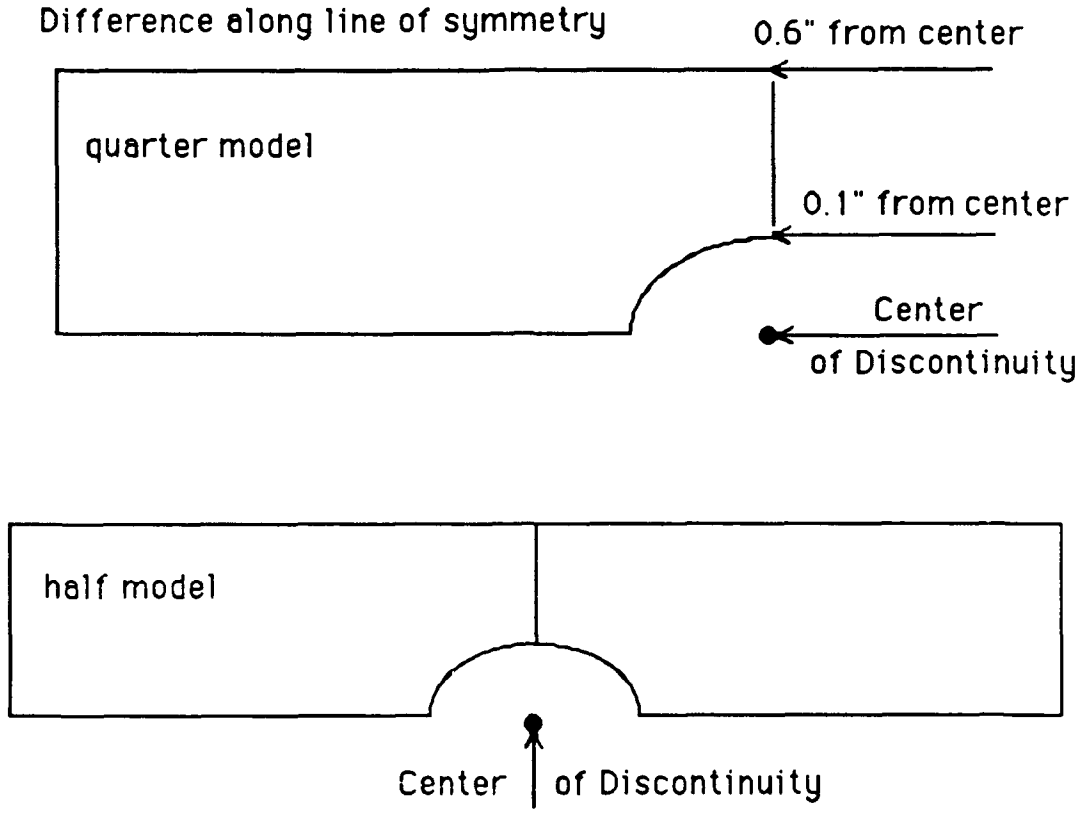

Figure 3-2. Size of half and Quarter Models

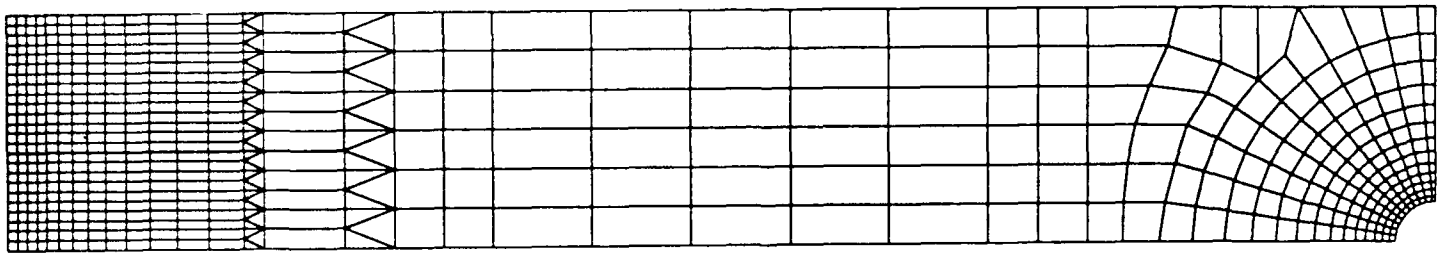

Figure 3-3. Quarter Notched Finite Element Model

The area around the discontinuity was modeled using a program to divide the radius of the notch by a specified number. This was the size of sides of the elements nearest the notch. From there, the elements were expanded very slowly to create a highly refined

model. The minimum size of the elements around the notch is 0.0046" by 0.0046" and were square. The maximum size is 0.5" by 0.1" and has an aspect ratio of five.

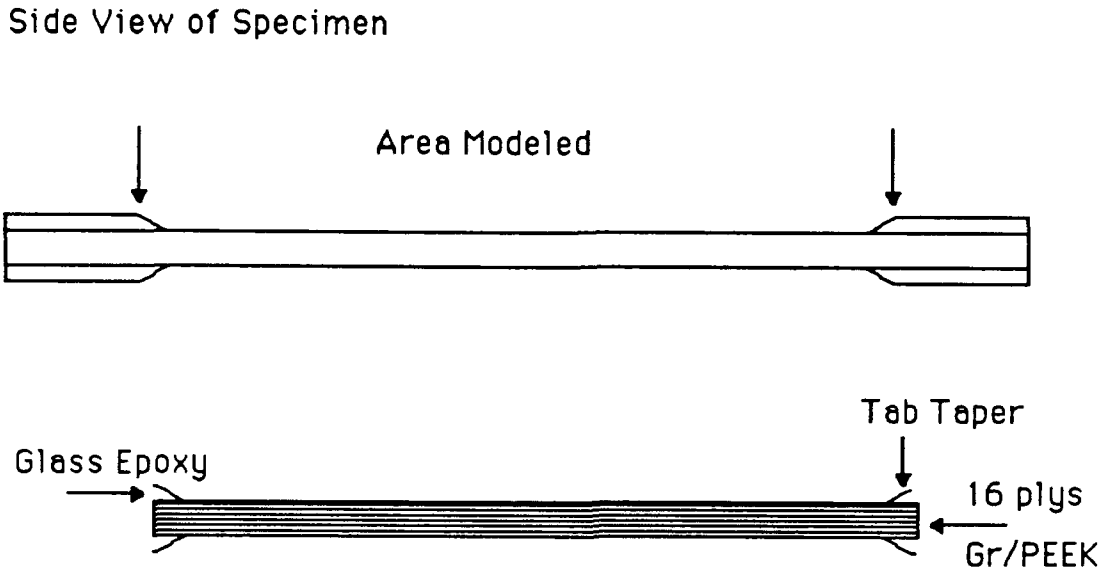

Figure 3-4. Side View of Modeled Region

The actual lay-up of the [±45°]s laminate has 16 plies. This program assumes only two plies. Each ply is 8 times as thick as one actual ply. In other words, instead of modeling 16 .00525" plies, eight .042" plies were modeled.

B. Modeling of the Glass Epoxy Fibers.

As shown in figure 3-4, the taper of the tabs was modeled. The material properties from Capt Martin's thesis were used for the lower strains. However, the cubic spline data was extrapolated up to 40 percent strain. Although Capt Daniels's thesis modeled the entire tab, it was not necessary for this thesis, since the fixture is assumed to remain undeformed and provide load according to the load cell.

C. Convergence Study.

The convergence study was done in the same way as Capt Daniels, and Capt Fisher. These were only quarter models of the specimen, so we needed to do a study. This is done by running the model as an isotropic material using the linear finite element program. From Peterson (17:21-24) and Griffel (10), equation (3-1) is applied.

$$K_t = \frac{\sigma_{max}}{\sigma_{nom}} \qquad (3\text{-}1)$$

K_t = Stress Concentration Factor

σ = load divided by area

Peterson and Griffel both give Kt =3.065 for a circular notch. Using the material properties from Capt Martin, our notched model gives $K_t = 2.915$. The notched model decided on was within 4.89% which was adequate. This is not surprizing since Capt Daniels's model with a hole had a difference of 4.64% and Capt Fisher 4.93%.

For the case without any discontinuity there is no stress concentration or $K_t \approx 1.0$. For the small model (Figure 3-5) the stress concentration varies up to 1.029 or 2.9% error. The large model difference is small enough to not show up on the computer print out.

Part of the reason for the error is that a quarter model was used. A half model would have a better ratio.

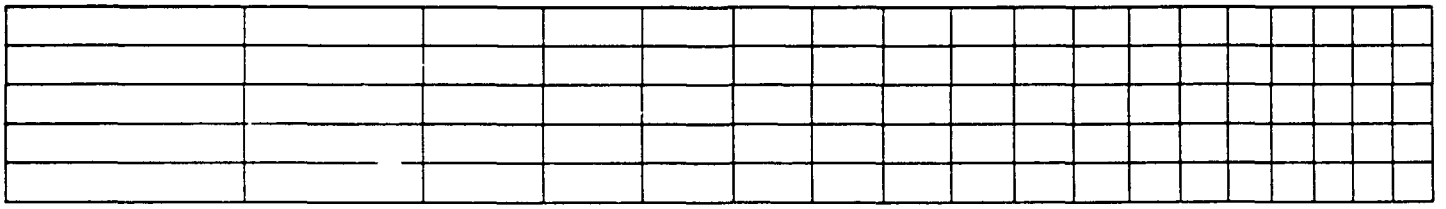

Figure 3-5. Small Quarter Model No Discontinuity

D. Boundary Conditions

The boundary conditions are shown in Figure 3-6. Nodes along the y-axis were fixed in the x direction. Nodes along the x-axis were fixed in the y direction. Nodes along the far side of the x-axis were displaced incrementally. All other nodes were allowed to move freely in either direction.

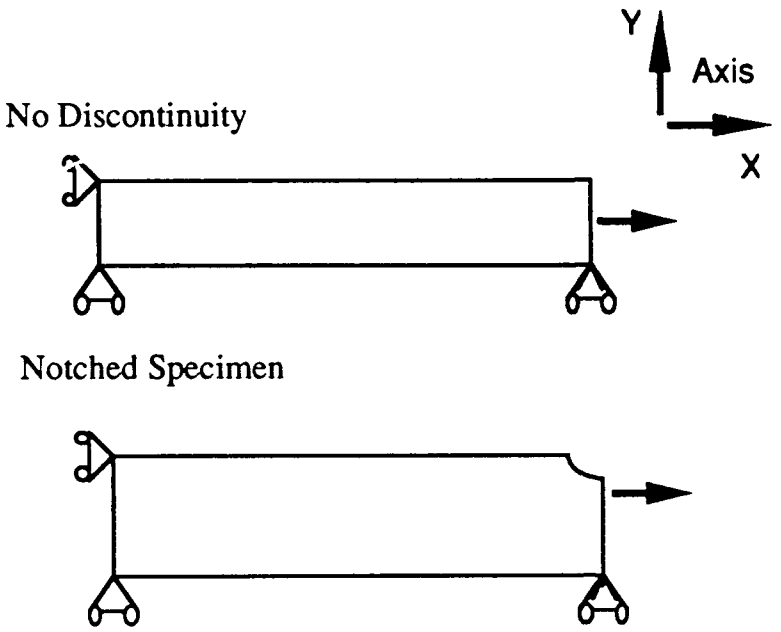

Figure 3-6. Boundary Conditions

This allows for 2 degrees of freedom for the unrestrained nodes.

IV. Experimentation

The purpose of the experimentation in this thesis is to compare the results with the analytical models. Experimentation was conducted at the facilities of the Structures Division, Flight Dynamics Laboratory (FDL), Wright-Patterson AFB, Ohio. Set up is shown in Figure 4-1. The voltmeter was used to show the load at the time the photograph was taken. For Figure 4-1b, take the voltage minus the voltage with no load and divide by two. This gives us 510 lbs applied at the time the photograph was taken. During the testing this number was checked with the value of the load cell and found to be almost identical.

Figure 4-1a. Photograph of Setup

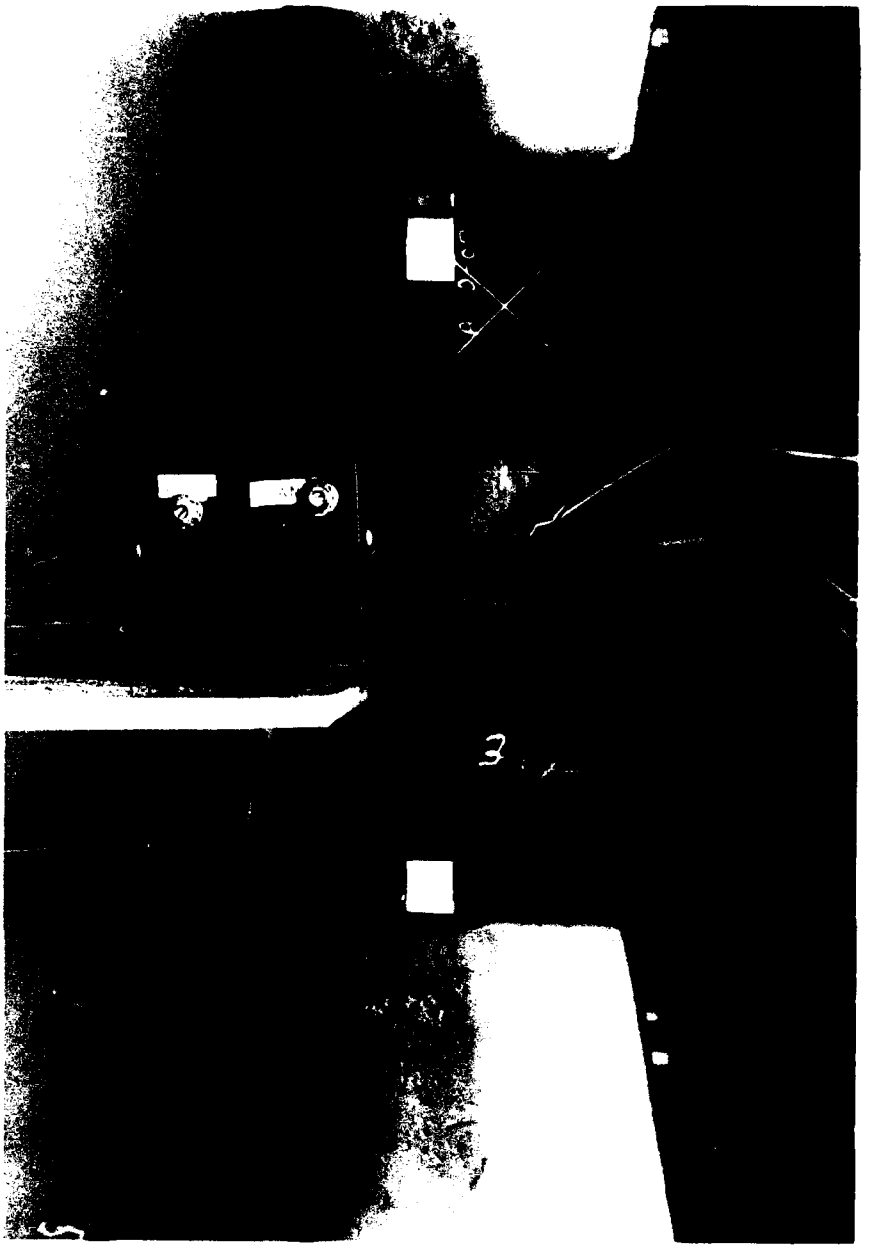

Figure 4-1b. Close-up Photograph of Setup

The voltmeter is used to show the load applied. To calculate the load, subtract the initial voltage, divide by two, and multiply 1000. For figure 4-1b, the load is 510 pounds.

The two models shown in figure 4-2 were tested using seven specimens of each type. High elongation gages were used for all experimentation. Stacked rosettes were not available for high strains,

therefore, rosettes are per figure 4-3. A complete list of materials used is provided in Appendix B

Gages located in center of specimen and 1" from tabs

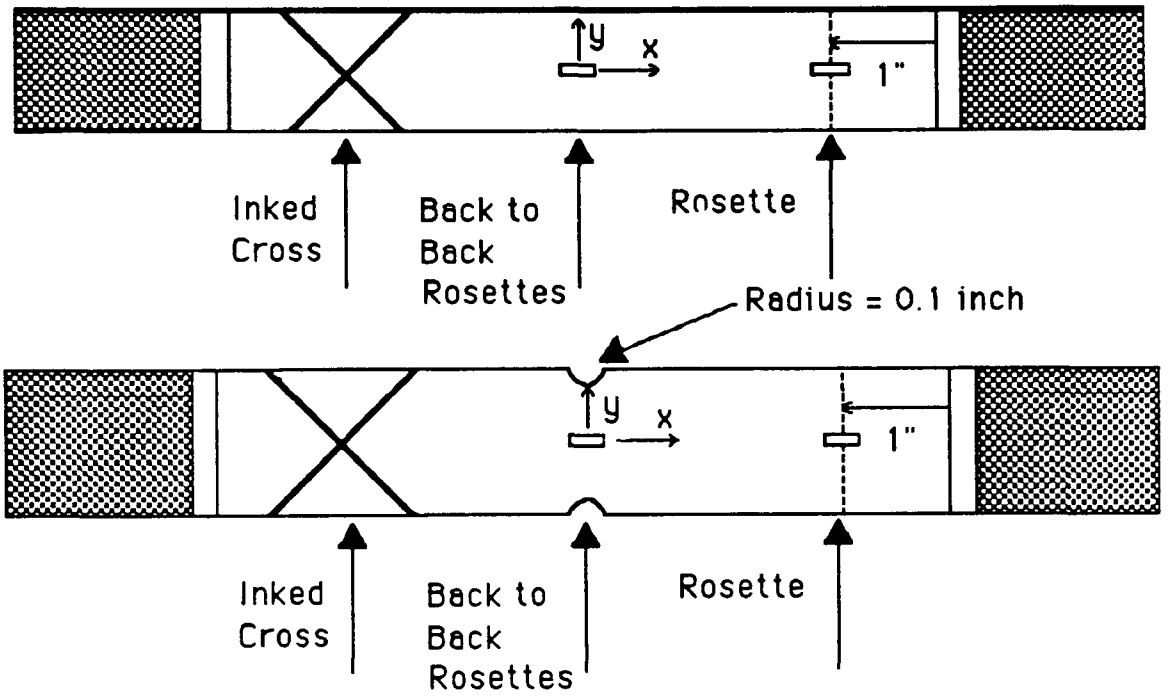

Figure 4-2. Gaged and Crossed Specimens

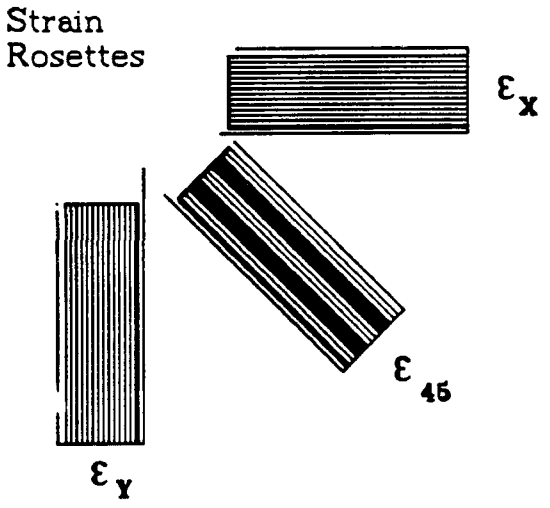

Figure 4-3. Electrix Industries High Elongation Rosettes

The Gr/PEEK panels were manufactured by the Fiberite Corporation, a subsidiary of Imperial Chemical Industries of Great Britain. The production information is described in the data sheets (7). The purchase order is provided in Appendix B. These panels were C-scanned to check for preexisting flaws. None were found. (The C-scan is provided in Appendix B) Only $(\pm 45°)_S$ 16 plies were used.

Table 4-1 Specimen Dimensions

Laminate Type	Ply Lay-up	Size	Ply Thickness
No discontinuity	$(\pm 45)_S$	10" X 1"	16 plies
Notched specimen (.1" radius)	$(\pm 45)_S$	10" X 1.2"	16 plies

After C-scanning the panels were cut into different sizes shown in table 4-1. Tabs were bonded to each specimen to allow the Instron machine to grip the specimen. The tabs were 1/16 inch thick G-10 glass epoxy (0/90 woven) and were bonded to the specimens using an adhesive which required curing in an autoclave.

High elongation strain rosettes (PAHE - 03 - 125RB -350 LEN and PAHE - 03-062RB - 350 LEN) were used. The gages were tested for proper resistances. Several gages were not within the specifications and needed to be replaced. These gages were attached with Micro Measurements M-Bond 610 for high elongation. These are the highest gages and adhesive found for this type of experiment. This

provided us with higher strain data than Fisher. The gages did not fail until almost 30% strain was reached.

Since, the material properties from Martin's experiments were used, no compression testing was done.

Camera work was provided by the Technical Photographic Division (4950TESTW/RMP). Pictures were taken of an "X" placed on the side opposite the strain gage. This showed the change of the 45° ply angle as the load was applied. The pictures were blown up and the angle digitized. Figure 4-7 shows the change in angle as the load was applied for the specimens without discontinuities. This was the average of two groups of photographs taken, one per specimen. Figure 4-8 shows the change in angle for the notched specimen. Only one set of photographs were taken.

A. Test Apparatus.

The Instron machine used to run these tests had a maximum load capacity of 20 kips. It was run at 0.05 inches per minute. Strain gage readings were recorded once every four seconds. This provided plenty of data, since each specimen with no discontinuity took 45-50 minutes to fail and each notched specimen took 20-25 minutes to fail.

A data file was created on the Fight Dynamics Laboratory (FDL) VAX which contained all the gage data, the load data and the time. From this a small program was created to divide the data into smaller sections and into a format readable by Cricket Graph, the graphics program used to make the graphs for this thesis. By sampling only 50-60 points out of 2000-4000 we only missed the small changes provided by the fibers failing at the beginning of the experiment.

Photographs were taken at approximately 2 feet from the specimen. The photographs were only taken of three different specimens. Preliminary photographs were taken on several of the other specimens.

B. Preliminary Results.

Material properties from Capt Martin and Fisher's experiments were valid only to approximately 5 - 10 percent strain. The present experiments provided better data at the higher strains. By using Capt Martin's finite element model data, the program predicts failure at slightly more than .25 inches for a specimen with no discontinuity. Experimentally, however, failure was found at around 2.1 inches. This is due primarily to the data being good only to about 5 percent strain for the gages used by Martin. (Figure 4-4) Since the angles are changing, the shear stress and strain must be updated. The shear data is calculated from equations 4-1 and 4-4. The tabular data is provided in Table 4-2.

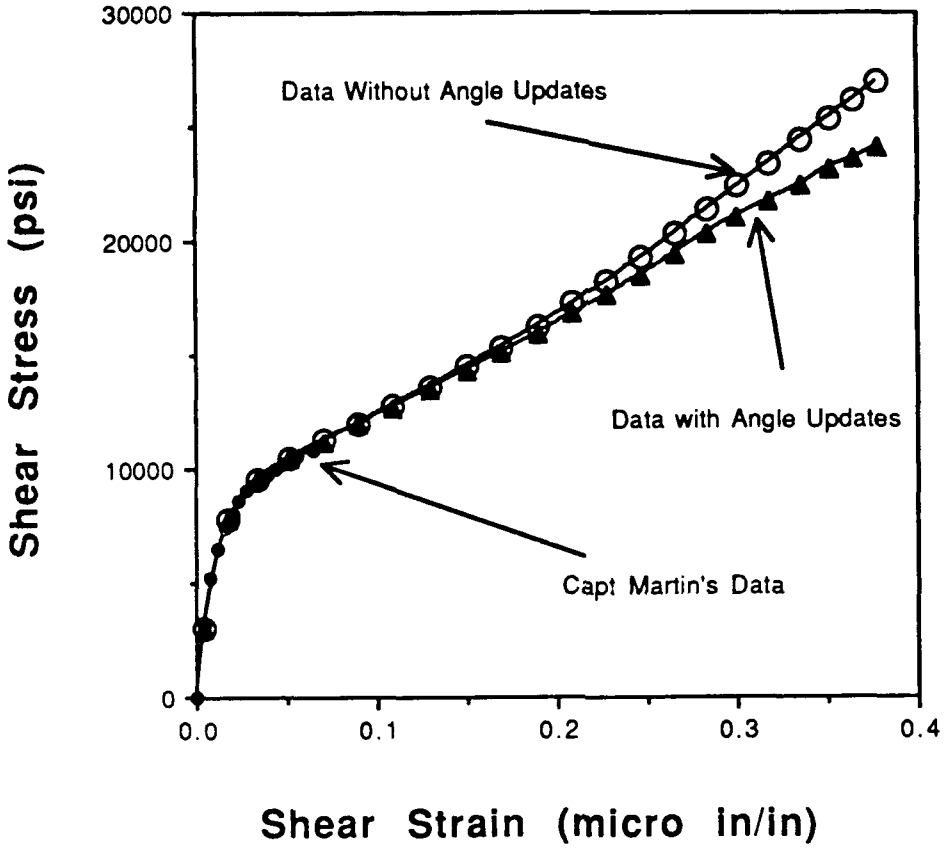

Figure 4-4. Experimental Shear Data Comparisons

The new values for shearing strain were calculated using equation 4-1 and 4-2.

$$\gamma_{12} = 2(\varepsilon_x - \varepsilon_y)\sin\theta\cos\theta \qquad (4\text{-}1)$$

where: ε_x = axial strain

ε_y = transverse strain

θ = fiber orientation (updated throughout program)

This equation comes from using the transformation matrix shown in equation 4-2. These basic equations come from several sources. (5:Section 2.1.2; 1-11) (12:48-51)

$$\begin{Bmatrix} \varepsilon_1 \\ \varepsilon_2 \\ \frac{\gamma_{12}}{2} \end{Bmatrix} = \begin{bmatrix} m^2 & n^2 & -2mn \\ n^2 & m^2 & 2mn \\ nm & -mn & m^2-n^2 \end{bmatrix} \begin{Bmatrix} \varepsilon_x \\ \varepsilon_y \\ \frac{\gamma_{xy}}{2} \end{Bmatrix} \qquad (4\text{-}2)$$

where: $m = \cos\theta$

$n = \sin\theta$

θ = fiber orientation (updated throughout program)

$$\gamma_{12} = 2(\varepsilon_x - \varepsilon_y)\sin\theta\cos\theta + \gamma_{xy}(\cos^2\theta - \sin^2\theta)$$

The shear strain (γ_{xy}) is small because the rosette is located at the line of symmetry. Therefore, equation 4-1 was used. ε_x is given from the C leg of the rosette. ε_y is given from the A leg of the rosette.

The same transformation matrix can be used to calculate shear stress also.

$$\begin{Bmatrix} \sigma_1 \\ \sigma_2 \\ \tau_{12} \end{Bmatrix} = \begin{bmatrix} m^2 & n^2 & -2mn \\ n^2 & m^2 & 2mn \\ nm & -mn & m^2-n^2 \end{bmatrix} \begin{Bmatrix} \sigma_x \\ \sigma_y \\ \tau_{xy} \end{Bmatrix} \qquad (4\text{-}3)$$

where: $m = \cos\theta$

$n = \sin\theta$

$\sigma_y = 0$

$\sigma_x = \frac{P}{b\,d}$

Assuming τ_{xy} is small, equation 4-4 results. This thesis does not look at changes to the width or thickness

$$\tau_{12} = \frac{P}{b\,d}\cos\theta\,\sin\theta \qquad (4\text{-}4)$$

P = load at end of specimen (lbs)

b = width of specimen (1.0")

d = thickness of specimen (.084")

θ = fiber orientation (degrees)

The angle was calculated using the cross on the specimen. (Figure 4-5) The cross was placed one inch from the tab, the same location as the strain gage, only on the other end.

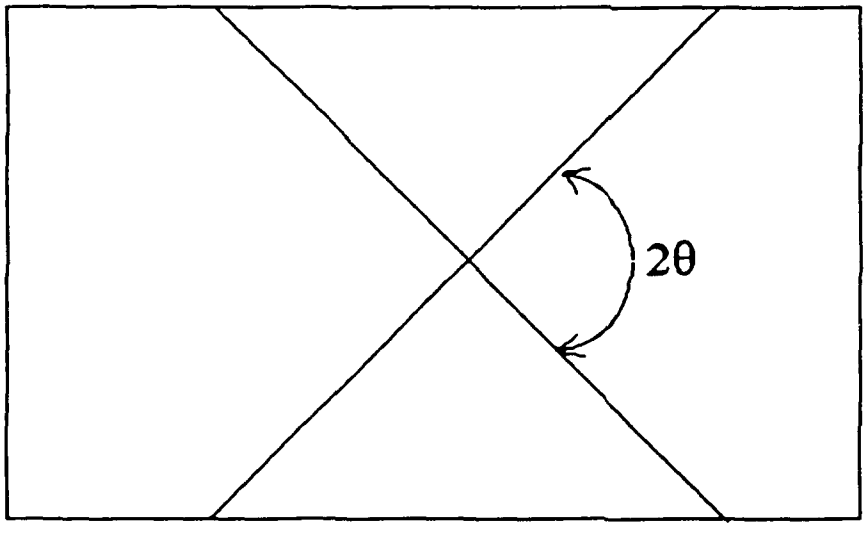

Figure 4-5. Angle Calculation from Cross on Specimen Displacement

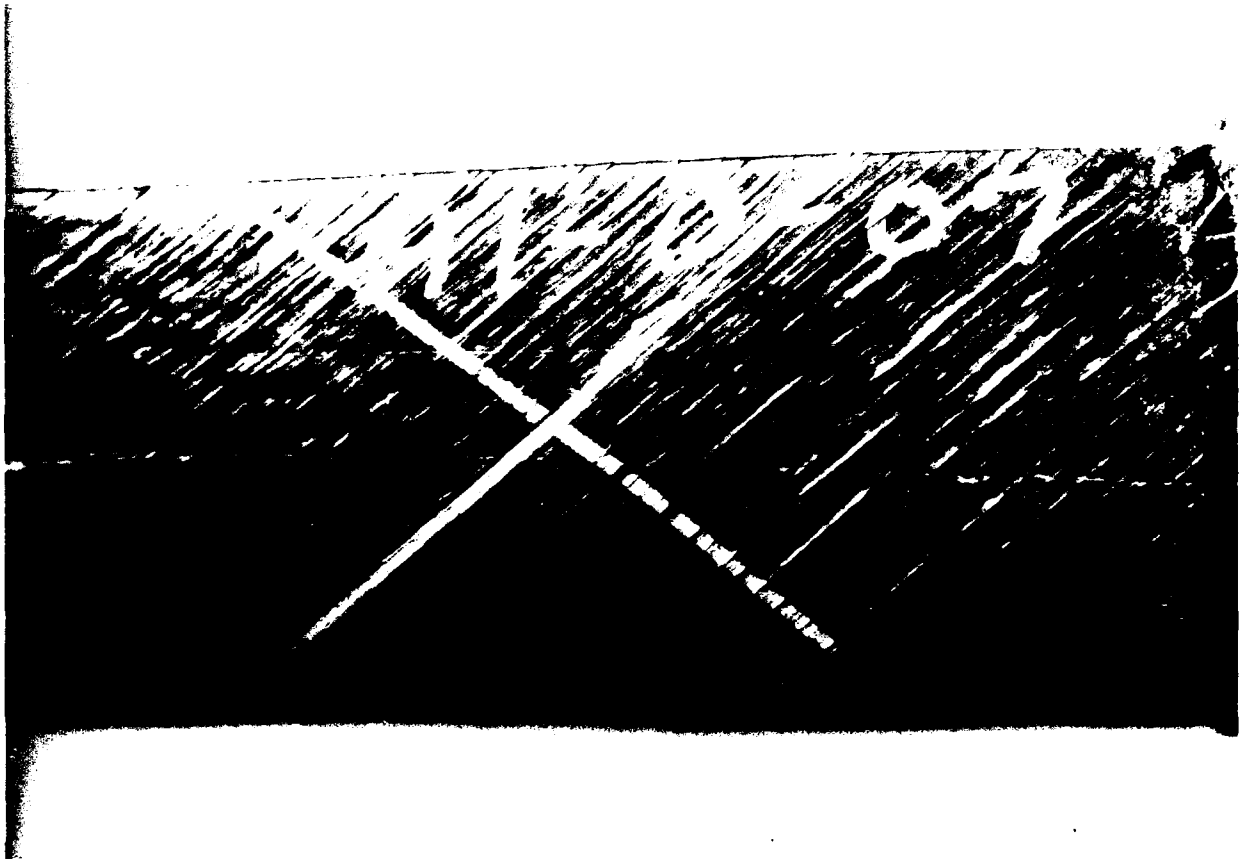

Figure 4-6. Photograph of Cross on Specimen

Table 4-2 Shear Data

Shear Strain	Shear Stress
0.000	0.0
0.005	2986.0
0.018	7743.0
0.034	9552.0
0.051	10420.0
0.070	11205.0
0.108	12730.0
0.129	13517.0

0.170	15146.0
0.209	16831.0
0.248	18530.0
0.283	20339.0
0.318	21724.0
0.351	23186.0
0.378	24690.0

The assumptions used by Fisher "...fibers retain their ±45 orientation." (8,4-7) This was admittedly a bad assumption, but, at low strain rates the error introduced was small. Obviously, this is not a good assumption for our tests. From the photographs, one can see that the angle change is significant. (Figure 4-7) The angle change for the notched specimen follows a similar pattern. (Figure 4-8) The increased load prior to fiber change is due to the wider specimen.

Angle changes for the notched specimen showed a similar pattern. It can be seen that the angles show little change before two thousand pounds are applied.

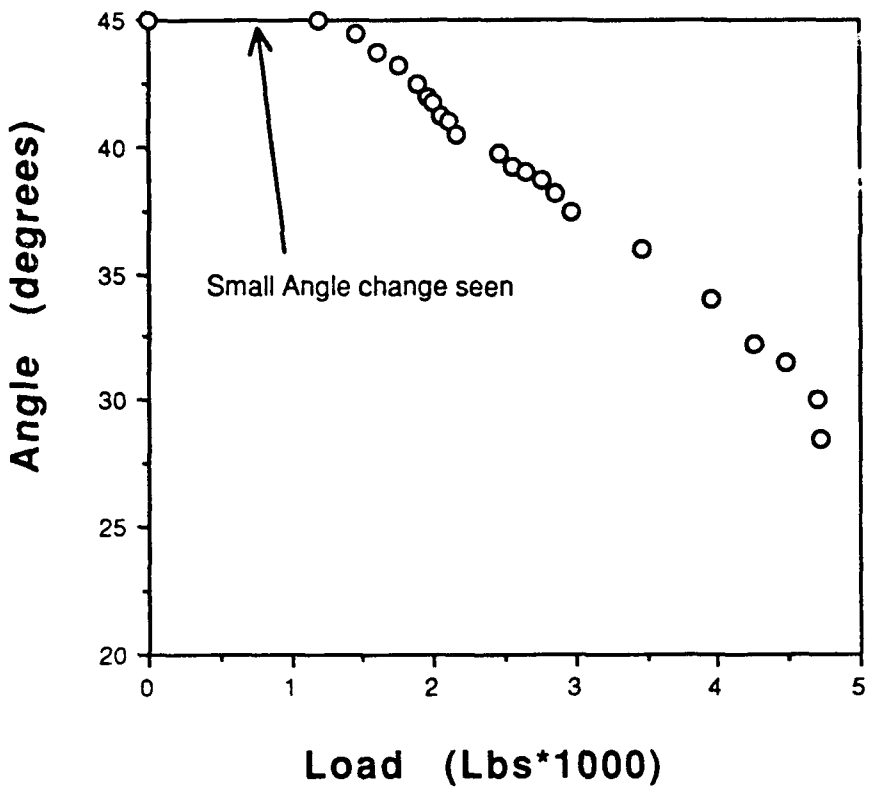

Figure 4-7. Angle Changes in Model without Discontinuity

C. Problems During Testing

One problem encountered was the strain gages. At first the strain gages saturated at 10 percent strain. The gages saturated because of the amount of current applied. This problem was solved by reducing the "gain factor" to 20. The gain factor is described in detail by a gage manufacturer (14). By reducing the gain factor one reduces the amount of current flowing through the gage. When the current gets to a certain level the gage saturates. This reduced the accuracy of the readings but allowed us to get reading beyond 10 percent strain. (Figure 4-2) The gages also peeled off the specimen at high strains.

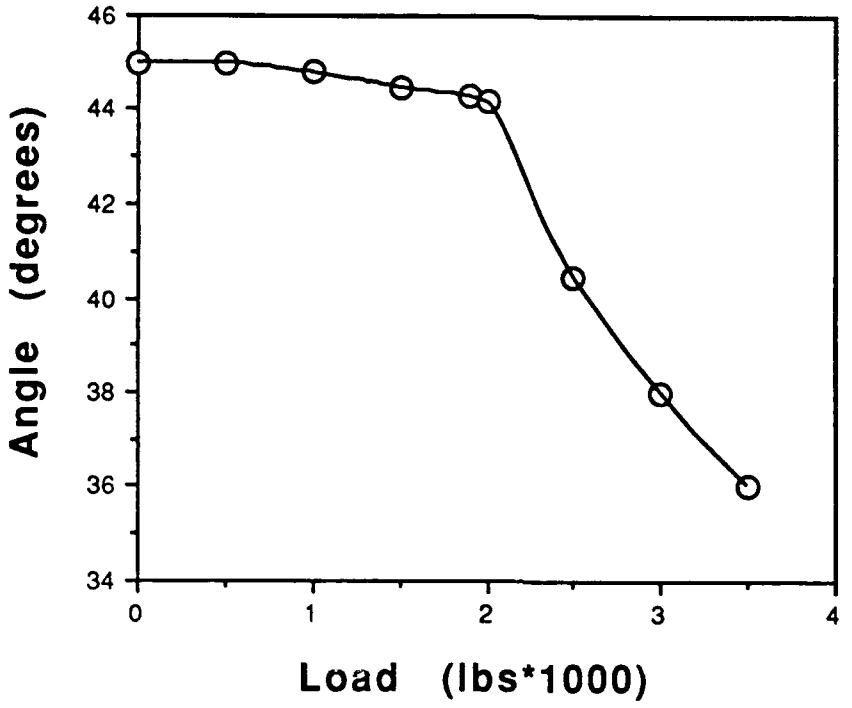

Figure 4-8. Angle Changes in Model with Notch

This problem was solved by running the experiments as soon as possible after the gages had been mounted. In addition, the leads were soldered directly to the specimen. The gages pulled off primarily because of the differences in axial and transverse strain at the location of the gages.

The tab material debonded (Figure 4-9). This is caused by the high stress concentrations at the corners. This was also experienced by the other three theses. During the high levels of strain it is more evident. This debonding begins at approximately 5 percent strain. The only way to alleviate this problem would have been to increase the length of the specimen. Since the plates were already manufactured and cut, this was not a possibility.

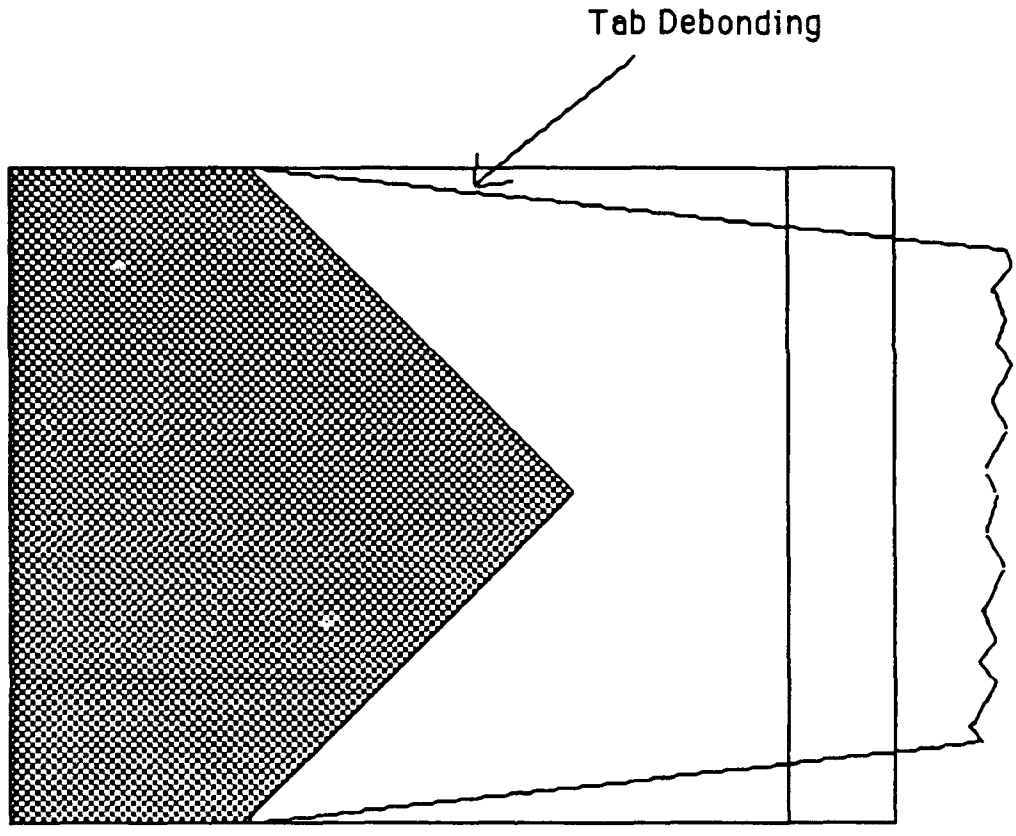

Figure 4-9. Sketch of Debonding

A stress/strain graph is shown in Figure 4-10. This graph shows the high rates from the gages without failure. This data is taken from the average of the two central gages for the last two specimens.

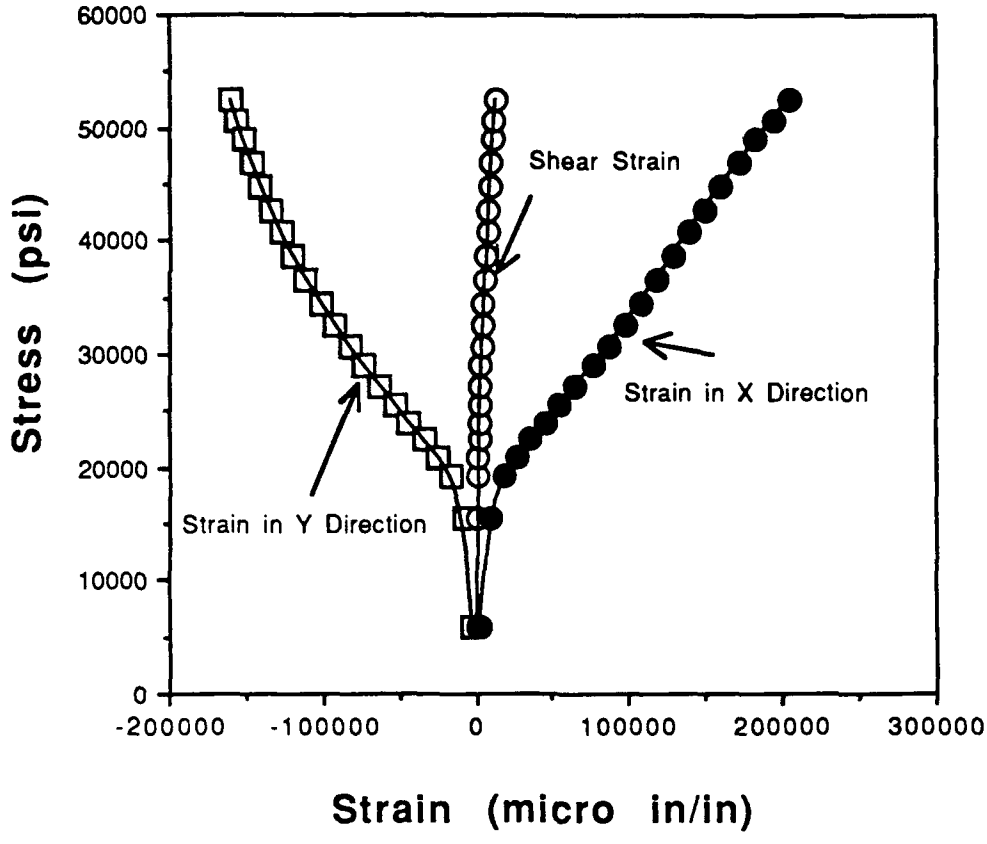

Figure 4-10. Stress vs Strain: No Discontinuity

V. Results and Discussion

This chapter will compare both the experimental data and the analytical data. This is done in two steps; comparison of experimentation to analytical data and comparison of linear to nonlinear programs.

A. Load, Displacement Comparison

First of all, plotting the standard load vs displacement curve shows that our model is reasonably accurate. Figure 5-1 shows the load versus displacement curve. This is the average of seven tests done on specimens with no discontinuity. As shown is section IV, the angle change is only necessary at high displacements. The experimental data was taken directly off the extensometer and the load cell. (Figure 5-1) For the analytical models we used an average of σ_x along the edge in equation 5-1.

$$P = \sigma_x \, b \, d \qquad (5\text{-}1)$$

P = load at end of specimen (lbs)

b = width of specimen (1.0")

d = thickness of specimen (0.084")

The displacements and loads were taken from the models shown in Figure 5-2. Because this is a quarter model we must multiply displacements at the edge by two. The nonlinear programs are run at displacement increments of .01". For the linear program the displacement is specified at the start of the program and run at different displacements.

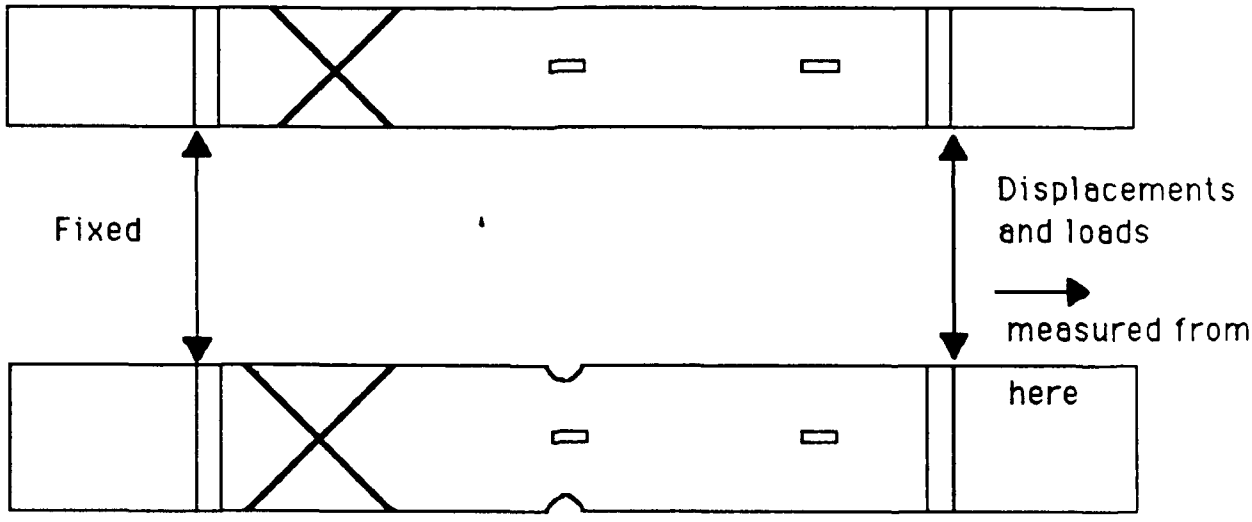

Figure 5-1. Experimental Displacement

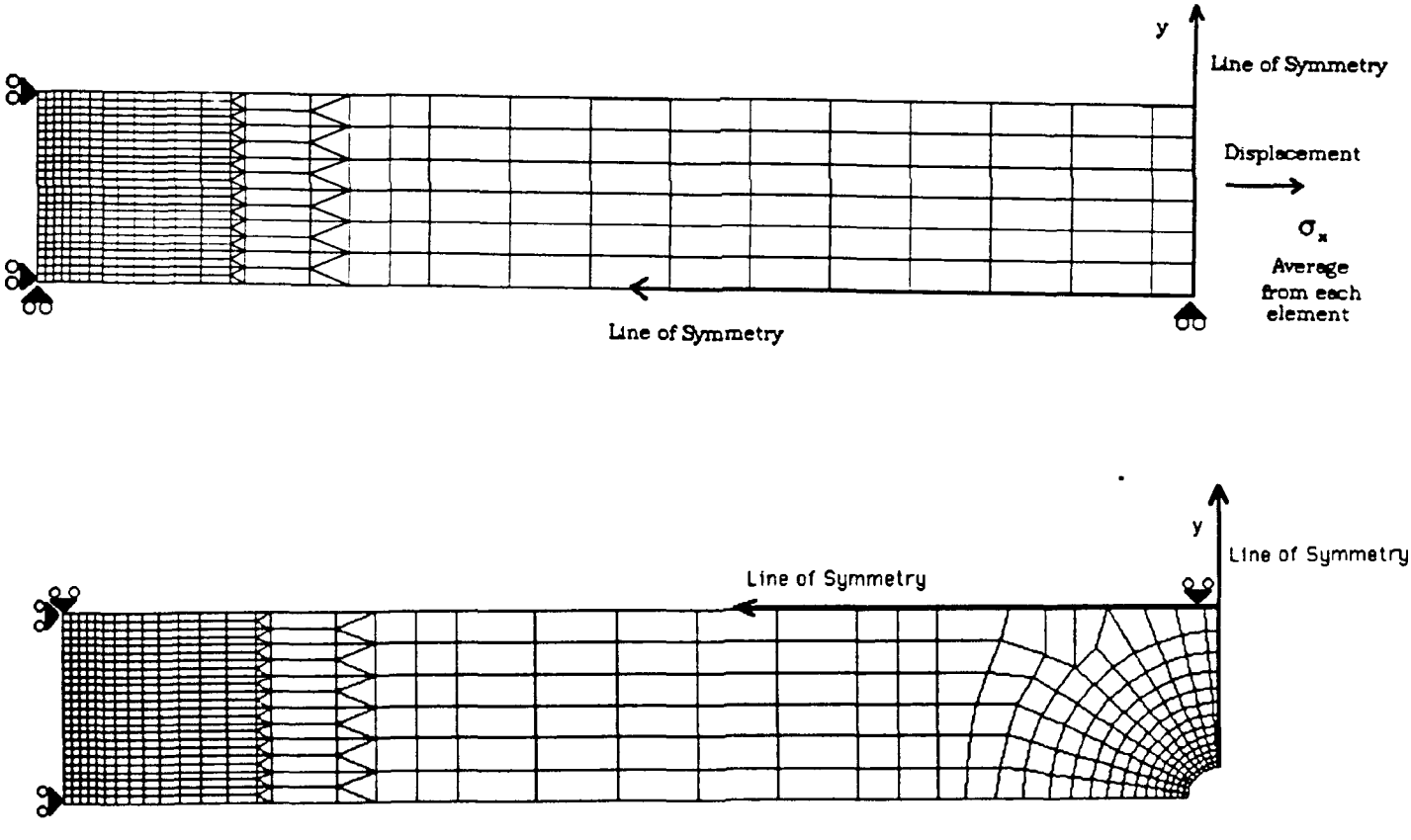

Figure 5-2. Analytical Displacements and Loads

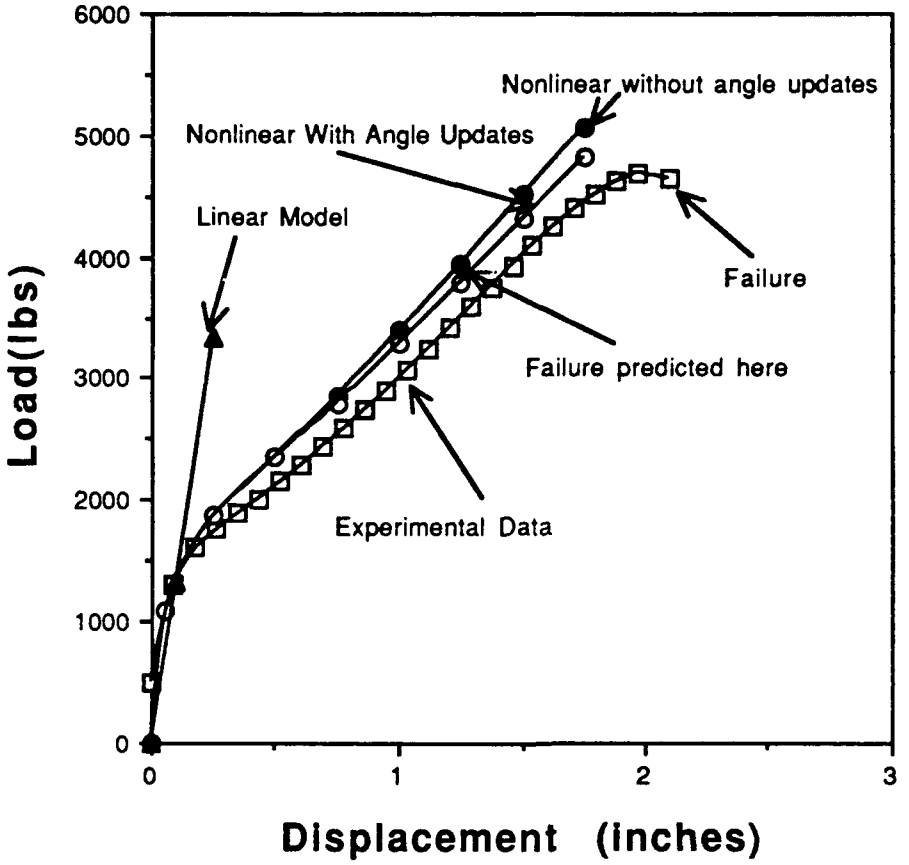

Figure 5-3. Load vs Displacement Curve for No Discontinuity.

From Figure 5-3, the updated model follows the experimental data most closely. The nonlinear model predicted failure at approximately 1.4 inches. Actual failure took place from 2.081 to 2.114 inches. This varied only slightly, compared to the load at failure. The load varied between approximately 3600 to 4600 (It was impossible to get an exact reading at failure because samples were only taken every 4 seconds). All the curves were approximately the same shape. The standard deviation for load is 356 lbs. For displacement the standard deviation is 0.012 inches.

The failure occurred at so much lower displacement because Capt Martin's data was cut off at about 5.6 percent strain. The computer assumed that at the end of the data failure had occurred.

Even with removing the failure criteria from the program, it would not run past 1.4 inches. It was only by extrapolating the data and removing the failure criteria from the curves were we able to get the results shown. To get a better result the Gr/PEEK should be tested for material properties up to failure (30% strain) and then used in the program.

The model does closely follows the curve. The difference is probably due to the change in material properties from our specimens to Capt Martin's specimens. In addition, the finite element model is naturally going to be stiffer than the experimental data. This is because one cannot have an infinite number of elements. Even within our own specimens, there is a variance between the load displacement curves.

Plotting the same curve using the notched specimen (Figure 5-4), failure is predicted even earlier. This is caused by the increase in stresses at the point of failure. Otherwise, the curve itself is a very close approximation to the experimental data.

This is also the average of seven specimens this time slightly wider (1.125 ") with .1" radius notches on both sides of the specimen. Displacements and loads are measured per Figure 5-1 for the experimental results and Figure 5-2 for the analytical results.

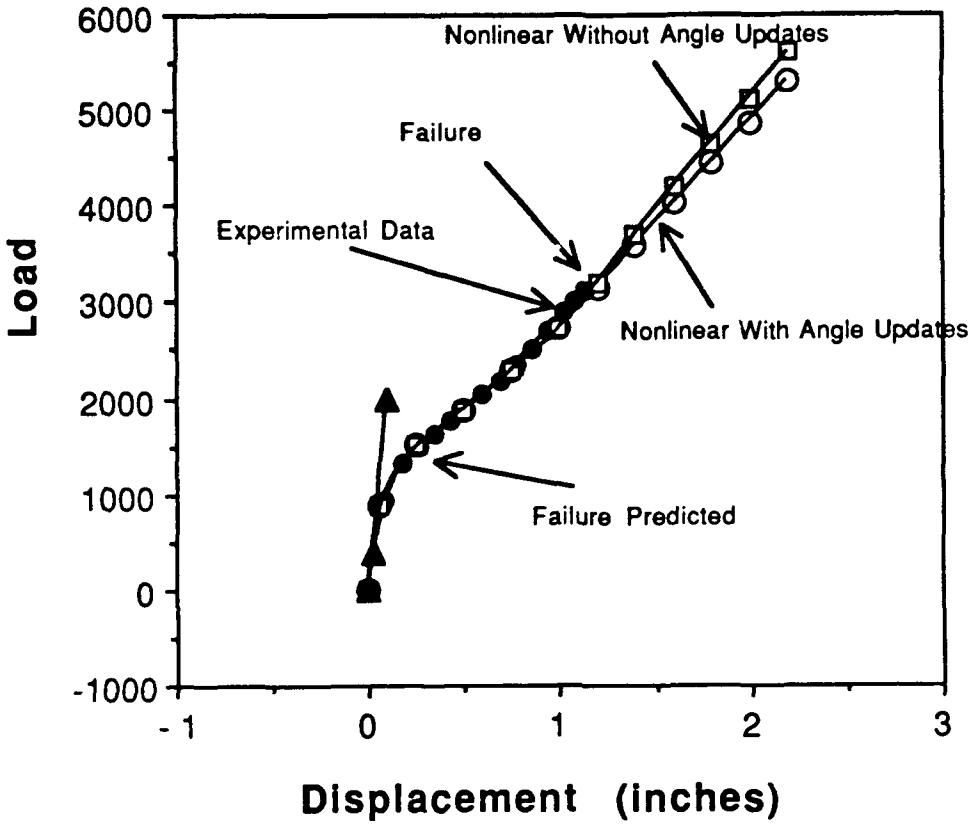

Figure 5-4. Load Displacement Curve for Notched Specimen

Updating the coordinates is necessary at even small displacements. This difference is caused by the increased stress from not allowing the elements to displace. This is only slightly better than the linear program above .02" or 1500 lbs. This is shown in figure 5-5.

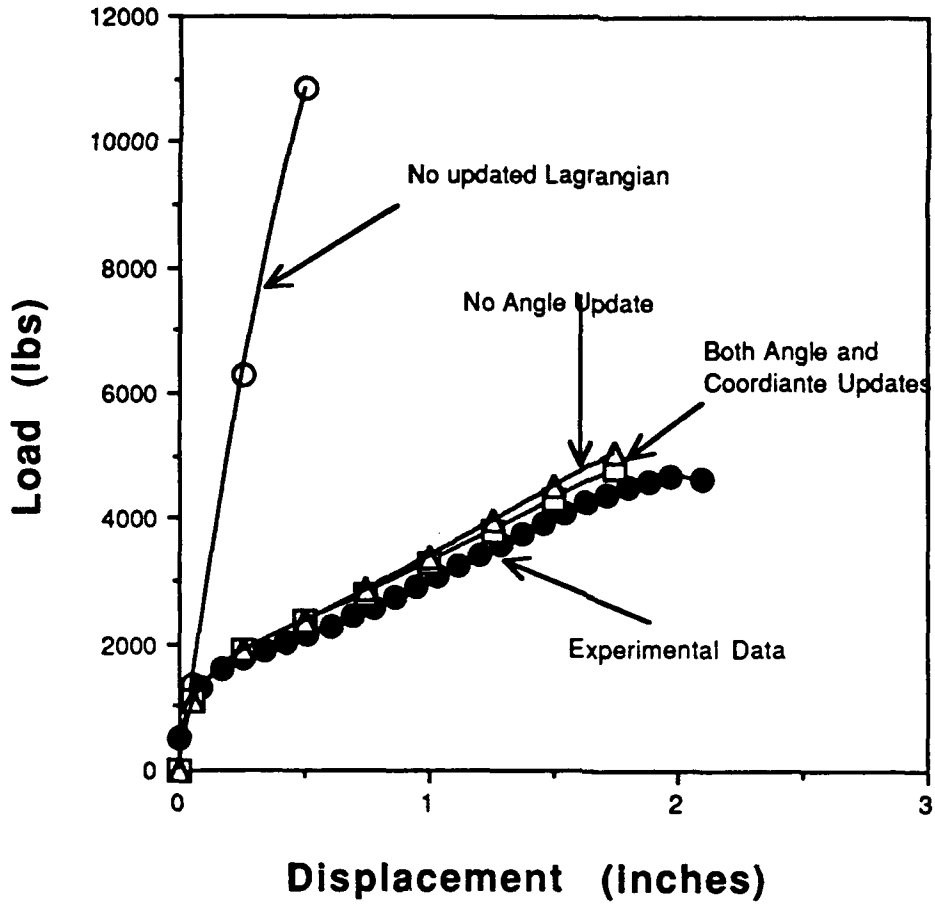

Figure 5-5. Load Displacement Curves including no updating of Coordinates for the specimen without a discontinuity

Another problem with the larger model is the use of triangular elements at the point of stress concentration. This could be part of the problem with the failure criteria. As the model displaces the finite element model also displaces. Therefore a smaller model was used to show the points of failure. This model is discussed in Chapter 3 as part of the convergence study.

B. Failure Comparison

From Figure 5-6a-d, the failure point is at approximately 1.5 inches from the tab. Figure 5-6b shows two failed specimens and two

prior to testing. Although there is a wide variance of ± 1 inch, this is approximately where the specimen fails experimentally. The nonlinear model predicted constant displacement along the edge. This is an obvious improvement in the linear model. The nonlinear model also predicted failure as shown.

Figure 5-6a. Photograph of Failure of Plain Specimen

Figure 5-6b. Comparison of Specimens

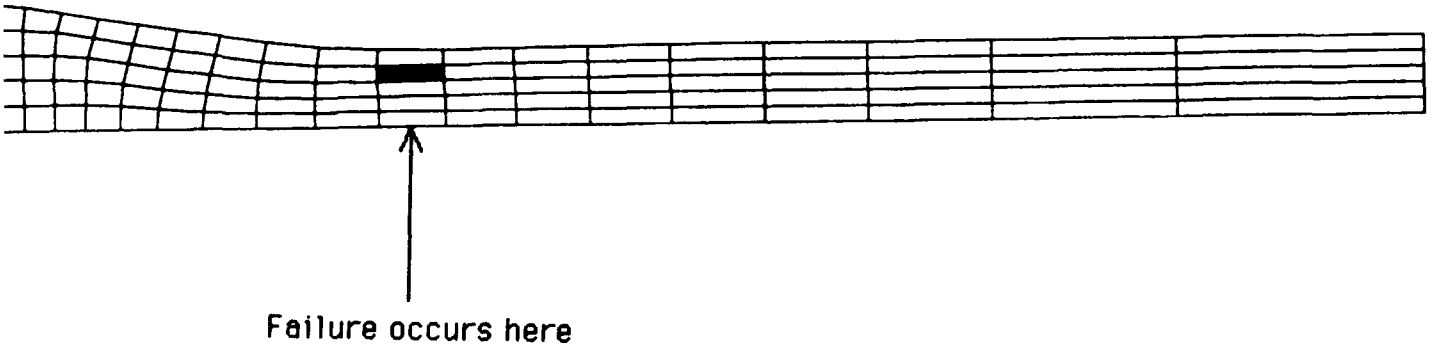

Figure 5-6c. Finite Element Failure (Small Model)

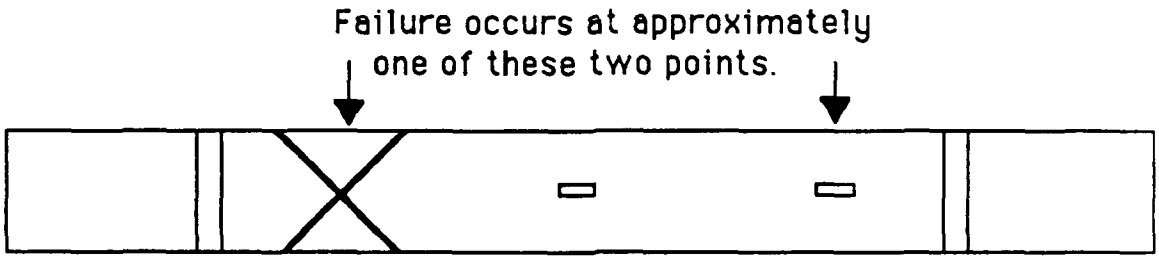

Figure 5-6d. Experimental Failures

From the Notched specimen, failure is predicted at slightly off the center line (Figure 5-7a). This is predicted by the nonlinear model (Figure 5-7b).

Figure 5-7a. Photograph of failure of Notched Specimen

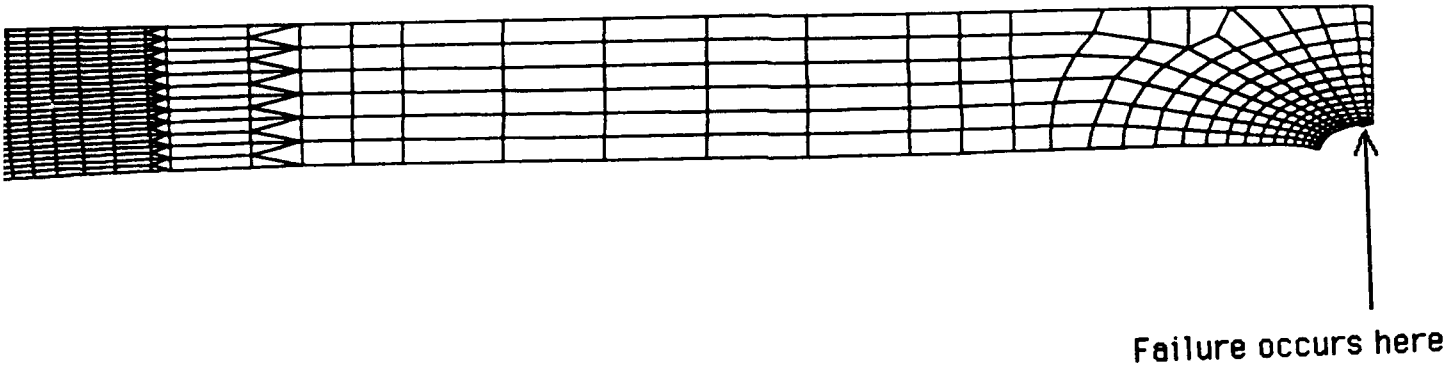

Figure 5-7b Displacement at failure of Notched Model

C. Displacement, Strain Comparisons

Figure 5-8 shows the difference between the strain (ε_x) in the x direction and the overall displacement. Both sets of data came directly off of the computer printouts. Examples of the printouts are shown in Appendices 1 and 3.

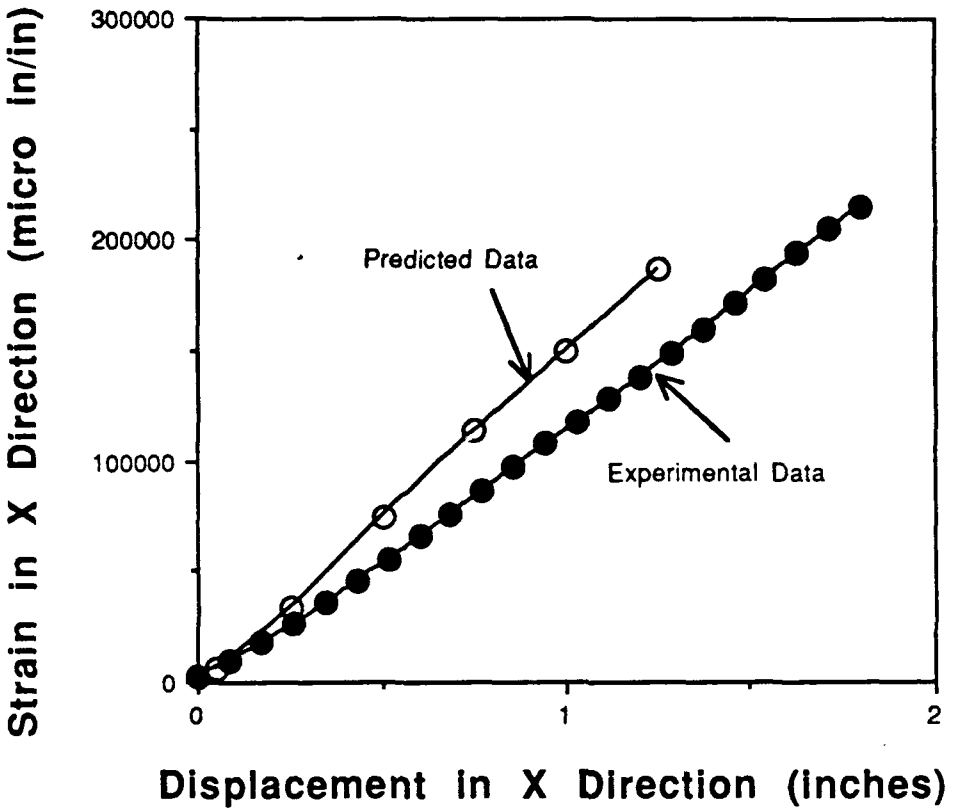

Figure 5-8. ε_x vs Displacement: No Discontinuity (Data as shown in figure 5-12)

Figure 5-9 is a graph shows the difference between the strain (ε_y) in the y direction and the overall displacement. This data also comes off the computer runs. One reason for the differences in strain for the predicted data could be the debonding discussed earlier in this section. This would account for the higher predicted stain in the x direction and the lesser strain in the y direction. Figure 5-10 and Figure 5-11 show much less differences. From the experiments we see much less debonding in the notched specimen.

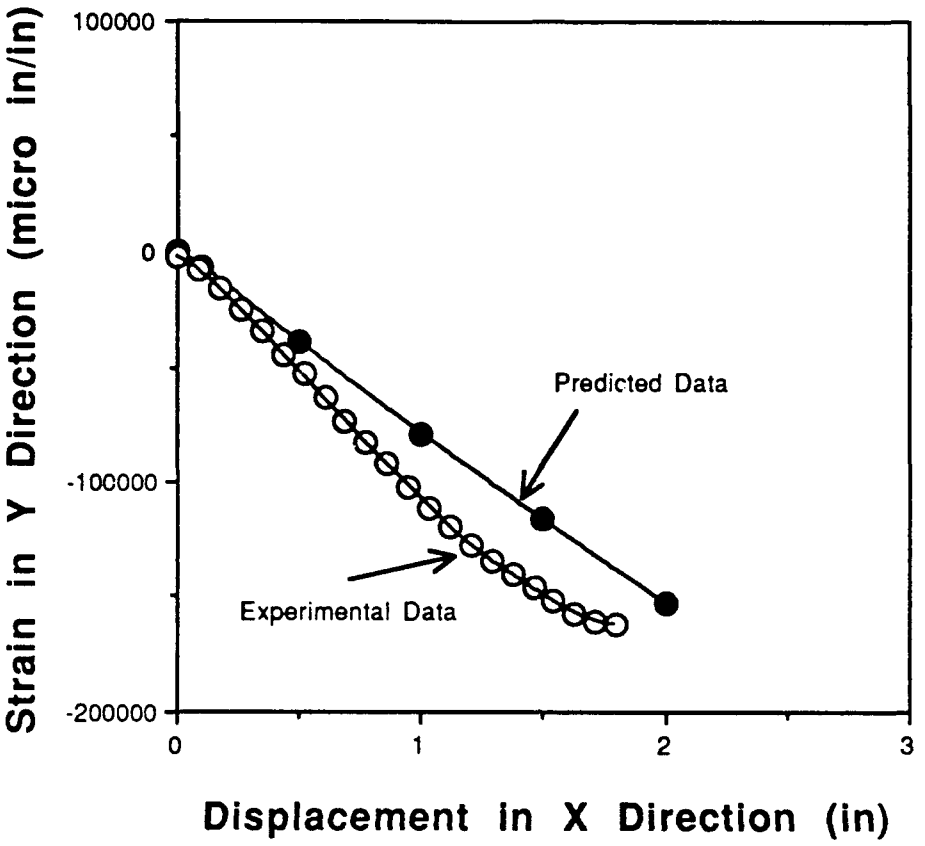

Figure 5-9. ε_y vs Displacement: No Discontinuity (Data as shown in figure 5-12)

Figures 5-10 and 5-11 show the same data as Figures 5-8 and 5-9 for the notched specimens.

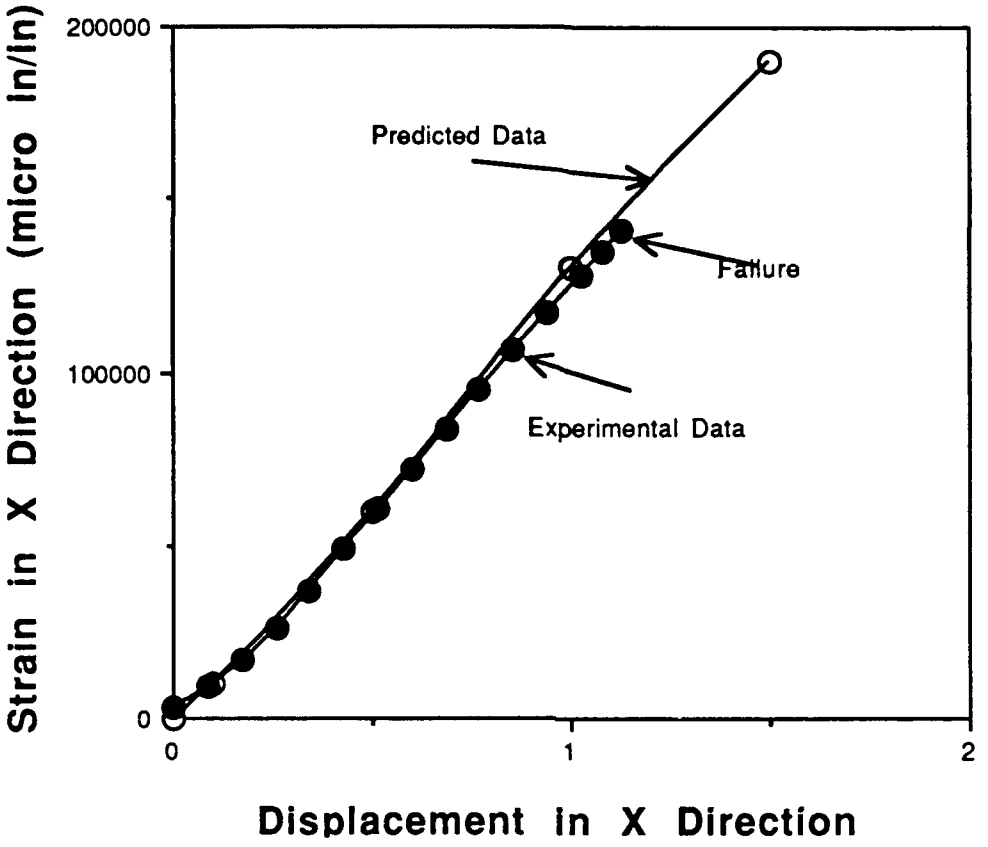

Figure 5-10. ε_X vs Displacement: Notched Specimen

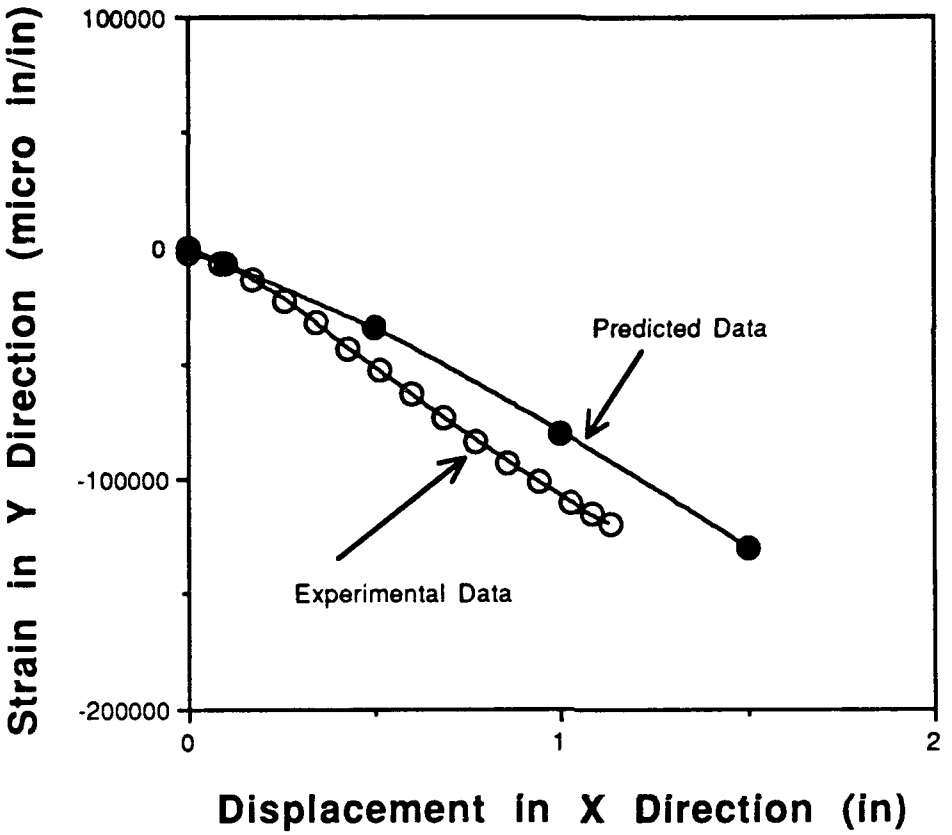

Figure 5-11. ε_y vs Displacement: Notched Specimen

D. Strain, Stress Position Comparisons

All graphs in this section are comparing stresses and strains at a point 1 inch from the tab (Figure 5-12).

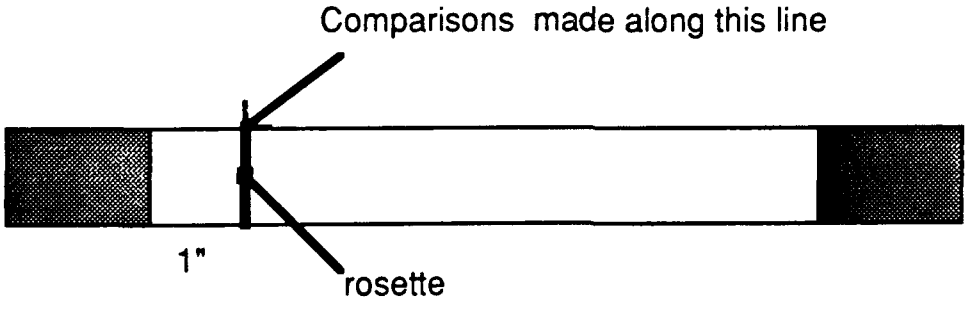

Figure 5-12. Line of Comparison for Analytical Models

From Figure 5-13 the linear model is beginning to fall apart. This is due to the nonlinearity of the geometry at 0.5" displacement.

The nonlinear program shows a smooth curve across the specimen. The contour plotting also shows this.

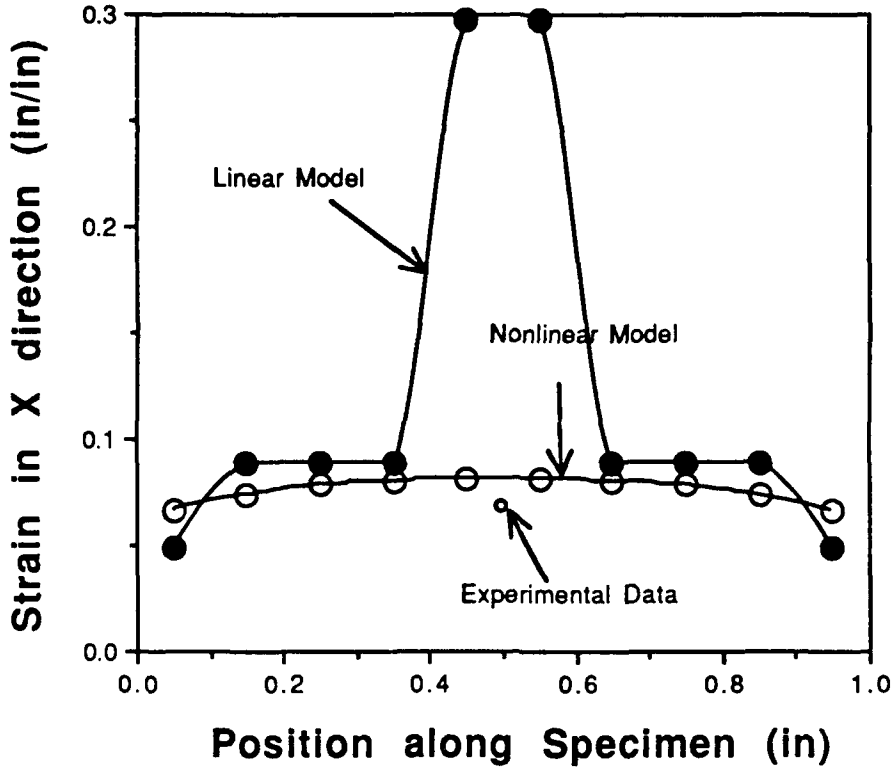

Figure 5-13. ε_x vs Position 1" from tab for 0.5" Total Displacement

Figure 5-14 also shows the problems with the linear models.

Figure 5-15 shows how the shear strain goes to zero at the line of symmetry and at the edges af the specimen. This is as expected per Figure 4-10 we see that shear strain is near zero at the center line. Figure 5-16 shows that shear strain does not go to zero in the linear model. Therefore, the nonlinear program provides far better data. This appears to be true for all properties.

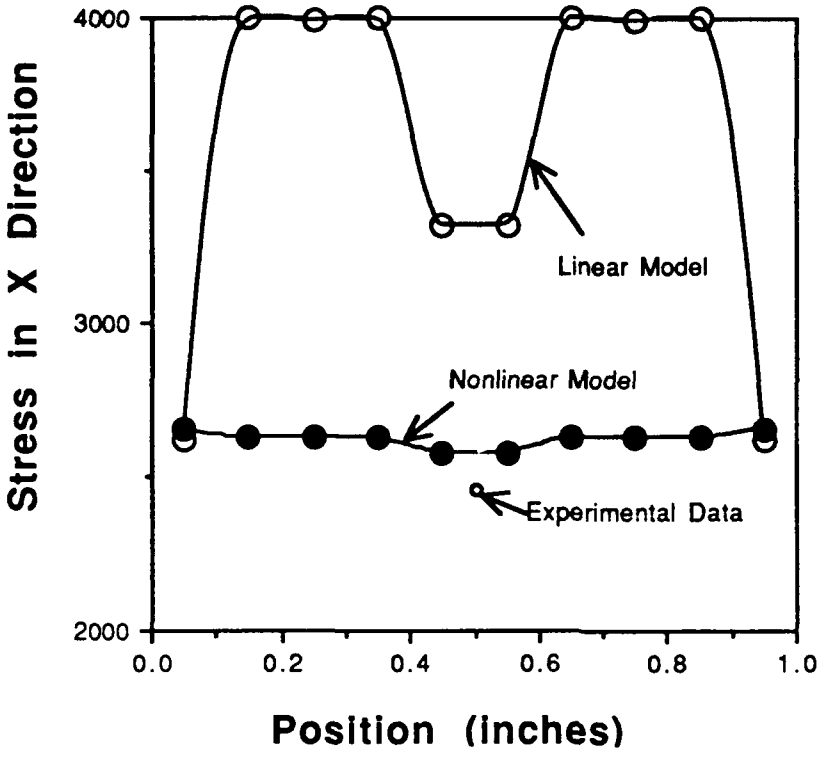

Figure 5-14. σ_x vs Position 0.5" Total Displacement

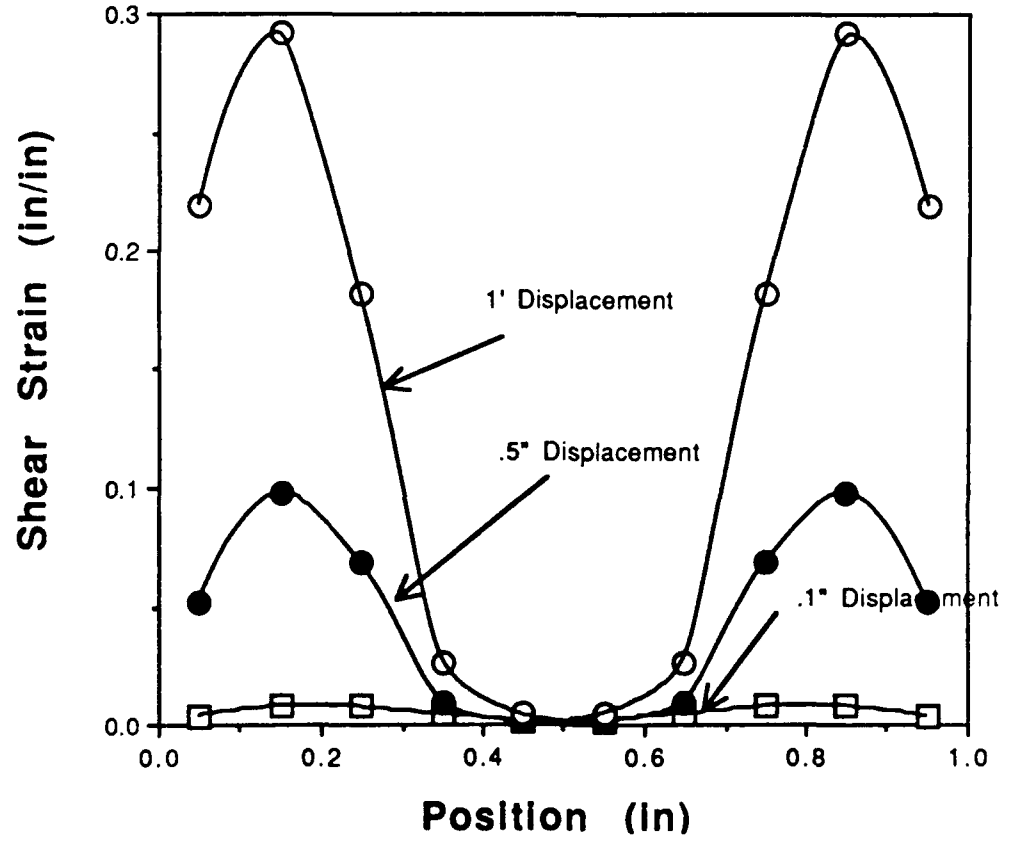

Figure 5-15. γ_{xy} vs Position at 0.1",0.5" and 1" Displacements

E. Contour Plotting

Contour plotting is done using a program written by Dr. Sandhu to show how stresses and strains are varying with respect to position. The stresses do not vary per ply due to the ±45° lay-up. This is very useful in comparing the different types of nonlinear programs. Figures 5-17a-d shows that with the fiber orientation updates there is a smoother transition across the specimen. Figures 5-17a-b are at a displacement of 1.5". Figures 5-17c-d are at a displacement of 2.5" These also indicate a smoother curve.

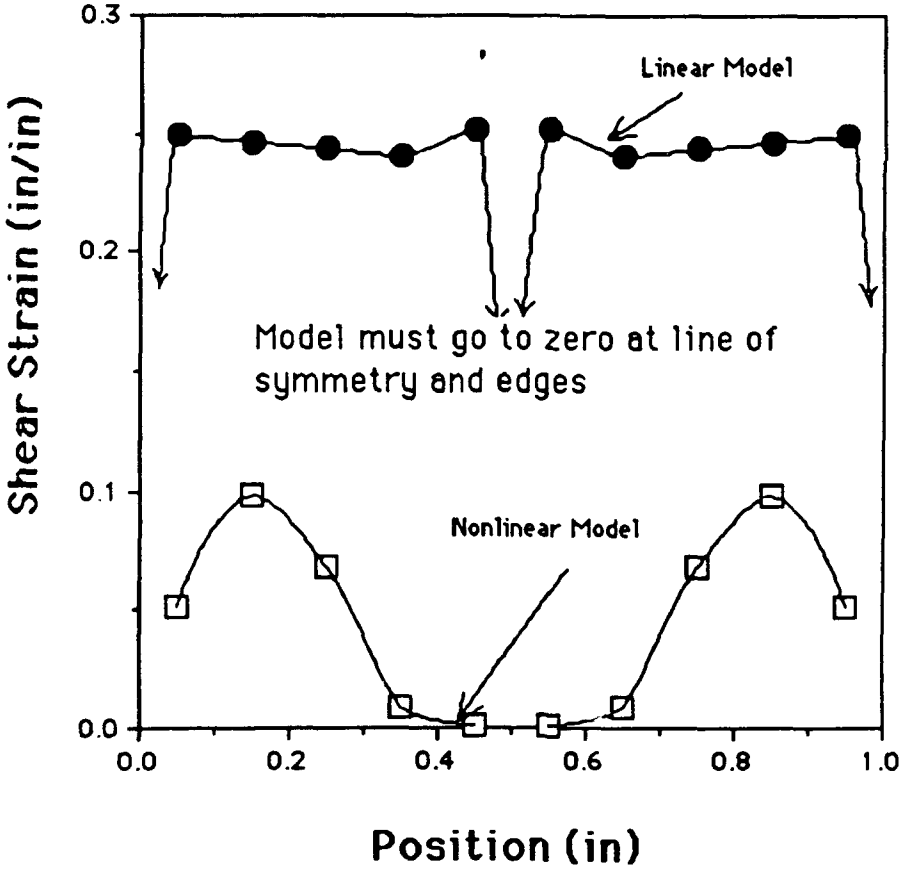

Figure 5-16. γ_{xy} vs Position at 0.5" Displacement

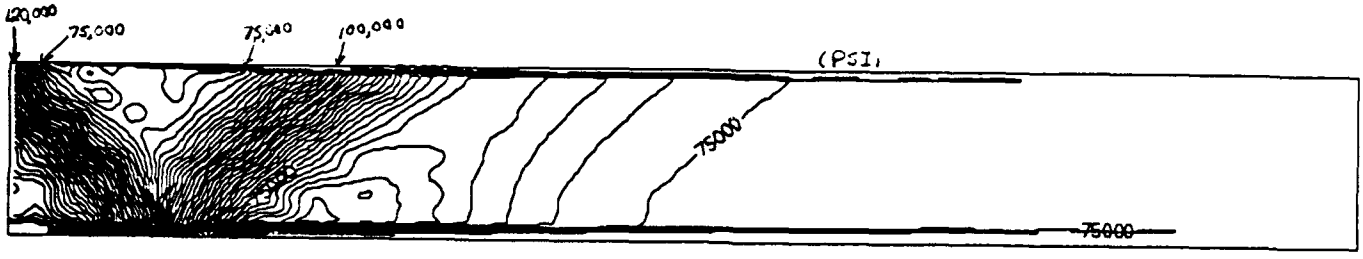

Figure 5-17a. σ_x for Nonlinear Program with Angle Updates(1.5")

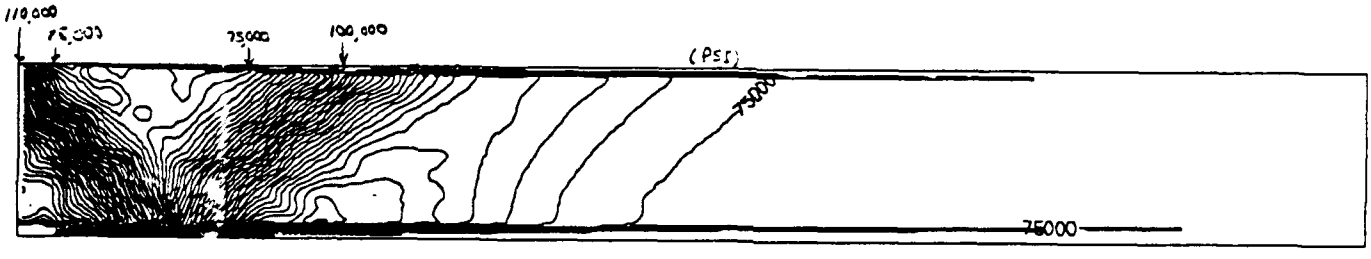

Figure 5-17b. σ_x for Nonlinear Program without Angle Updates(1.5")

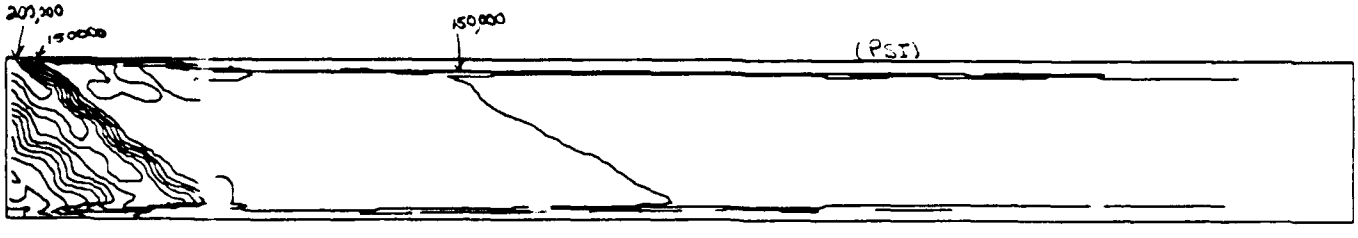

Figure 5-17c. σ_x for Nonlinear Program with Angle Updates(2.5")

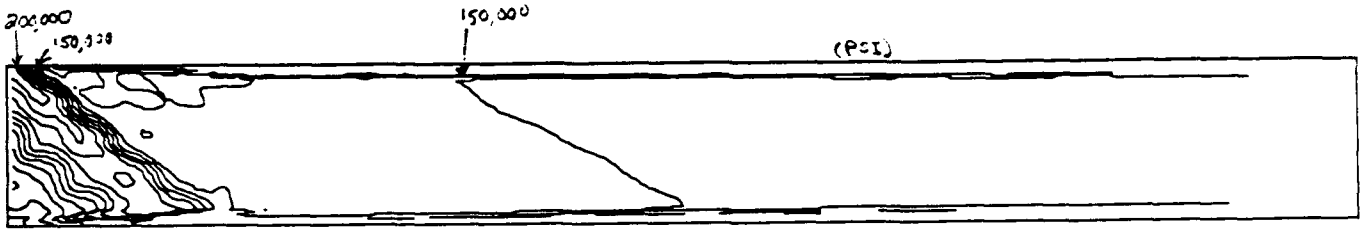

Figure 5-17d. σ_x for Nonlinear Program without Angle Updates(2.5")

Figure 5-18 is at the same displacement as Figure 5-13. This is also a plot of strain in the x direction. Figure 5-13 goes across the entire specimen where Figure 5-18 is only across a quarter of the specimen.

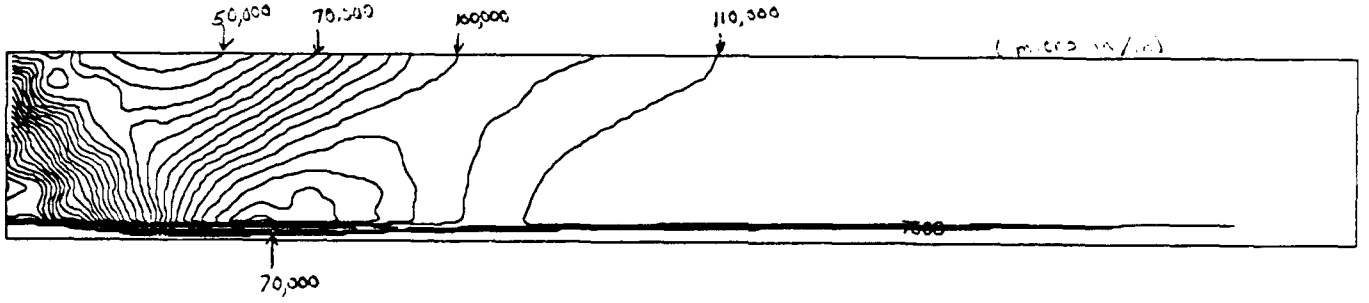

Figure 5-18. ε_x for Nonlinear Program with Angle Updates(0.5")

In addition to showing the smoother curve for the plot of angle updated data, Figures 5-19a and b show the strain concentration at the edge upper left corner. This follows the experimental results, which causes the debonding. These plots were made at 0.5 inches which is where debonding begins. Figure 5-20 shows the beginning of debonding at 0.5 inch displacement (Look carefully at the upper clamp). The strands of the glass epoxy can be seen in the upper left hand corner.

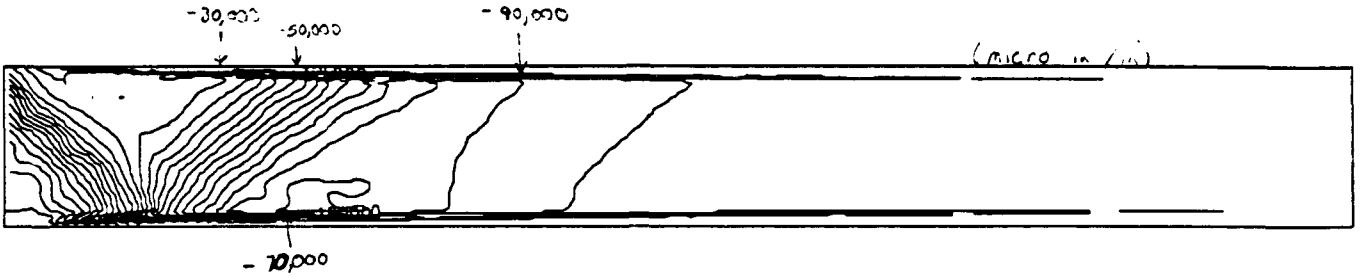

Figure 5-19a. ε_y for Nonlinear Program with Angle Updates(0.5")

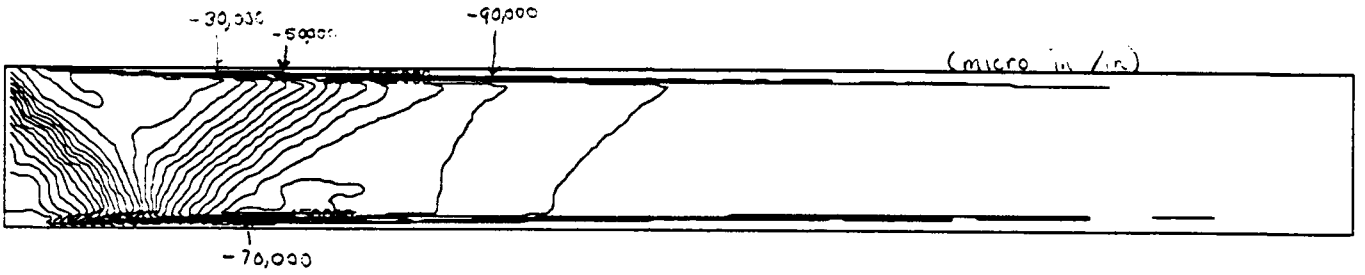

Figure 5-19b. ε_y for Nonlinear Program without Angle Updates(0.5")

Figure 5-21 shows the stress concentration slightly off the center of the circular discontinuity. This also follows the experimental results shown in Figure 5-5a.

Figures 5-22a and b shows that the linear model indicates the shear concentration at the center of the circular discontinuity. Since it is the shearing strain which causes the failure, the nonlinear model shows better results.

F. Displacement Modeling

There is also a plotting program to show how the specimen is displacing as the load is applied by plotting the updated coordinates.

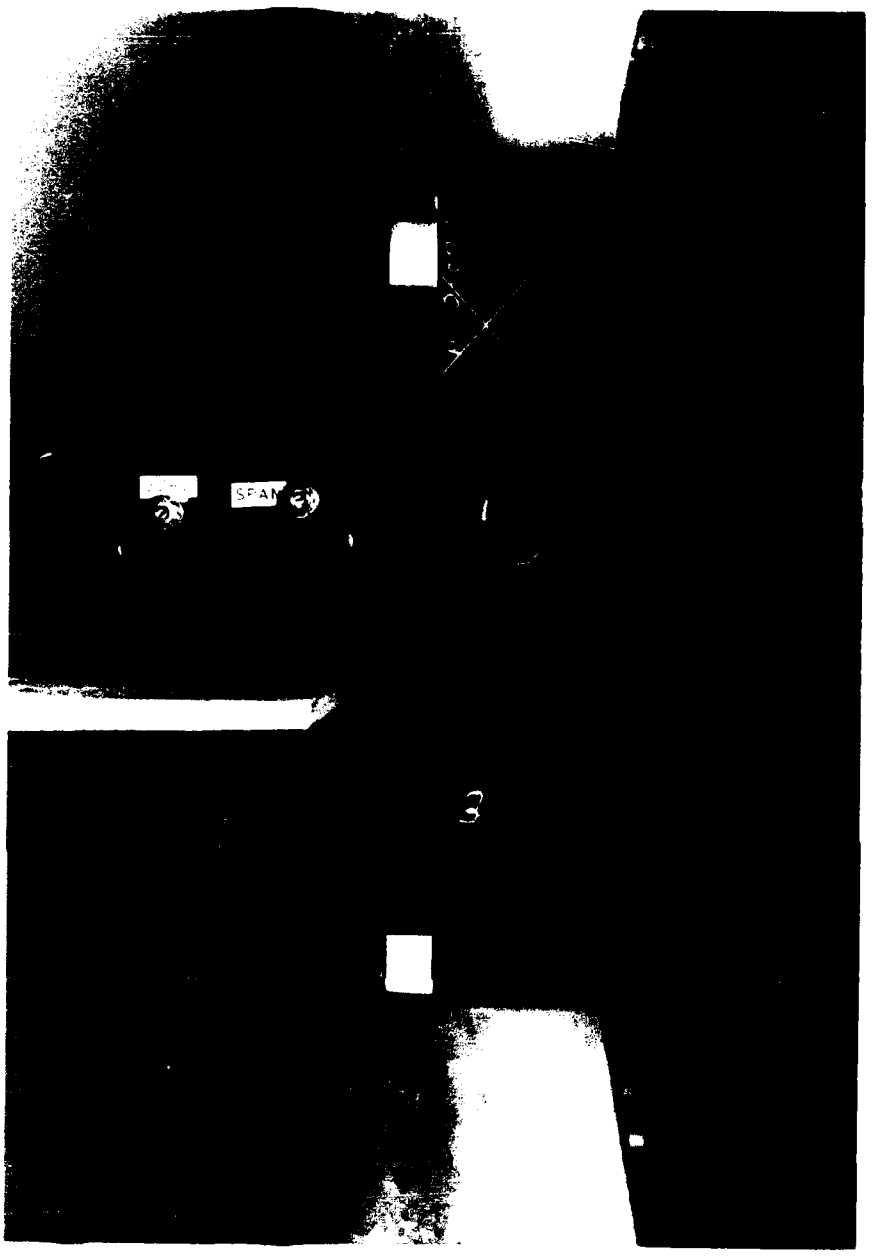

Figure 5-20. Photograph at 0.5" Displacement

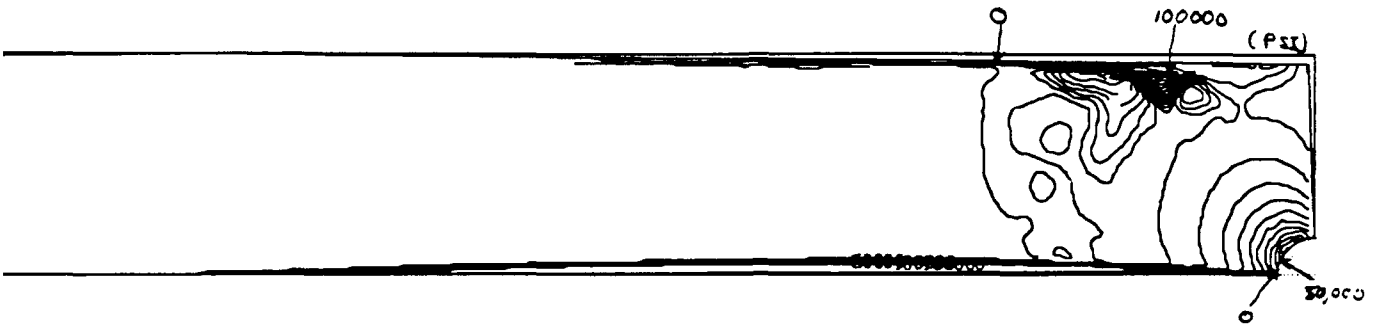

Figure 5-21. σ_x for Nonlinear Program with Angle Updates(0.5")

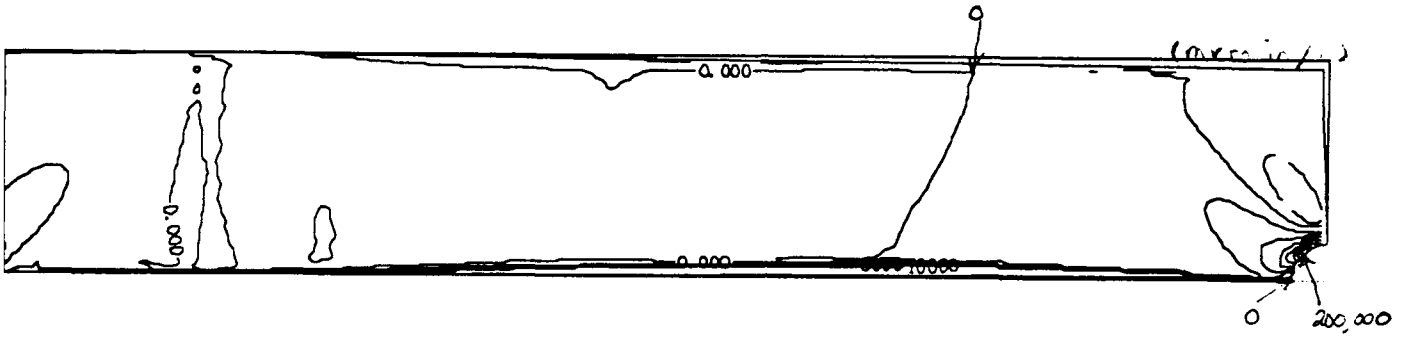

Figure 5-22a. γ_{xy} for Nonlinear Program with Angle Updates(0.5")

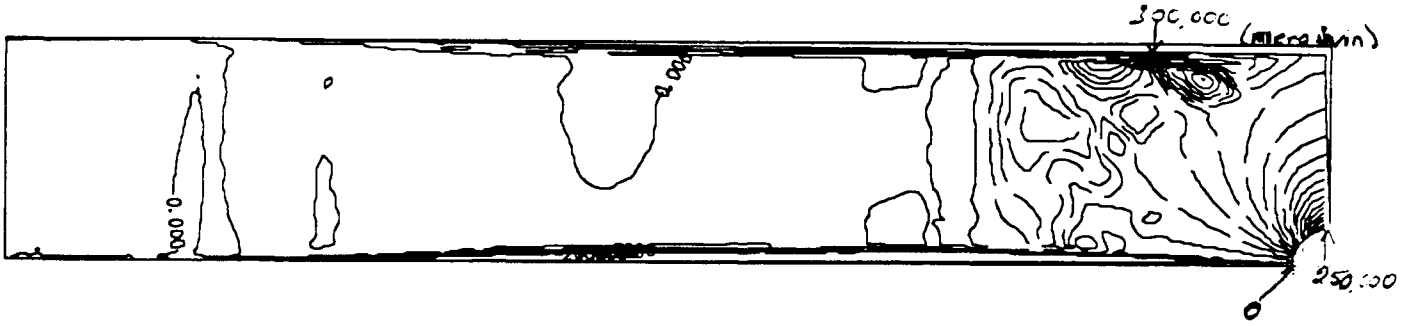

Figure 5-22b. γ_{xy} for Linear Program(0.5")

Figures 5-23a-g show how the nonlinear programs deformation is slightly more at the point about 1 inch from the tab of the specimen which is where the specimen fails. The displacements have become

smooth at about one inch from the tab. As the displacements continue, the elements are less and less rectangular around the one inch point where the failure occurs.

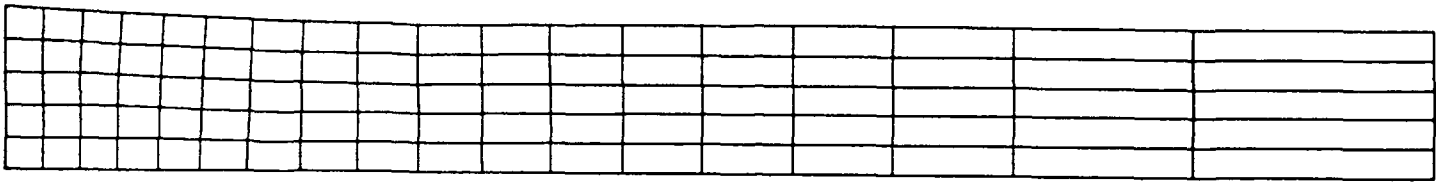

Figure 5-23a. Displacement for Nonlinear Program with Angle Updates (0.1")

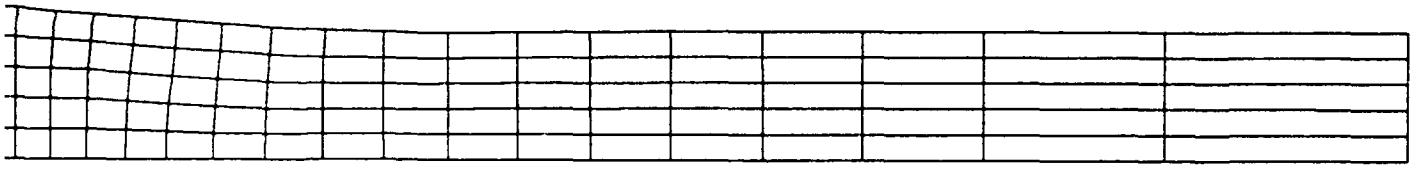

Figure 5-23b. Displacement for Nonlinear Program with Angle Updates (0.25")

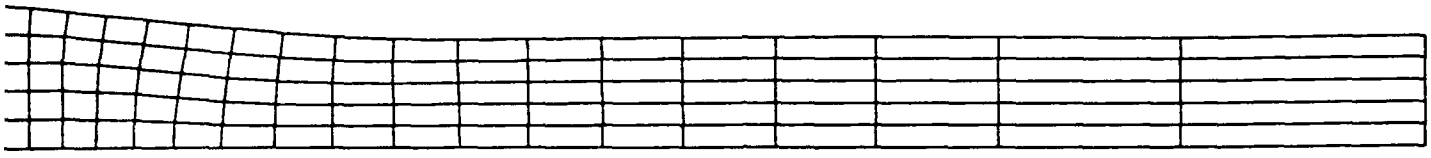

Figure 5-23c. Displacement for Nonlinear Program with Angle Updates (0.5")

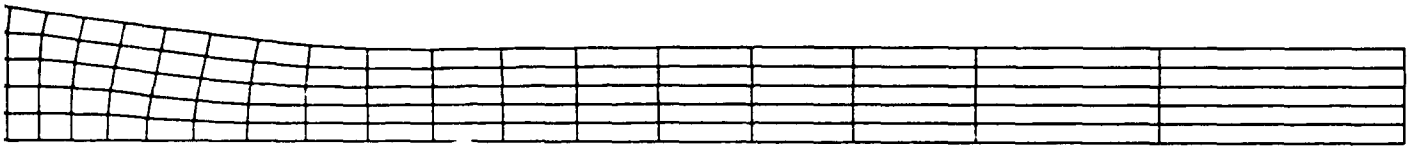

Figure 5-23d. Displacement for Nonlinear Program with Angle Updates (0.75")

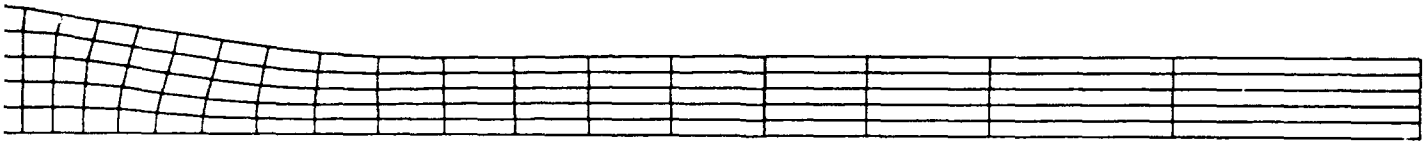

Figure 5-23e. Displacement for Nonlinear Program with Angle Updates (1")

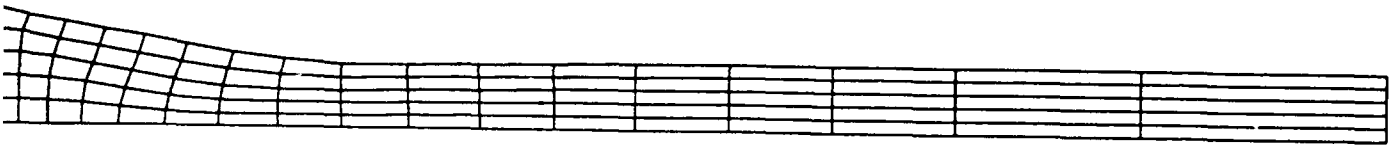

Figure 5-23f. Displacement for Nonlinear Program with Angle Updates(1.5")

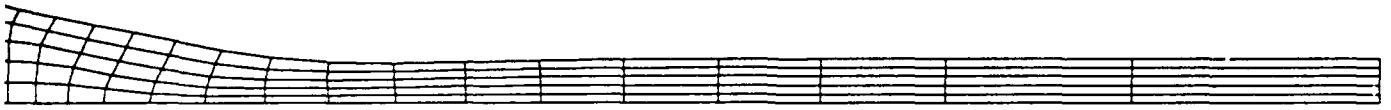

Figure 5-23g. Displacement for Nonlinear Program with Angle Updates(2")

A similar sequence of displacements is shown for the notched model in Figures 24a-c. Figure 5-24c is after the specimen has failed.

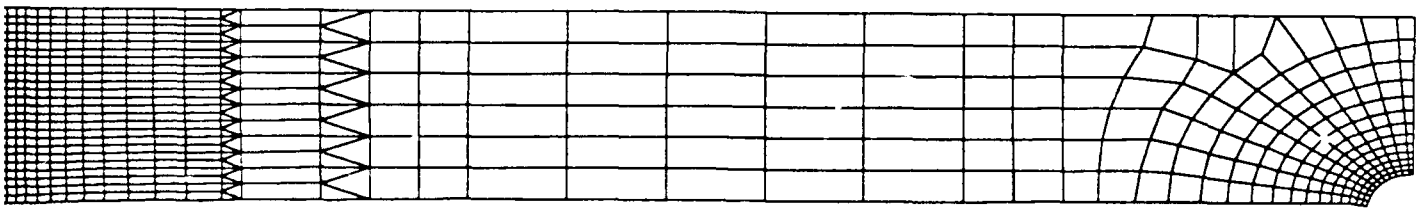

Figure 5-24a. Displacements for Nonlinear Program with Angle Updates(0.5")

Figure 5-24b. Displacements for Nonlinear Program with Angle Updates(1")

Figure 5-24c. Displacements for Nonlinear Program with Angle Updates(2")

VI. Conclusions

From the data collected, the changes appear to provide the program a better method of predicting stresses, strains, loads, and failures for large strains. Updated Lagrangian is essential for nonlinear materials at strains above 5 percent. Angle updating is important at strains above 10 percent. This updating should in no way hinder any of the original program capabilities.

The use of equation 2-9 for the calculation of the change in fiber orientation is accurate even at high strain. This is far easier than calculating the angle by examining the displaced elements.

The failure criteria may have several problems. For one, three dimensional effects are not taken into effect. Another, the energy of the interply scissoring is not taken into account. A third is that the tab debonds at these high strains.

The high elongation gages worked well even above the their stated maximum. The failures in the gages were usually due to the glue failing, the gages saturating, the gages peeling off, or the connection breaking. The gages themselves held to failure. When the specimens were tested the day after applying the gages the glue did not fail.

Recommendations

By running more experiments with high elongation gages this data could be even better. This would provide better data for the cubic splines used by the program.

By increasing the length of the specimen one might avoid the debonding of the tabs. One might also use tapered tabs. (4) This

Appendix A: Program Inputs, and Outputs

Input Data For Modified PLSTR2 (small model):

```
PLATE WITH NO DISCONTINUITY
  114  185    2    0    0.        0.        0.        2    0    0    0    1    1
    2   75  185    0    3    1  300
    1   11   0.0       0.0
    2   10   0.0       0.1
    3   10   0.0       0.2
    4   10   0.0       0.3
    5   10   0.0       0.4
    6   10   0.0       0.5
    7    1   0.10000   0.00000
    8        0.10000   0.10000
   12        0.10000   0.50000
   13    1   0.20000   0.00000
   14        0.20000   0.10000
   18        0.20000   0.50000
   19    1    .30000   0.00000
   20         .30000   0.10000
   24         .30000   0.50000
   25    1    .41000   0.00000
   26         .41000   0.10000
   30         .41000   0.50000
   31    1    .52000   0.00000
   32         .52000   0.10000
   36         .52000   0.50000
   37    1    .64000   0.00000
   38         .64000   0.10000
   42         .64000   0.50000
   43    1    .77000   0.00000
   44         .77000   0.10000
   48         .77000   0.50000
   49    1    .91000   0.00000
   50         .91000   0.10000
   54         .91000   0.50000
   55    1   1.0600    0.00000
   56        1.0600    0.10000
   60        1.06000   0.50000
   61    1   1.22000   0.00000
   62        1.22000   0.10000
   66        1.22000   0.50000
   67    1   1.39000   0.00000
   68        1.39000   0.10000
   72        1.39000   0.50000
   73    1   1.57000   0.00000
   74        1.57000   0.10000
   78        1.57000   0.50000
   79    1   1.77000   0.00000
   80        1.77000   0.10000
   84        1.77000   0.50000
   85    1   2.00000   0.00000
   86        2.00000   0.10000
   90        2.00000   0.50000
   91    1   2.25000   0.00000
   92        2.25000   0.10000
   96        2.25000   0.50000
   97    1   2.55000   0.00000
   98        2.55000   0.10000
```

```
102          2.55000    0.50000
103     1    3.0        0.0
104          3.0        0.1
108          3.0        0.5
109    11    3.60000    0.00000        .025
110    10    3.60000    0.10000        .025
111    10    3.6          .2           .025
112    10    3.6          .3           .025
113    10    3.6          .4           .025
114    10    3.60000    0.50000        .025
0.0          45.0       -45.0
.042         .042       .042
   2     1     1
   1     7     8     2     1     2     0.     .042
  15    11    12     6     5     1  -45.0     .042
  16    13    14     8     7     1   45.0     .042                          2
  25    17    18    12    11     1  -45.0     .042                          2
  26    19    20    14    13     1   45.0     .042                          2
  35    23    24    18    17     1  -45.0     .042                          2
  36    25    26    20    19     1   45.0     .042                          2
  45    29    30    24    23     1  -45.0     .042                          2
  46    31    32    26    25     1   45.0     .042                          2
  55    35    36    30    29     1  -45.0     .042                          2
  56    37    38    32    31     1   45.0     .042                          2
  65    41    42    36    35     1  -45.0     .042                          2
  66    43    44    38    37     1   45.0     .042                          2
  75    47    48    42    41     1  -45.0     .042                          2
  76    49    50    44    43     1   45.0     .042                          2
  85    53    54    48    47     1  -45.0     .042                          2
  86    55    56    50    49     1   45.0     .042                          2
  95    59    60    54    53     1  -45.0     .042                          2
  96    61    62    56    55     1   45.0     .042                          2
 105    65    66    60    59     1  -45.0     .042                          2
 106    67    68    62    61     1   45.0     .042                          2
 115    71    72    66    65     1  -45.0     .042                          2
 116    73    74    68    67     1   45.0     .042                          2
 125    77    78    72    71     1  -45.0     .042                          2
 126    79    80    74    73     1   45.0     .042                          2
 135    83    84    78    77     1  -45.0     .042                          2
 136    85    86    80    79     1   45.0     .042                          2
 145    89    90    84    83     1  -45.0     .042                          2
 146    91    92    86    85     1   45.0     .042                          2
 155    95    96    90    89     1  -45.0     .042                          2
 156    97    98    92    91     1   45.0     .042                          2
 165   101   102    96    95     1  -45.0     .042                          2
 166   103   104    98    97     1   45.0     .042                          2
 175   107   108   102   101     1  -45.0     .042                          2
 176   109   110   104   103     1   45.0     .042                          2
 185   113   114   108   107     1  -45.0     .042                          2
   2
  17    16    15    20    15    17    16
   0.0000       0.        0.0010  19500.       0.0020  39000.
   0.0030   58500.        0.0040  78100.       0.0050  97800.
   0.006   118000.        0.007  138500.       0.008  159000.
   0.009   180000.        0.01   202000.       0.011  224500.
   0.012   247500.        0.013  271000.       0.014  295000.
   0.141   290739.        0.15   319000.
   0.0000       0.        0.0008  15000.       0.0016  30000.
   0.0024   44500.        0.0032  58500.       0.0040  72500.
   0.0048   86000.        0.0056  99000.       0.0064 111500.
```

would also avoid the stress concentration causing the debonding. This would mean shaping the tabs in the shape of the deformation shown in Figure 4-9.

```
    0 0072 124000.      0.0080 136000.      0.0088 148000.
    0.0096 159000.      0.0104 170000.      0.110  178000.
    0.112  180500.
    0.0000      0.      0.001    1550.      0.002    3100.
    0.003    4600.      0.004    6050.      0.005    7450.
    0.006    8850.      0.007   10200.      0.008   11500.
    0.009   12550.      0.010   13300.      0.011   13900.
    0.012   14300.      0.129  145860.      0.13   146000.
    0.0000      0.      0.002    3200.      0.004    6400.
    0.006    9600.      0.008   12750.      0.010   15500.
    0.012   18000.      0.014   20250       0.016   22200.
    0.018   24050.      0.020   25730.      0.022   27300.
    0.024   28700.      0.026   29900.      0.028   30900.
    0.030   31800.      0.032   32500.      0.034   33100.
    0.352  334000.      0.36    336000.
    0.0000      0.0     0.005   2986.0      0.0180  7743.0
    0.034    9552.0     0.051   10420.0     0.070   11205.0
    0.108   12730.0     0.129   13517.0     0.170   15146.0
    0.209   16831.0     0.248   18530.0     0.283   20339.0
    0.318   21724.0     0.351   23186.0     0.378   24690.0
    0.0000    0.305     0.001     0.310     0.002     0.315
    0.003     0.3167    0.004     0.3165    0.005     0.315
    0.006     0.312     0.007     0.3085    0.008     0.305
    0.009     0.3025    0.010     0.3       0.011     0.298
    0.012     0.296     0.013     0.2943    0.014     0.293
    0.500     0.2929    0.550     0.292
    0.0000    0.34      0.0008    0.35      0.0016    0.356
    0.0024    0.359     0.0032    0.3615    0.0040    0.3635
    0.0048    0.365     0.0056    0.3662    0.0064    0.3673
    0 0072    0.3684    0.0080    0.3695    0.0088    0.3705
    0.0096    0.3715    0.0104    0.3725    0.500     0.3733
    0.510     0.3735
19500000. 18750000. 1550000.  1600000.  812500.
   26   26   26   26   21   26   26
  0 000000      0.00   .001000   4141.90   .002000   8119.04
    .003000  11927.77   .004000  15502.54   .005000  18744.10
    .006000  21988.71   .007000  25053.58   .008000  28184.42
    .009000  31303.99   .010000  34287.47   .011000  37326.15
    .012000  40375.34   .013000  43413.02   .014000  46419.94
    .015000  49386.09   .016000  52321.32   .017000  55175.65
    .018000  58001.02   .019000  60855.01   .020000  63722.05
    .021000  66514.80   .022000  69295.50   .023000  72089.79
 0.27573  832174.6  0.321468  943451.29
  0.000000      0.00   .001000   4141.90   .002000   8119.04
    .003000  11927.77   .004000  15502.54   .005000  18744.10
    .006000  21988.71   .007000  25053.58   .008000  28184.42
    .009000  31303.99   .010000  34287.47   .011000  37326.15
    .012000  40375.34   .013000  43413.02   .014000  46419.94
    .015000  49386.09   .016000  52321.32   .017000  55175.65
    .018000  58001.02   .019000  60855.01   .020000  63722.05
    .021000  66514.80   .022000  69295.50   .023000  72089.79
 0.27573  832174.6  0.321468  943451.29
  0.000000      0.00   .001000   4141.90   .002000   8119.04
    .003000  11927.77   .004000  15502.54   .005000  18744.10
    .006000  21988.71   .007000  25053.58   .008000  28184.42
    .009000  31303.99   .010000  34287.47   .011000  37326.15
    .012000  40375.34   .013000  43413.02   .014000  46419.94
    .015000  49386.09   .016000  52321.32   .017000  55175.65
    .018000  58001.02   .019000  60855.01   .020000  63722.05
    .021000  66514.80   .022000  69295.50   .023000  72089.79
```

```
 0.27573  832174.6  0.321468  943451.29
  0.000000      0.00   .001000   4141.90   .002000   8119.04
    .003000  11927.77   .004000  15502.54   .005000  18744.10
    .006000  21988.71   .007000  25053.58   .008000  28184.42
    .009000  31303.99   .010000  34287.47   .011000  37326.15
    .012000  40375.34   .013000  43413.02   .014000  46419.94
    .015000  49386.09   .016000  52321.32   .017000  55175.65
    .018000  58001.02   .019000  60855.01   .020000  63722.05
    .021000  66514.80   .022000  69295.50   .023000  72089.79
 0.27573  832174.6  0.321468  943451.29
  0.000000      0.00   .005000   2855.55   .010000   4471.86
    .015000   5442.37   .020000   5973.45   .025000   6410.88
    .030000   6690.98   .035000   6900.77   .040000   7054.57
    .045000   7179.76   .050000   7287.89   .055000   7396.03
    .060000   7463.32   .065000   7589.96   .070000   7690.74
    .075000   7749.71   .080000   7895.29   .085000   8039.59
    .090000   8185.200.151743   9430.85   0.213487  10676.49
  0.0000000.1302935   .001000   .130293   .002000   .129309
    .003000   .127840   .004000   .122488   .005000   .113358
    .006000   .104879   .007000   .097967   .008000   .092782
    .009000   .087801   .010000   .084354   .011000   .081168
    .012000   .078120   .013000   .074784   .014000   .071385
    .015000   .067775   .016000   .063838   .017000   .058719
    .018000   .054426   .019000   .050026   .020000   .045578
    .021000   .041045   .022000   .037599   .023000   .034035
0.27573   0.25534   0.321468  0.17033
  0.0000000.1302935   .001000   .130293   .002000   .129309
    .003000   .127840   .004000   .122488   .005000   .113358
    .006000   .104879   .007000   .097967   .008000   .092782
    .009000   .087801   .010000   .084354   .011000   .081168
    .012000   .078120   .013000   .074784   .014000   .071385
    .015000   .067775   .016000   .063838   .017000   .058719
    .018000   .054426   .019000   .050026   .020000   .045578
    .021000   .041045   .022000   .037599   .023000   .034035
0.27573   0.25534   0.321468  0.17033
4141900.  4141900.  4141900.  4141900.  571110.
```

Output Data:

```
1PLATE WITH NO DISCONTINUITY
  NUMBER OF NODAL POINTS-------  114
  NUMBER OF ELEMENTS-----------  185
  NUMBER OF DIFF. MATERIALS----    2
  NUMBER OF PRESSURE CARDSS----    0
  X-ACCELERATION---------------  0.0000E+00
  Y-ACCELERATION---------------  0.0000E+00
  REFERENCE TEMPERATURE--------  0.0000E+00
  MATERIAL COMBINATION
  ** ISO.=1 ANISO.=2 BOTH=3 **     2
  NUMBER OF ISOTROPIC MATERIALS    0
  TYPE OF OUTPUT---------------    0
  **** ** ***** NCONTR---------    1
  NUMBER OF ITERATION----------    0
  NONLINEAR ANALYSIS NONLIN=1--
  LINEAR ANALYSIS NONLIN=0-----
  NONLIN-----------------------    1
  NOPSHN-----------------------    2
  MAX. NO. OF INRETS-MAXINR----   75
  MAXIMUM ELEM. OUTPUT MAXEL---  185
  MAX. NO. OF INRETS-MAXINR----   75
  MAXIMUM ELEM. OUTPUT MAXEL---  185
  MINIMUM ELEM. OUTPUT MINEL---    0
  DEPTH-WISE ELEMENTS MAXDPT---    3
  MDIS=0 FORCE LOADING---------
  MDIS=1 DISPLACEMENT LOADING--
  TYPE OF LOADING  MDIS--------    1
```

NODAL POINT	TYPE	X ORDINATE	Y ORDINATE	X LOAD OR DISPLACEMENT	Y LOAD OR DISPLACEMENT	TEMPERATURE
1	11	0.00000	0.00000	0.0000000E+00	0.0000000E+00	0.000
2	10	0.00000	0.10000	0.0000000E+00	0.0000000E+00	0.000
3	10	0.00000	0.20000	0.0000000E+00	0.0000000E+00	0.000
4	10	0.00000	0.30000	0.0000000E+00	0.0000000E+00	0.000
5	10	0.00000	0.40000	0.0000000E+00	0.0000000E+00	0.000
6	10	0.00000	0.50000	0.0000000E+00	0.0000000E+00	0.000
7	1	0.10000	0.00000	0.0000000E+00	0.0000000E+00	0.000
8	0	0.10000	0.10000	0.0000000E+00	0.0000000E+00	0.000
9	0	0.10000	0.20000	0.0000000E+00	0.0000000E+00	0.000
10	0	0.10000	0.30000	0.0000000E+00	0.0000000E+00	0.000
11	0	0.10000	0.40000	0.0000000E+00	0.0000000E+00	0.000
12	0	0.10000	0.50000	0.0000000E+00	0.0000000E+00	0.000
13	1	0.20000	0.00000	0.0000000E+00	0.0000000E+00	0.000
14	0	0.20000	0.10000	0.0000000E+00	0.0000000E+00	0.000
15	0	0.20000	0.20000	0.0000000E+00	0.0000000E+00	0.000
16	0	0.20000	0.30000	0.0000000E+00	0.0000000E+00	0.000
17	0	0.20000	0.40000	0.0000000E+00	0.0000000E+00	0.000
18	0	0.20000	0.50000	0.0000000E+00	0.0000000E+00	0.000
19	1	0.30000	0.00000	0.0000000E+00	0.0000000E+00	0.000

After all the nodes and elements are shown, the program writes the cubic spline data:

BAND WIDTH---------- 16

FOR THIS PROGRAM THE LOCATION OF AA USED IS = 9411 AND IN IA IS = 1412
1

MATERIAL 1

STRAIN 0 DEG.(TEN)	STRESS 0 DEG.(TEN)	STRAIN 0 DEG.(COM)	STRESS 0 DEG.(COM)
0.00000000E+00	0.00000000E+00	0.00000000E+00	0.00000000E+00
0.10000000E-02	0.19500000E+05	0.80000000E-03	0.15000000E+05
0.20000000E-02	0.39000000E+05	0.16000000E-02	0.30000000E+05
0.30000000E-02	0.58500000E+05	0.24000000E-02	0.44500000E+05
0.40000000E-02	0.78100000E+05	0.32000000E-02	0.58500000E+05
0.50000000E-02	0.97800000E+05	0.40000000E-02	0.72500000E+05
0.60000000E-02	0.11800000E+06	0.48000000E-02	0.86000000E+05
0.70000000E-02	0.13850000E+06	0.56000000E-02	0.99000000E+05
0.80000000E-02	0.15900000E+06	0.64000000E-02	0.11150000E+06
0.90000000E-02	0.18000000E+06	0.72000000E-02	0.12400000E+06
0.10000000E-01	0.20200000E+06	0.80000000E-02	0.13600000E+06
0.11000000E-01	0.22450000E+06	0.88000000E-02	0.14800000E+06
0.12000000E-01	0.24750000E+06	0.96000000E-02	0.15900000E+06
0.13000000E-01	0.27100000E+06	0.10400000E-01	0.17000000E+06
0.14000000E-01	0.29500000E+06	0.11000000E-01	0.17800000E+06
0.14100000E-01	0.29739300E+06	0.11200000E-01	0.18050000E+06
0.15000000E-01	0.31900000E+06	0.00000000E+00	0.00000000E+00

STRAIN 90DEG.(TEN)	STRESS 90DEG.(TEN)	STRAIN 90DEG.(COM)	STRESS 90DEG.(COM)	SHEAR STRAIN	SHE
0.00000000E+00	0.00000000E+00	0.00000000E+00	0.00000000E+00	0.00000000E+00	0.0(
0.10000000E-02	0.15500000E+04	0.20000000E-02	0.32000000E+04	0.50000000E-02	0.2!
0.20000000E-02	0.31000000E+04	0.40000000E-02	0.64000000E+04	0.18000000E-01	0.7:
0.30000000E-02	0.46000000E+04	0.60000000E-02	0.96000000E+04	0.34000000E-01	0.9!
0.40000000E-02	0.60500000E+04	0.80000000E-02	0.12750000E+05	0.51000000E-01	0.1(
0.50000000E-02	0.74500000E+04	0.10000000E-01	0.15500000E+05	0.70000000E-01	0.1)
0.60000000E-02	0.88500000E+04	0.12000000E-01	0.18000000E+05	0.10800000E+00	0.1:
0.70000000E-02	0.10200000E+05	0.14000000E-01	0.20250000E+05	0.12900000E+00	0.1:
0.80000000E-02	0.11500000E+05	0.16000000E-01	0.22200000E+05	0.17000000E+00	0.1!
0.90000000E-02	0.12550000E+05	0.18000000E-01	0.24050000E+05	0.20900000E+00	0.1(
0.10000000E-01	0.13300000E+05	0.20000000E-01	0.25730000E+05	0.24800000E+00	0.1(
0.11000000E-01	0.13900000E+05	0.22000000E-01	0.27300000E+05	0.28300000E+00	0.2(
0.12000000E-01	0.14300000E+05	0.24000000E-01	0.28700000E+05	0.31800000E+00	0.2)
0.12900000E-01	0.14586000E+05	0.26000000E-01	0.29900000E+05	0.35100000E+00	0.2:
0.13000000E-01	0.14600000E+05	0.28000000E-01	0.30900000E+05	0.37800000E+00	0.2(
0.00000000E+00	0.00000000E+00	0.30000000E-01	0.31800000E+05	0.00000000E+00	0.0(
0.00000000E+00	0.00000000E+00	0.32000000E-01	0.32500000E+05	0.00000000E+00	0.0(
0.00000000E+00	0.00000000E+00	0.34000000E-01	0.33100000E+05	0.00000000E+00	0.0(
0.00000000E+00	0.00000000E+00	0.35200000E-01	0.33400000E+05	0.00000000E+00	0.0(
0.00000000E+00	0.00000000E+00	0.36000000E-01	0.33600000E+05	0.00000000E+00	0.0(

STRAIN 0 DEG.(TEN)	TEN. POSSONS RATIO	STRAIN 90DEG.(COM)	COM. POSSONS RATIO
0.00000000E+00	0.30500000E+00	0.00000000E+00	0.34000000E+00
0.10000000E-02	0.31000000E+00	0.80000000E-03	0.35000000E+00
0.20000000E-02	0.31500000E+00	0.16000000E-02	0.35600000E+00
0.30000000E-02	0.31670000E+00	0.24000000E-02	0.35900000E+00
0.40000000E-02	0.31650000E+00	0.32000000E-02	0.36150000E+00
0.50000000E-02	0.31500000E+00	0.40000000E-02	0.36350000E+00
0.60000000E-02	0.31200000E+00	0.48000000E-02	0.36500000E+00
0.70000000E-02	0.30850000E+00	0.56000000E-02	0.36620000E+00
0.80000000E-02	0.30500000E+00	0.64000000E-02	0.36730000E+00
0.90000000E-02	0.30250000E+00	0.72000000E-02	0.36840000E+00
0.10000000E-01	0.30000000E+00	0.80000000E-02	0.36950000E+00
0.11000000E-01	0.29800000E+00	0.88000000E-02	0.37050000E+00

0.12000000E-01	0.29600000E+00	0.96000000E-02	0.37150000E+00
0.13000000E-01	0.29430000E+00	0.10400000E-01	0.37250000E+00
0.14000000E-01	0.29300000E+00	0.11000000E-01	0.37330000E+00
0.14100000E-01	0.29290000E+00	0.11200000E-01	0.37350000E+00
0.15000000E-01	0.29200000E+00	0.00000000E+00	0.00000000E+00

INITIAL MODULI OF ELASTICITY

E1T= 0.19500000E+08 E1C= 0.18750000E+08 E2T= 0.15500000E+07 E2C= 0.16000000E+07 G12= 0.81250000E

MATERIAL	ENERGY-LLT	ENERGY-LLC	ENERGY-TTT	ENERGY-TTC	EN
1	0.20101491E+04	0.10398971E+04	0.11331091E+03	0.75100690E+03	0.538(

1

MATERIAL 2

STRAIN 0 DEG.(TEN)	STRESS 0 DEG.(TEN)	STRAIN 0 DEG.(COM)	STRESS 0 DEG.(COM)
0.00000000E+00	0.00000000E+00	0.00000000E+00	0.00000000E+00
0.10000000E-02	0.41419000E+04	0.10000000E-02	0.41419000E+04
0.20000000E-02	0.81190400E+04	0.20000000E-02	0.81190400E+04
0.30000000E-02	0.11927770E+05	0.30000000E-02	0.11927770E+05
0.40000000E-02	0.15502540E+05	0.40000000E-02	0.15502540E+05
0.50000000E-02	0.18744100E+05	0.50000000E-02	0.18744100E+05
0.60000000E-02	0.21988710E+05	0.60000000E-02	0.21988710E+05
0.70000000E-02	0.25053580E+05	0.70000000E-02	0.25053580E+05
0.80000000E-02	0.28184420E+05	0.80000000E-02	0.28184420E+05
0.90000000E-02	0.31303990E+05	0.90000000E-02	0.31303990E+05
0.10000000E-01	0.34287470E+05	0.10000000E-01	0.34287470E+05
0.11000000E-01	0.37326150E+05	0.11000000E-01	0.37326150E+05
0.12000000E-01	0.40375340E+05	0.12000000E-01	0.40375340E+05
0.13000000E-01	0.43413020E+05	0.13000000E-01	0.43413020E+05
0.14000000E-01	0.46419940E+05	0.14000000E-01	0.46419940E+05
0.15000000E-01	0.49386090E+05	0.15000000E-01	0.49386090E+05
0.16000000E-01	0.52321320E+05	0.16000000E-01	0.52321320E+05
0.17000000E-01	0.55175650E+05	0.17000000E-01	0.55175650E+05
0.18000000E-01	0.58001020E+05	0.18000000E-01	0.58001020E+05
0.19000000E-01	0.60855010E+05	0.19000000E-01	0.60855010E+05
0.20000000E-01	0.63722050E+05	0.20000000E-01	0.63722050E+05
0.21000000E-01	0.66514800E+05	0.21000000E-01	0.66514800E+05
0.22000000E-01	0.69295500E+05	0.22000000E-01	0.69295500E+05
0.23000000E-01	0.72089790E+05	0.23000000E-01	0.72089790E+05
0.27573000E+00	0.83217460E+06	0.27573000E+00	0.83217460E+06
0.32146800E+00	0.94345129E+06	0.32146800E+00	0.94345129E+06

STRAIN 90DEG.(TEN)	STRESS 90DEG.(TEN)	STRAIN 90DEG.(COM)	STRESS 90DEG.(COM)	SHEAR STRAIN	SHE
0.00000000E+00	0.00000000E+00	0.00000000E+00	0.00000000E+00	0.00000000E+00	0.0(
0.10000000E-02	0.41419000E+04	0.10000000E-02	0.41419000E+04	0.50000000E-02	0.2(
0.20000000E-02	0.81190400E+04	0.20000000E-02	0.81190400E+04	0.10000000E-01	0.4(
0.30000000E-02	0.11927770E+05	0.30000000E-02	0.11927770E+05	0.15000000E-01	0.5(
0.40000000E-02	0.15502540E+05	0.40000000E-02	0.15502540E+05	0.20000000E-01	0.5(
0.50000000E-02	0.18744100E+05	0.50000000E-02	0.18744100E+05	0.25000000E-01	0.6(
0.60000000E-02	0.21988710E+05	0.60000000E-02	0.21988710E+05	0.30000000E-01	0.6(
0.70000000E-02	0.25053580E+05	0.70000000E-02	0.25053580E+05	0.35000000E-01	0.6(
0.80000000E-02	0.28184420E+05	0.80000000E-02	0.28184420E+05	0.40000000E-01	0.7(
0.90000000E-02	0.31303990E+05	0.90000000E-02	0.31303990E+05	0.45000000E-01	0.7(
0.10000000E-01	0.34287470E+05	0.10000000E-01	0.34287470E+05	0.50000000E-01	0.7(
0.11000000E-01	0.37326150E+05	0.11000000E-01	0.37326150E+05	0.55000000E-01	0.7(
0.12000000E-01	0.40375340E+05	0.12000000E-01	0.40375340E+05	0.60000000E-01	0.7(
0.13000000E-01	0.43413020E+05	0.13000000E-01	0.43413020E+05	0.65000000E-01	0.7(
0.14000000E-01	0.46419940E+05	0.14000000E-01	0.46419940E+05	0.70000000E-01	0.7(
0.15000000E-01	0.49386090E+05	0.15000000E-01	0.49386090E+05	0.75000000E-01	0.7(
0.16000000E-01	0.52321320E+05	0.16000000E-01	0.52321320E+05	0.80000000E-01	0.7(
0.17000000E-01	0.55175650E+05	0.17000000E-01	0.55175650E+05	0.85000000E-01	0.8(
0.18000000E-01	0.58001020E+05	0.18000000E-01	0.58001020E+05	0.90000000E-01	0.8(
0.19000000E-01	0.60855010E+05	0.19000000E-01	0.60855010E+05	0.15174300E+00	0.9(
0.20000000E-01	0.63722050E+05	0.20000000E-01	0.63722050E+05	0.21348700E+00	0.1(
0.21000000E-01	0.66514800E+05	0.21000000E-01	0.66514800E+05	0.00000000E+00	0.0(
0.22000000E-01	0.69295500E+05	0.22000000E-01	0.69295500E+05	0.00000000E+00	0.0(
0.23000000E-01	0.72089790E+05	0.23000000E-01	0.72089790E+05	0.00000000E+00	0.0(
0.27573000E+00	0.83217460E+06	0.27573000E+00	0.83217460E+06	0.00000000E+00	0.0(

0.32146800E+00 0.94345129E+06 0.32146800E+00 0.94345129E+06 0.00000000E+00 0.0(

STRAIN 0 DEG.(TEN)	TEN. POSSONS RATIO	STRAIN 90DEG.(COM)	COM. POSSONS RATIO
0.00000000E+00	0.13029350E+00	0.00000000E+00	0.13029350E+00
0.10000000E-02	0.13029300E+00	0.10000000E-02	0.13029300E+00
0.20000000E-02	0.12930900E+00	0.20000000E-02	0.12930900E+00
0.30000000E-02	0.12784000E+00	0.30000000E-02	0.12784000E+00
0.40000000E-02	0.12248800E+00	0.40000000E-02	0.12248800E+00
0.50000000E-02	0.11335800E+00	0.50000000E-02	0.11335800E+00
0.60000000E-02	0.10487900E+00	0.60000000E-02	0.10487900E+00
0.70000000E-02	0.97967000E-01	0.70000000E-02	0.97967000E-01
0.80000000E-02	0.92782000E-01	0.80000000E-02	0.92782000E-01
0.90000000E-02	0.87801000E-01	0.90000000E-02	0.87801000E-01
0.10000000E-01	0.84354000E-01	0.10000000E-01	0.84354000E-01
0.11000000E-01	0.81168000E-01	0.11000000E-01	0.81168000E-01
0.12000000E-01	0.78120000E-01	0.12000000E-01	0.78120000E-01
0.13000000E-01	0.74784000E-01	0.13000000E-01	0.74784000E-01
0.14000000E-01	0.71385000E-01	0.14000000E-01	0.71385000E-01
0.15000000E-01	0.67775000E-01	0.15000000E-01	0.67775000E-01
0.16000000E-01	0.63838000E-01	0.16000000E-01	0.63838000E-01
0.17000000E-01	0.58719000E-01	0.17000000E-01	0.58719000E-01
0.18000000E-01	0.54426000E-01	0.18000000E-01	0.54426000E-01
0.19000000E-01	0.50026000E-01	0.19000000E-01	0.50026000E-01
0.20000000E-01	0.45578000E-01	0.20000000E-01	0.45578000E-01
0.21000000E-01	0.41045000E-01	0.21000000E-01	0.41045000E-01
0.22000000E-01	0.37599000E-01	0.22000000E-01	0.37599000E-01
0.23000000E-01	0.34035000E-01	0.23000000E-01	0.34035000E-01
0.27573000E+00	0.25534000E+00	0.27573000E+00	0.25534000E+00
0.18000000E-01	0.54426000E-01	0.18000000E-01	0.54426000E-01
0.19000000E-01	0.50026000E-01	0.19000000E-01	0.50026000E-01

```
0.22000000E-01      0.37599000E-01      0.22000000E-01      0.37599000E-01
0.23000000E-01      0.34035000E-01      0.23000000E-01      0.34035000E-01
0.27573000E+00      0.25534000E+00      0.27573000E+00      0.25534000E+00
0.32146800E+00      0.17033000E+00      0.32146800E+00      0.17033000E+00
```

The program now reads the Initial values of the material properties:

```
INITIAL MODULI OF ELASTICITY
E1T= 0.41419000E+07  E1C= 0.41419000E+07  E2T= 0.41419000E+07  E2C= 0.41419000E+07  G12= 0.57111000E
MATERIAL          ENERGY-LLT          ENERGY-LLC          ENERGY-TTT          ENERGY-TTC          EN
   2      0.11639355E+06      0.11639355E+06      0.11639355E+06      0.11639355E+06      0.11395671
```

The iterations are now listed and the increment given in the far right hand column:

```
ITERATION CONTROLS
ITERATION    2  CHECK1    0.00000000E+00  CHECK2    0.12406354E+02  DECHK     0.10000000E+01 SCALE     0.10000
ITERATION CONTROLS
ITERATION    3  CHECK1    0.12406354E+02  CHECK2    0.13138208E+02  DECHK     0.55704235E-01 SCALE     0.10000
ITERATION CONTROLS
ITERATION    4  CHECK1    0.13138208E+02  CHECK2    0.13201918E+02  DECHK     0.48258377E-02 SCALE     0.10000
ITERATION CONTROLS
ITERATION    5  CHECK1    0.13201918E+02  CHECK2    0.13213167E+02  DECHK     0.85131919E-03 SCALE     0.10000
```

The program now writes the new angles after the first iteration:

```
THE ANGLES HAVE BEEN CHANGED
        1   0.00000000E+00       2   0.44997487E+02       3  -0.44997487E+02       4   0.00000000E+00
        5   0.44991883E+02       6  -0.44991883E+02       7   0.00000000E+00       8   0.44980874E+02
        9  -0.44980874E+02      10   0.00000000E+00      11   0.44942155E+02      12  -0.44942155E+02
       13   0.00000000E+00      14   0.44929219E+02      15  -0.44929219E+02      16   0.44992181E+02
       17  -0.44992181E+02      18   0.44973111E+02      19  -0.44973111E+02      20   0.44938856E+02
       21  -0.44938856E+02      22   0.44888812E+02      23  -0.44888812E+02      24   0.44900062E+02
       25  -0.44900062E+02      26   0.44985753E+02      27  -0.44985753E+02      28   0.44952023E+02
       29  -0.44952023E+02      30   0.44914241E+02      31  -0.44914241E+02      32   0.44916338E+02
       33  -0.44916338E+02      34   0.44989454E+02      35  -0.44989454E+02      36   0.44979148E+02
       37  -0.44979148E+02      38   0.44943508E+02      39  -0.44943508E+02      40   0.44939870E+02
       41  -0.44939870E+02      42   0.44980161E+02      43  -0.44980161E+02      44   0.44997305E+02
       45  -0.44997305E+02      46   0.44984222E+02      47  -0.44984222E+02      48   0.44970504E+02
       49  -0.44970504E+02      50   0.44986742E+02      51  -0.44986742E+02      52   0.44996012E+02
       53  -0.44996012E+02      54   0.44999032E+02      55  -0.44999032E+02      56   0.44997119E+02
       57  -0.44997119E+02      58   0.44990347E+02      59  -0.44990347E+02      60   0.44992033E+02
       61  -0.44992033E+02      62   0.44996933E+02      63  -0.44996933E+02      64   0.44999974E+02
       65  -0.44999974E+02      66   0.44988447E+02      67  -0.44988447E+02      68   0.44977245E+02
       69  -0.44977245E+02      70   0.44980688E+02      71  -0.44980688E+02      72   0.44989946E+02
       73  -0.44989946E+02      74   0.44998159E+02      75  -0.44998159E+02      76   0.44994168E+02
       77  -0.44994168E+02      78   0.44983482E+02      79  -0.44983482E+02      80   0.44979781E+02
       81  -0.44979781E+02      82   0.44985037E+02      83  -0.44985037E+02      84   0.44995490E+02
       85  -0.44995490E+02      86   0.44997658E+02      87  -0.44997658E+02      88   0.44992489E+02
       89  -0.44992489E+02      90   0.44987421E+02      91  -0.44987421E+02      92   0.44986932E+02
       93  -0.44986932E+02      94   0.44993927E+02      95  -0.44993927E+02      96   0.44999051E+02
       97  -0.44999051E+02      98   0.44997130E+02      99  -0.44997130E+02     100   0.44995139E+02
      101  -0.44995139E+02     102   0.44993728E+02     103  -0.44993728E+02     104   0.44995518E+02
      105  -0.44995518E+02     106   0.44999980E+02     107  -0.44999980E+02     108   0.44999935E+02
      109  -0.44999935E+02     110   0.44999789E+02     111  -0.44999789E+02     112   0.44999316E+02
      113  -0.44999316E+02     114   0.44998645E+02     115  -0.44998645E+02     116   0.44999375E+02
      117  -0.44999375E+02     118   0.44998312E+02     119  -0.44998312E+02     120   0.44997801E+02
      121  -0.44997801E+02     122   0.44998163E+02     123  -0.44998163E+02     124   0.44999531E+02
      125  -0.44999531E+02     126   0.44999287E+02     127  -0.44999287E+02     128   0.44998086E+02
      129  -0.44998086E+02     130   0.44997505E+02     131  -0.44997505E+02     132   0.44997784E+02
      133  -0.44997784E+02     134   0.44999012E+02     135  -0.44999012E+02     136   0.44999652E+02
      137  -0.44999652E+02     138   0.44999044E+02     139  -0.44999044E+02     140   0.44998681E+02
      141  -0.44998681E+02     142   0.44998677E+02     143  -0.44998677E+02     144   0.44999102E+02
      145  -0.44999102E+02     146   0.44999988E+02     147  -0.44999988E+02     148   0.44999936E+02
      149  -0.44999936E+02     150   0.44999825E+02     151  -0.44999825E+02     152   0.44999676E+02
      153  -0.44999676E+02     154   0.44999582E+02     155  -0.44999582E+02     156   0.44999897E+02
      157  -0.44999897E+02     158   0.44999730E+02     159  -0.44999730E+02     160   0.44999674E+02
      161  -0.44999674E+02     162   0.44999769E+02     163  -0.44999769E+02     164   0.44999978E+02
      165  -0.44999978E+02     166   0.44999954E+02     167  -0.44999954E+02     168   0.44999868E+02
      167  -0.44999897E+02     158   0.44999730E+02     159  -0.44999730E+02     160   0.44999674E+02
      161  -0.44999674E+02     162   0.44999769E+02     163  -0.44999769E+02     164   0.44999978E+02
      165  -0.44999978E+02     166   0.44999954E+02     167  -0.44999954E+02     168   0.44999868E+02
      169  -0.44999868E+02     170   0.44999805E+02     171  -0.44999805E+02     172   0.44999781E+02
      173  -0.44999781E+02     174   0.44999814E+02     175  -0.44999814E+02     176   0.45000000E+02
      177  -0.45000000E+02     178   0.44999998E+02     179  -0.44999998E+02     180   0.44999990E+02
      181  -0.44999990E+02     182   0.44999973E+02     183  -0.44999973E+02     184   0.44999950E+02
      185  -0.44999950E+02
```

The program now writes the dispalcements for the increment:

1 LOAD INCREMENT 1

DISPLACEMENTS

N.P.	UX	UY	N.P.	UX	UY	N.P.	UX	
1	0.00000000E+00	0.00000000E+00	2	0.00000000E+00	-0.35198089E-03	3	0.00000000E+00	-0.6
4	0.00000000E+00	-0.10315992E-02	5	0.00000000E+00	-0.13142859E-02	6	0.00000000E+00	-0.1
7	0.36206947E-03	0.00000000E+00	8	0.36184309E-03	-0.35467879E-03	9	0.35996848E-03	-0.7
10	0.35178756E-03	-0.10408004E-02	11	0.35850726E-03	-0.13791095E-02	12	0.53584429E-03	-0.1
13	0.83956609E-03	0.00000000E+00	14	0.84004871E-03	-0.36403318E-03	15	0.84215591E-03	-0.7
16	0.86446990E-03	-0.11039131E-02	17	0.97480282E-03	-0.15624221E-02	18	0.12190940E-02	-0.2
19	0.13396937E-02	0.00000000E+00	20	0.13457754E-02	-0.38717426E-03	21	0.13774393E-02	-0.7
22	0.14770619E-02	-0.12591805E-02	23	0.16656396E-02	-0.18034098E-02	24	0.18561292E-02	-0.2
25	0.19445875E-02	0.00000000E+00	26	0.19694844E-02	-0.44793927E-03	27	0.20572164E-02	-0.9
28	0.22110034E-02	-0.14720179E-02	29	0.23769577E-02	-0.20059500E-02	30	0.25378994E-02	-0.2
31	0.26465411E-02	0.00000000E+00	32	0.26881159E-02	-0.54125260E-03	33	0.27974615E-02	-0.1
34	0.29317096E-02	-0.16446009E-02	35	0.30712892E-02	-0.21745587E-02	36	0.32118812E-02	-0.2
37	0.35262694E-02	0.00000000E+00	38	0.35561231E-02	-0.62294459E-03	39	0.36283323E-02	-0.1
40	0.37231587E-02	-0.17856706E-02	41	0.38306582E-02	-0.23257020E-02	42	0.39463370E-02	-0.2
43	0.45358382E-02	0.00000000E+00	44	0.45418125E-02	-0.65204554E-03	45	0.45656780E-02	-0.1
46	0.46109380E-02	-0.18771946E-02	47	0.46749382E-02	-0.24419199E-02	48	0.47541202E-02	-0.2
49	0.56150797E-02	0.00000000E+00	50	0.56122027E-02	-0.64688238E-03	51	0.56073918E-02	-0.1
52	0.56099956E-02	-0.19063353E-02	53	0.56265747E-02	-0.25012164E-02	54	0.56594425E-02	-0.3
55	0.67458005E-02	0.00000000E+00	56	0.67410611E-02	-0.63137052E-03	57	0.67278492E-02	-0.1
58	0.67099234E-02	-0.18860288E-02	59	0.66941553E-02	-0.24999308E-02	60	0.66873201E-02	-0.3
61	0.79241721E-02	0.00000000E+00	62	0.79198149E-02	-0.61504982E-03	63	0.79070433E-02	-0.1
64	0.78870539E-02	-0.18469108E-02	65	0.78627326E-02	-0.24632287E-02	66	0.78389903E-02	-0.3
67	0.91526949E-02	0.00000000E+00	68	0.91497429E-02	-0.60258552E-03	69	0.91410946E-02	-0.1
70	0.91273430E-02	-0.18132106E-02	71	0.91094397E-02	-0.24237952E-02	72	0.90887974E-02	-0.3
73	0.10439456E-01	0.00000000E+00	74	0.10438221E-01	-0.59635740E-03	75	0.10434583E-01	-0.1
76	0.10428676E-01	-0.17947807E-02	77	0.10420528E-01	-0.23991806E-02	78	0.10409931E-01	-0.3
79	0.11865828E-01	0.00000000E+00	80	0.11865879E-01	-0.59564859E-03	81	0.11865935E-01	-0.1
82	0.11865710E-01	-0.17903256E-02	83	0.11864761E-01	-0.23905981E-02	84	0.11862544E-01	-0.2
85	0.13510346E-01	0.00000000E+00	86	0.13510824E-01	-0.59779583E-03	87	0.13512145E-01	-0.1
88	0.13514004E-01	-0.17940396E-02	89	0.13515987E-01	-0.23927986E-02	90	0.13517639E-01	-0.2
91	0.15303372E-01	0.00000000E+00	92	0.15303678E-01	-0.59979029E-03	93	0.15304557E-01	-0.1
94	0.15305905E-01	-0.17988770E-02	95	0 15307578E-01	-0.23980410E-02	96	0.15309434E-01	-0.2
97	0.17456127E-01	0.00000000E+00	98	0.17458194E-01	-0.60054673E-03	99	0.17458397E-01	-0.1
100	0.17458742E-01	-0.18012669E-02	101	0.17459226E-01	-0.24013166E-02	102	0.17459834E-01	-0.3
103	0.20690585E-01	0.00000000E+00	104	0.20690564E-01	-0.60050910E-03	105	0.20690507E-01	-0.1
106	0.20690437E-01	-0.18014703E-02	107	0.20690380E-01	-0.24018946E-02	108	0.20690368E-01	-0.3
109	0.25000000E-01	0.00000000E+00	110	0.25000000E-01	-0.60038355E-03	111	0.25000000E-01	-0.1

The program now prints the stresses, strains, and failure criteria numbers:

1 STRESSES / STRAINS / ENERGY CONTRIBUTIONS

ELEM.	X	Y	-XX	-YY	-XY	-LL	-TT	-LT	ENER. LEVE
1	0.050	0.050	0.1272E+05	-0.1235E+05	-0.9210E+01	0.1272E+05	-0.1235E+05	-0.9210E+01	
			0.3620E-02	-0.3533E-02	-0.1462E-04	0.3620E-02	-0.3533E-02	-0.1462E-04	
						0.2265E-03	0.2161E-03	0.5908E-07	0.442
2	0.050	0.050	0.4714E+04	-0.3627E+04	-0.4640E+03	0.10[illegible]8E+04	0.7982E+02	0.4170E+04	
			0.3620E-02	-0.3533E-02	-0.1462E-04	0.[illegible]044E-04	0.3582E-04	0.7153E-02	
						0.1234E-04	0.8760E-05	0.2835E-02	0.285
3	0.050	0.050	0.4582E+04	-0.3759E+04	0.3160E+03	0.7276E+03	0.9565E+02	-0.4170E+04	
			0.3620E-02	-0.3533E-02	-0.1462E-04	0.3582E-04	0.5044E-04	-0.7153E-02	
						0.6223E-05	0.1737E-04	0.2835E-02	0.285
4	0.050	0.149	0.1270E+05	-0.1217E+05	-0.2974E+02	0.1270E+05	-0.1217E+05	-0.2974E+02	
			0.3609E-02	-0.3484E-02	-0.4722E-04	0.3609E-02	-0.3484E-02	-0.4722E-04	
						0.2252E-03	0.2102E-03	0.6163E-06	0.435
5	0.050	0.149	0.5049E+04	-0.3231E+04	-0.8067E+03	0.1716E+04	0.1021E+03	0.4140E+04	
			0.3609E-02	-0.3484E-02	-0.4722E-04	0.8639E-04	0.3917E-04	0.7093E-02	
						0.3620E-04	0.1047E-04	0.2789E-02	0.283
6	0.050	0.149	0.4622E+04	-0.3658E+04	0.3286E+03	0.8104E+03	0.1533E+03	-0.4140E+04	
			0.3609E-02	-0.3484E-02	-0.4722E-04	0.3917E-04	0.8639E-04	-0.7093E-02	
						0.7440E-05	0.5095E-04	0.2789E-02	0.284
7	0.050	0.249	0.1257E+05	-0.1168E+0[illegible]	-0.7009E+02	0.1257E+05	-0.1168E+05	-0.7009E+02	
			0.3559E-02	-0.3345E-02	-0.1113E-03	0.3559E-02	-0.3345E-02	-0.1113E-03	
						0.2191E-03	0.1942E-03	0.3422E-05	0.416
8	0.050	0.249	0.5730E+04	-0.2358E+04	-0.1529E+04	0.3215E+04	0.1571E+03	0.4044E+04	
			0.3559E-02	-0.3345E-02	-0.1113E-03	0.1624E-03	0.5116E-04	0.6904E-02	
						0.1280E-03	0.1787E-04	0.2649E-02	0.279
9	0.050	0.249	0.4724E+04	-0.3365E+04	0.4023E+03	0.1082E+04	0.2775E+03	-0.4044E+04	
			0.3559E-02	-0.3345E-02	-0.1113E-03	0.5116E-04	0.1624E-03	-0.6904E-02	
						0.1269E-04	0.1801E-03	0.2649E-02	0.284
10	0.050	0.349	0.1266E+05	-0.1077E+05	-0.2119E+03	0.1266E+05	-0.1077E+05	-0.2119E+03	
			0.3551E-02	-0.3105E-02	-0.3365E-03	0.3551E-02	-0.3105E-02	-0.3365E-03	
						0.2182E-03	0.1678E-03	0.3129E-04	0.417
11	0.050	0.349	0.7912E+04	0.7754E+02	-0.3722E+04	0.7717E+04	0.2724E+03	0.3917E+04	
			0.3551E-02	-0.3105E-02	-0.3365E-03	0.3915E-03	0.5498E-04	0.6656E-02	
						0.7434E-03	0.2064E-04	0.2469E-02	0.323
12	0.050	0.349	0.4869E+04	-0.2966E+04	0.3149E+03	0.1266E+04	0.6365E+03	-0.3917E+04	
			0.3551E-02	-0.3105E-02	-0.3365E-03	0.5498E-04	0.3915E-03	-0.6656E-02	
						0.1466E-04	0.1047E-02	0.2469E-02	0.351
13	0.050	0.448	0.1593E+05	-0.1110E+05	-0.2593E+03	0.1593E+05	-0.1110E+05	-0.2593E+03	
			0.4472E-02	-0.3307E-02	-0.4118E-03	0.4472E-02	-0.3307E-02	-0.4118E-03	
						0.3410E-03	0.1899E-03	0.4685E-04	0.577
14	0.050	0.448	0.1279E+05	0.3836E+04	-0.7350E+04	0.1566E+05	0.9642E+03	0.4478E+04	
			0.4472E-02	-0.3307E-02	-0.4118E-03	0.7881E-03	0.3764E-03	0.7779E-02	
						0.3013E-02	0.9671E-03	0.3327E-02	0.730
15	0.050	0.448	0.9067E+04	0.1118E+03	0.3180E+04	0.7769E+04	0.1410E+04	-0.4478E+04	
			0.4472E-02	-0.3307E-02	-0.4118E-03	0.3764E-03	0.7881E-03	-0.7779E-02	
						0.6869E-03	0.4243E-02	0.3327E-02	0.825
16	0.151	0.050	0.1153E+05	0.2015E+04	-0.5588E+04	0.1236E+05	0.1183E+04	0.4755E+04	
			0.4779E-02	-0.3594E-02	-0.4549E-04	0.6152E-03	0.5697E-03	0.8372E-02	
						0.1836E-02	0.2217E-02	0.3824E-02	0.787
17	0.151	0.050	0.1111E+05	0.1604E+04	0.5127E+04	0.1149E+05	0.1232E+04	-0.4755E+04	
			0.4779E-02	-0.3594E-02	-0.4549E-04	0.5697E-03	0.6152E-03	-0.8372E-02	
						0.1574E-02	0.2585E-02	0.3824E-02	0.798
18	0.151	0.149	0.1235E+05	0.2847E+04	-0.6414E+04	0.1401E+05	0.1183E+04	0.4750E+04	
			0.4802E-02	-0.3558E-02	-0.1564E-03	0.7000E-03	0.5436E-03	0.8360E-02	
						0.2376E-02	0.2018E-02	0.3814E-02	0.820
19	0.151	0.149	0.1093E+05	0.1432E+04	0.4830E+04	0.1101E+05	0.1352E+04	-0.4750E+04	
			0.4802E-02	-0.3558E-02	-0.1564E-03	0.5436E-03	0.7000E-03	-0.8360E-02	
						0.1433E-02	0.3347E-02	0.3814E-02	0.859

Appendix B. Equipment List

Strain Gages:

Electrix Industries; Lombard IL

High Elongation Rosettes (Specially manufactured)

Part Number: PAHE - 3 - 125RB -350 LEN

Part Number: PAHE - 3 - 062RB -350 LEN

Strain Gage Adhesive:

Micro Measurements; Raliegh, NC

M-Bond 610 High Elongation

Recommend use as soon as possible after application.

Tab Adhesive:

Scotch 3M Structural Adhesive AF - 163 - 2

Miscellaneous Equipment:

Instron 20 kip (thousand pounds) universal test machine

Voltmeter

Summagraphics Digitizer

C-Scan and Gr/PEEK Data sheet attached. The next four pages are C-Scans of the panels used. The last page is the order form describing exactly how the material was produced.

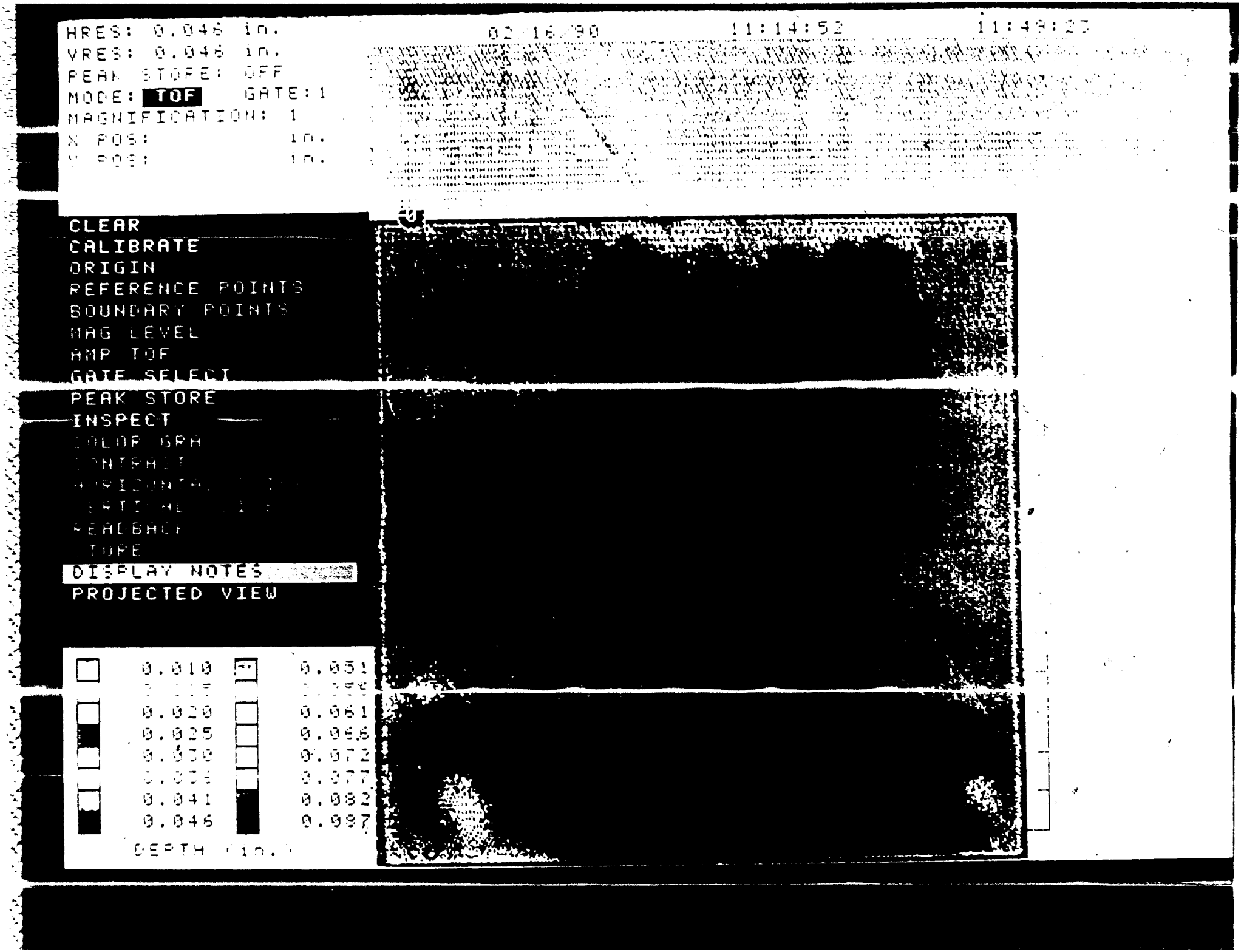
HRES: 0.046 in.
VRES: 0.046 in.
PEAK STORE: OFF
MODE: TOF GATE: 1
MAGNIFICATION: 1
X POS: in.
Y POS: in.
02 16 90
11:14:52
CLEAR
CALIBRATE
ORIGIN
REFERENCE POINTS
BOUNDARY POINTS
MAG LEVEL
AMP TOF
GATE SELECT
PEAK STORE
INSPECT
PROJECTED VIEW
0.010
0.020
0.025
0.041
0.046
0.051
0.061
0.066
0.072
0.077
0.082
0.087
DEPTH (in.)

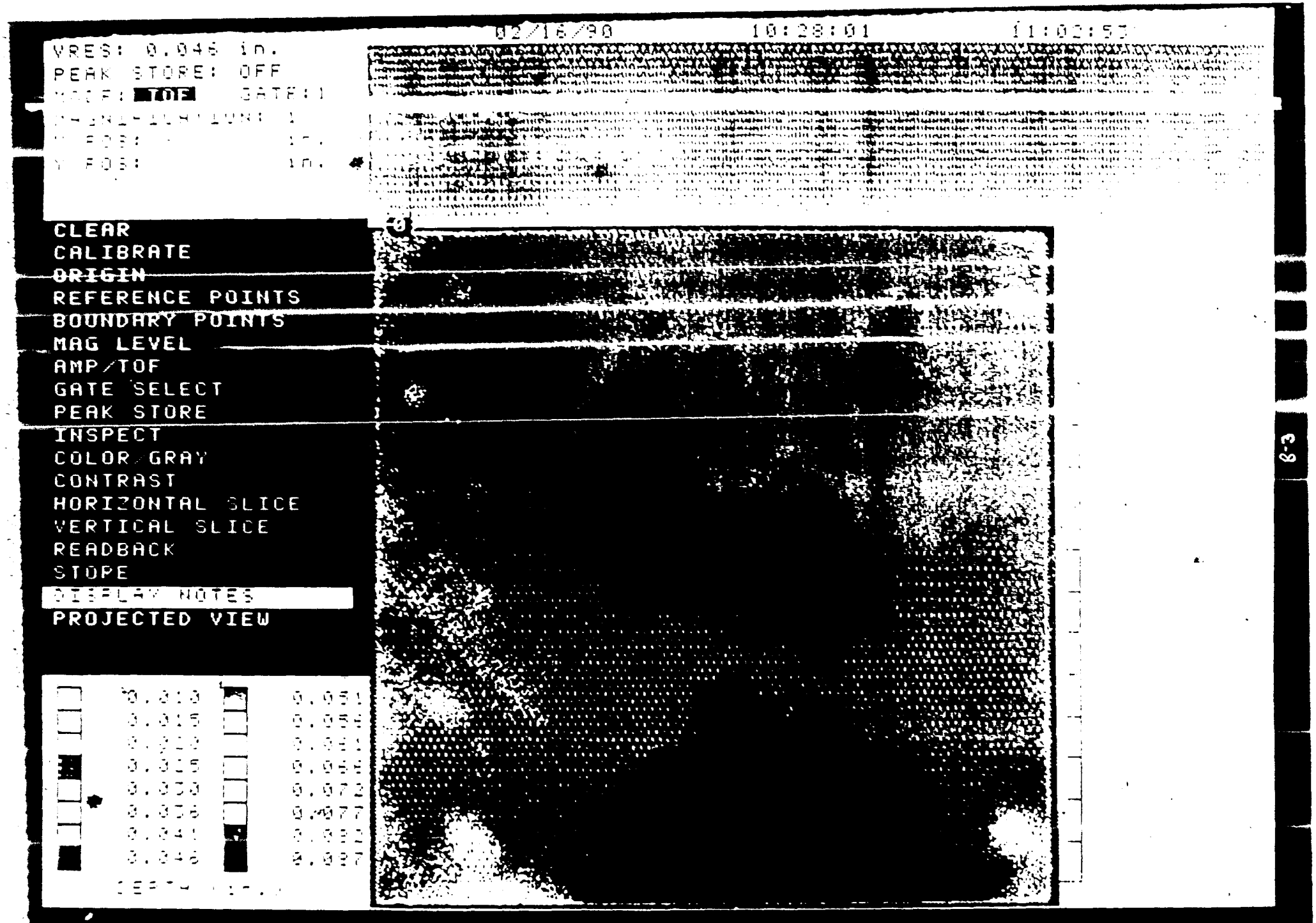
02/16/90
10:28:01
11:02:57
VRES: 0.046 in.
PEAK STORE: OFF
MAG LEVEL
CLEAR
CALIBRATE
ORIGIN
REFERENCE POINTS
BOUNDARY POINTS
MAG LEVEL
AMP/TOF
GATE SELECT
PEAK STORE
INSPECT
COLOR/GRAY
CONTRAST
HORIZONTAL SLICE
VERTICAL SLICE
READBACK
STORE
DISPLAY NOTES
PROJECTED VIEW
8-3

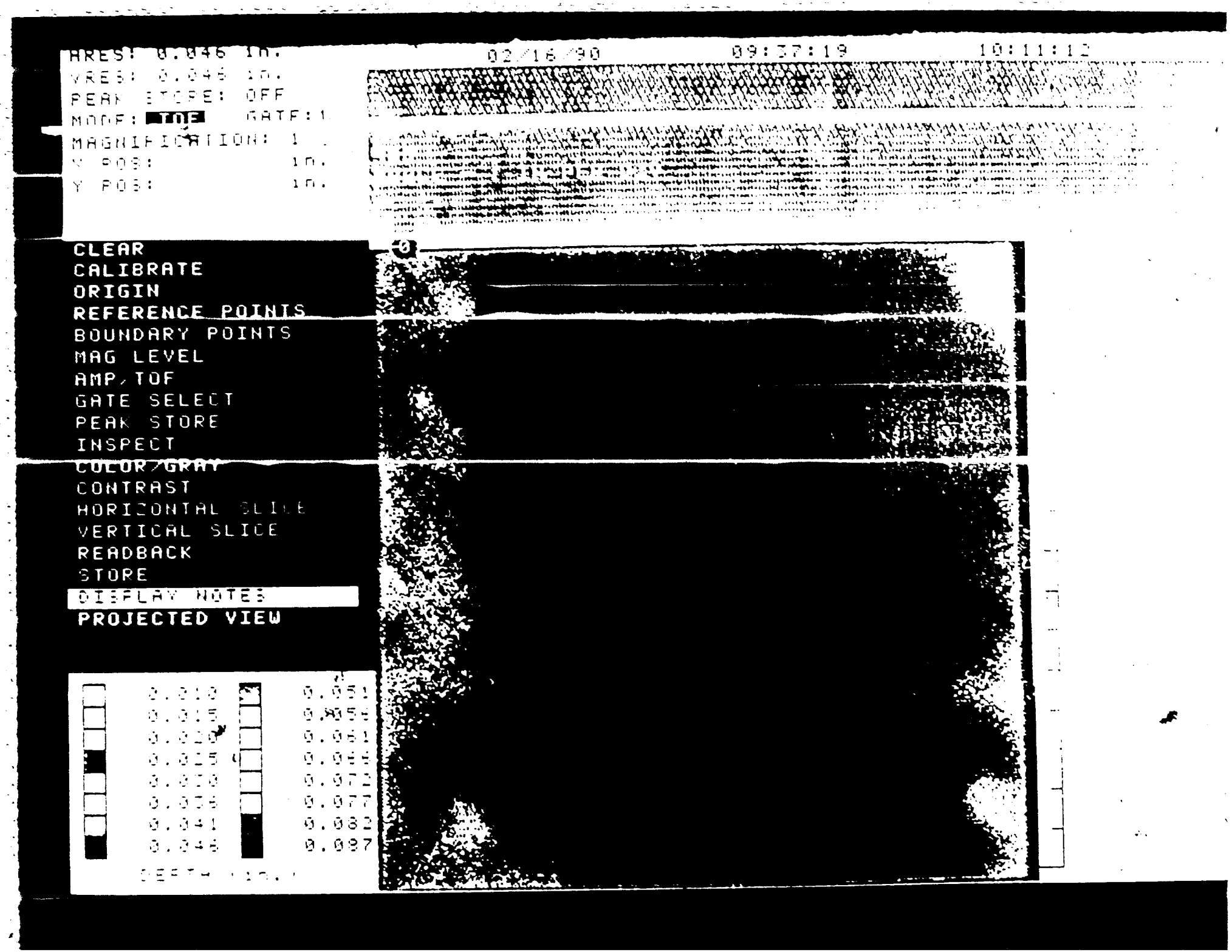
HRES: 0.046 in.
02/16/90
09:37:19
10:11:12
VRES: 0.046 in.
PEAK STORE: OFF
MODE: TOF
GATE:1
MAGNIFICATION: 1
X POS: 10.
Y POS: 10.
CLEAR
CALIBRATE
ORIGIN
REFERENCE POINTS
BOUNDARY POINTS
MAG LEVEL
AMP/TOF
GATE SELECT
PEAK STORE
INSPECT
COLOR/GRAY
CONTRAST
HORIZONTAL SLICE
VERTICAL SLICE
READBACK
STORE
DISPLAY NOTES
PROJECTED VIEW
0.010
0.015
0.020
0.025
0.030
0.035
0.041
0.046
0.051
0.056
0.061
0.066
0.072
0.077
0.082
0.087
DEPTH (in.)

PO Box No 54 Wilton Works
Middlesbrough Cleveland
TS6 8JA England

Telephone (0642) 43 Direct Line
(0642) 454144 Switchboard
Telex 587461
Cables. ICIWilton Middlesbrough Telex

Fax (0642) 433022

Nearest Airport — Teesside 19 miles

APC DEVELOPMENT LABORATORY

FIBERITE®

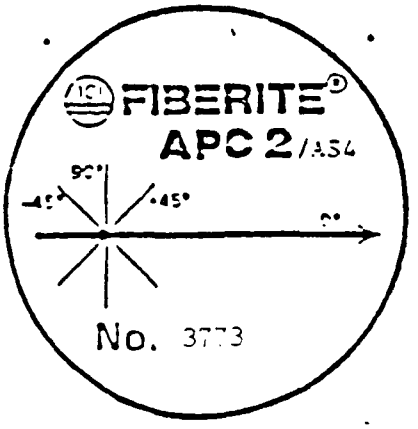

Date 11 April 1989

CUSTOMER:- Wright Patterson A.F.B
CUSTOMER ORDER NO:- F33615-89-M3187

PLEASE FIND ENCLOSED 3 PLAQUES OF APC-2 CODED 3773/1 to 3

THE LAYUP PATTERN IS $[+45/-45]_{4S}$ A_1, A_2, A_3
TO THE CONVENTION SHOWN ABOVE.

THE CONSTRUCTION IS 16 Ply Quasi Isotropic

FIBRE AREAL WEIGHT PER PLY IN NOMINALLY 145 g/m^2

RESIN CONTENT IS NOMINALLY 32 %w/w

PRE-PREG BATCH NO. F/01/36

FIBRE BATCH NO. AS4 12K 746-4N

POLYMER BATCH NO. MNH 18-18

ROLL NUMBERS USED FOR LAMINATE PRODUCTION. 59, 83B

SIGNATURE K. Thompson.

QUALITY CONTROL SUPERVISOR

K. THOMPSON
QC SUPERVISOR

Appendix C. Strain Gage Data

lntout of the Experimental Data

ge readings at start:

F><LF><LF>			CAL0	CAL1	CAL2	S/N 1
AN	0	10	8003	8005		
AN	2	0	-191	-191		
AN	3	-1	-194	-194		
AN	4	-2	-193	-193		
AN	5	-2	-194	-194		
AN	6	0	-192	-192		
AN	7	0	-192	-192		
AN	10	-1	-197	-197		
AN	11	-1	-195	-195		
AN	12	0	-192	-192		

ad and gain settings:

F>CHAN	NAME	TY	B	C T	FAC T	Y	U BL	CH	PLOT PARA
A	KB	KC	UM	X GF					
0 LOAD		20 0	0 0	0 0	4988.00000 0	0.00000 0.000 0 0	0	0	0 0 0
0000 0.0000		0.0000	0.0000	1 0.000					

rst a listing of from the load cell. A reading is made every four
conds:

F><LF>S/N 1 MONTH 09 DAY 12 YEAR 90 CHAN 0 0 TRANSDUCER LOAD

PAGE 1

F>	TIME SEC	COUNTS DEC	LOAD LBS	TIME SEC	COUNTS DEC	LOAD LBS	TIME SEC	COUNTS DE
	36.492	43.000	20.594	1873.433	2441.000	1517 .056	2079.973	2957.0
	40.570	41.000	19.345	1877.570	2460.000	1528 .913	2084.094	2967.0
	44.652	44.000	21.218	1881.683	2477.000	1539 .522	2088.223	2977.0
	48.730	40.000	18.721	1885.820	2491.000	1548 .258	2092.371	2983.0
	52.832	42.000	19.969	1889.933	2505.000	1556 .995	2096.492	2991.0
	1687.422	192.000	113.576	1894.070	2522.000	1567		

ch channel specifies a different gage: (Strain is micro strain)
annel 2 is the A gage of the first rosette.

F><LF><LF>S/N 1 MONTH 09 DAY 12 YEAR 90 CHAN 0 2 TRANSDUCER SG1A

PAGE 1

F>	TIME SEC	COUNTS DEC	U-STRAIN	TIME SEC	COUNTS DEC	U-STRAIN	TIME SEC	COUNTS DEC
	36.492	-4.000	-117.903	1873.433	-435.000	-12656.312	2079.973	-1078.000
	40.570	-4.000	-117.903	1877.570	-446.000	-12972.081	2084.094	-1092.000
	44.652	-4.000	-117.903	1881.683	-458.000	-13316.318	2088.223	-1107.000
	48.730	-4.000	-117.903	1885.820	-470.000	-13660.308	2092.371	-1122.000
	52.832	-4.000	-117.903	1889.933	-481.000	-13975.415	2096.492	-1137.000
	1687.422	-15.000	-441.988	1894.070	-493.000	-14318.933	2100.613	-1152.000
	1691.563	-22.000	-648.111	1898.172	-506.000	-14699.797	2104.730	-1167.000
	1695.683	-30.000	-883.573	1902.313	-517.000	-15005.226	2108.871	-1182.000

Bibliography

1. Betts, K., "Adaptivity Reshapes FE Analysis." Mechanical Engineering, 22 (October 1990), pp.59-64.

2. Cook, R.D. Concepts and Applications of Finite Element Analysis. New York: John Wiley & Sons, 1981.

3. Cron, S.M., A.N. Palazotto, and R.S. Sandhu, "A Failure Criterion Evaluation for Composite Materials." Composite Materials: Testing and Design, 9 (1990), pp.494-507.

4. Cron, S.M. Improvement of End Boundary Conditions for Off-Axis Tension Specimen Use. MS Thesis, AFIT/GAE/AA/85D-3. School of Engineering, Air Force Institute of Technology (AU), Wright-Patterson AFB, OH. December 1985.

5. DOD/NASA Advanced Composites Design Guide: Volume II, Analysis. Structures/Dynamics Division Flight Dynamics Laboratory, Air Force Wright-Patterson AFB, OH, July 1983.

6. Daniels J.A. A Study of Failure Characteristics in Thermoplastic Composite Laminates Due to an Eccentric Circular Discontinuity. MS Thesis, AFIT/GAE/ENY/89D-06. School of Engineering, Air Force Institute of Technology (AU), Wright-Patterson AFB, OH. December 1989.

7. Fiberite Corporation, a subsidiary of Imperial Chemical Industries (ICI). APC-2 PEEK/Carbon Fibre Composite. Manufacture's Data Sheets Orange, CA, April 1989.

8. Fisher, J.M. A Study of Failure Characteristics in Thermoplastic Composite Material at High Temperature. MS Thesis, AFIT/GAE/AA/88D-15. School of Engineering, Air Force Institute of Technology (AU), Wright-Patterson AFB, OH. December 1988.

9. Ghantous, N.Y. Geometric Nonlinear Analysis of Plane Frame Structures. MS Thesis, Ohio State University, Columbus OH, 1985.

10. Griffel, W. Handbook of Formulas for Stress and Strain. New York: Fredric Unger Publishing Co., 1966.

11. James, M.R. et al. "A High Accuracy Automated Strain-Field Mapper." Journal of Experimental Mechanics. 31, (March 1990) pp.60-67.

12. Jones, R.M. Mechanics of Composite Materials. New York: McGraw-Hill,1975.

13. Martin, J. A Study of Failure Characteristics in Thermoplastic Composite Material. MS Thesis, AFIT/GA/AA/88M-2. School of Engineering, Air Force Institute of Technology (AU), Wright-Patterson AFB, OH. March 1988.

14. Micro-Measurements Catalog 500, Part B - Strain Gage Technical Data, Measurements Group Inc., Raleigh, NC, Copyright 1988.

15. Owen, J.E. and E. Hinton Finite Elements in Plasticity: Theory and Practice. Swansea, U. K.: Pineridge Press Limited, 1980.

16. Palazotto, A.N. Class handouts and notes in MECH 642, Finite Element Analysis. School of Engineering, Air Force Institute of Technology (AU), Wright-Patterson AFB, OH, January 1990.

17. Peterson, R.E. Stress Concentration Factors. New York: John Wiley and Sons, 1974.

18. Saada, A.S. Elasticity: Theory and Applications. Malabar FL: Robert E Krieger Publishing Co., 1987.

19. Sandhu, R. S. Analytical-Experimental Correlation of the Behavior of 0°,±45°,90° Family of AS/3501-5 Graphite Epoxy Composite Laminates Under Uniaxial Tensile Loading. Air Force Flight Dynamics Laboratory, AFFDL-TR-79-3064, MAY 1979.

20. Sandhu, R.S., G.P. Sendeckyj and R.L. Gallo "Modeling of the Failure Process in Notched Laminates." Composite Materials: Recent Advances in the Mechanics of Composite Material, IUTAM symposium, August 1983, Pergamon Press, 1983.

21. Sandhu, R. S. "Nonlinear Behavior of Unidirectional and Angle Ply Laminates." Journal of Aircraft, 13, No. 2 (February 1976), pp.104-111.

22. Sandhu, R.S. A Survey of Failure Theories of Isotropic and Anisotropic Materials. Technical Report AFFDL-TR-72-71, AD 756889, Air Force Flight Dynamics Laboratory, Wright-Patterson AFB, OH, January 1972.

23. Sandhu, R.S. Ultimate Strength Analysis of Symmetric Laminates. Technical Report AFFDL-TR-73-137, Air Force Flight Dynamics Laboratory, Wright-Patterson AFB, OH. (1974).

Vita

Captain Stephen C. Gould [redacted] He graduated from Worthington Senior High School in 1977. After two years at Worthington Community College, he transferred to the University of Minnesota in Minneapolis, Minnesota, where he received his bachelors degree in December 1981. After spending time at the U. S. Bureau of Mines in Minneapolis as a mechanical engineer, he went to Officer's Training School (OTS) where he received his commission. His first assignment was at Aeronautical Systems Division (ASD) Wright-Patterson AFB, OH. Lt Gould was named the program manager for the Advanced Synthetic Aperture Radar System (ASARS). There he was responsible for managing a multi-million dollar radar program. He entered the School of Engineering, at the Air Force Institute of Technology, in May 1989.

[redacted]

REPORT DOCUMENTATION PAGE

Form Approved
OMB No. 0704-0188

Public reporting burden for this collection of information is estimated to average 1 hour per response, including the time for reviewing instructions, searching existing data sources, gathering and maintaining the data needed, and completing and reviewing the collection of information. Send comments regarding this burden estimate or any other aspect of this collection of information, including suggestions for reducing this burden to Washington Headquarters Services, Directorate for information Operations and Reports, 1215 Jefferson Davis Highway, Suite 1204, Arlington, VA 22202-4302, and to the Office of Management and Budget, Paperwork Reduction Project (0704-0188), Washington DC 20503

1. AGENCY USE ONLY (Leave blank)	2. REPORT DATE	3. REPORT TYPE AND DATES COVERED
	December 1990	Master's Thesis

4. TITLE AND SUBTITLE

INVESTIGATION OF STRAIN CHARACTERISTICS OF GRAPHITE POLYETHERETHER KETONE USING A NONLINEAR ANALYSIS AND EXPERIMENTAL METHODS

5. FUNDING NUMBERS

6. AUTHOR(S)

Stephen C. Gould, Captain, USAF

7. PERFORMING ORGANIZATION NAME(S) AND ADDRESS(ES)

Air Force Institute of Technology, WPAFB OH 45433-6583

8. PERFORMING ORGANIZATION REPORT NUMBER

AFIT/GAE/ENY/90D-08

9. SPONSORING MONITORING AGENCY NAME(S) AND ADDRESS(ES)

Structures Division [FIBCA]
Flight Dynamics Laboratory
Wright Reseach and Development Center
Wright-Patterson AFB, OH 45433

10. SPONSORING/MONITORING AGENCY REPORT NUMBER

11. SUPPLEMENTARY NOTES

12a. DISTRIBUTION AVAILABILITY STATEMENT

Approved for public release; distribution unlimited

12b. DISTRIBUTION CODE

13. ABSTRACT (Maximum 200 words)

A geometric nonlinear technique is incorporated in a current finite element program. This nonlinear program allows material nonlinearity for calculating the stresses, strains, and failure of composites. The improved program uses an updated Langrangian to calculate the stresses and strains. In addition, it updates the fiber orientation due to displacement in order to calculate the updated stiffness matrix. This method is valuable for large strain values.

The analytical data were compared to experimental data obtained from Graphite PolyEtherEther Ketone (Gr/PEEK) laminates. To obtain data two geometries were used. Digitized photographs were used to measure the angle change for large strains.

14. SUBJECT TERMS

Composites, Strain, Finite Elements, Updated LaGrangian, Fiber Orientation

15. NUMBER OF PAGES

106

16. PRICE CODE

17. SECURITY CLASSIFICATION OF REPORT	18. SECURITY CLASSIFICATION OF THIS PAGE	19. SECURITY CLASSIFICATION OF ABSTRACT	20. LIMITATION OF ABSTRACT
Unclassified	Unclassified	Unclassified	UL

GENERAL INSTRUCTIONS FOR COMPLETING SF 298

The Report Documentation Page (RDP) is used in announcing and cataloging reports. It is important that this information be consistent with the rest of the report, particularly the cover and title page. Instructions for filling in each block of the form follow. It is important to **stay within the lines to meet optical scanning requirements.**

Block 1. Agency Use Only (Leave Blank)

Block 2. Report Date. Full publication date including day, month, and year, if available (e.g. 1 Jan 88). Must cite at least the year.

Block 3. Type of Report and Dates Covered. State whether report is interim, final, etc. If applicable, enter inclusive report dates (e.g. 10 Jun 87 - 30 Jun 88).

Block 4. Title and Subtitle. A title is taken from the part of the report that provides the most meaningful and complete information. When a report is prepared in more than one volume, repeat the primary title, add volume number, and include subtitle for the specific volume. On classified documents enter the title classification in parentheses.

Block 5. Funding Numbers. To include contract and grant numbers; may include program element number(s), project number(s), task number(s), and work unit number(s). Use the following labels:

C	- Contract	**PR**	- Project
G	- Grant	**TA**	- Task
PE	- Program Element	**WU**	- Work Unit Accession No.

Block 6. Author(s). Name(s) of person(s) responsible for writing the report, performing the research, or credited with the content of the report. If editor or compiler, this should follow the name(s).

Block 7. Performing Organization Name(s) and Address(es). Self-explanatory.

Block 8. Performing Organization Report Number. Enter the unique alphanumeric report number(s) assigned by the organization performing the report.

Block 9. Sponsoring/Monitoring Agency Names(s) and Address(es). Self-explanatory.

Block 10. Sponsoring/Monitoring Agency. Report Number. (If known)

Block 11. Supplementary Notes. Enter information not included elsewhere such as: Prepared in cooperation with...; Trans. of ..., To be published in .... When a report is revised, include a statement whether the new report supersedes or supplements the older report.

Block 12a. Distribution/Availablity Statement. Denote public availability or limitation. Cite any availability to the public. Enter additional limitations or special markings in all capitals (e.g. NOFORN, REL, ITAR)

DOD - See DoDD 5230.24, "Distribution Statements on Technical Documents."
DOE - See authorities
NASA - See Handbook NHB 2200.2.
NTIS - Leave blank.

Block 12b. Distribution Code.

DOD - DOD - Leave blank
DOE - DOE - Enter DOE distribution categories from the Standard Distribution for Unclassified Scientific and Technical Reports
NASA - NASA - Leave blank
NTIS - NTIS - Leave blank.

Block 13. Abstract. Include a brief (Maximum 200 words) factual summary of the most significant information contained in the report.

Block 14. Subject Terms. Keywords or phrases identifying major subjects in the report.

Block 15. Number of Pages. Enter the total number of pages.

Block 16. Price Code. Enter appropriate price code (NTIS only).

Blocks 17. - 19. Security Classifications. Self-explanatory. Enter U.S. Security Classification in accordance with U.S. Security Regulations (i.e., UNCLASSIFIED). If form contains classified information, stamp classification on the top and bottom of the page.

Block 20. Limitation of Abstract. This block must be completed to assign a limitation to the abstract. Enter either UL (unlimited) or SAR (same as report). An entry in this block is necessary if the abstract is to be limited. If blank, the abstract is assumed to be unlimited.